Ni(II) and Pd(II) based catalysts for α-olefin polymerisation

by

LUCKY MONI

A thesis submitted in fulfilment of the

requirement for the degree of

Master of Science

at University of Cape Town

Supervisor: Prof. J.R. Moss (UCT)

June 1999

DECLARATION

I, undersigned, hereby declare that the work contained in this thesis is my own original work and that I have not previously in its entirety or in part submitted it at any university for a degree and all the sources I have used or quoted have been indicated and acknowledged by means of complete references.

.....

Lucky Moni

Acknowledgements

I wish to extend my thanks to:

my supervisor, Professor J. R. Moss for all the time and support he gave me,
members of the Inorganic Research for all the support they gave,
Foundation for Research and Development (FRD) for the financial support,
I would like to thank my family and my friends for the all the support,
finally, I would like to thank the University of Cape Town for giving me an opportunity to better my future,

Abstract

A variety of Ni(II) and Pd(II) based catalysts have been synthesised and used in homopolymerisation of ethylene and 1-hexene at room temperature. These catalysts are of the type (R-DAB)MRX, where R-DAB = dimine ligand, such as glyoxal-bis (2,6-diisopropylphenyl)imine or diacetyl-bis(2,6-diisopropylphenyl)imine, glyoxal-bis(2,6-dimethylpheny)imine and diacetyl-bis(2,6-dimethylphenyl)imine, M = transition metal, such as Ni(II) or Pd(II), R = akyl group, and X = halide. These complexes were characterised by ^{1}H and ^{13}C NMR and elemental analysis and the results are discussed. All these complexes were known compounds, we only modified the synthesis methods of other complexes.

These complexes were then used as catalysts in the polymerisation of 1-hexene and ethylene at room temperatures. All the nickel based catalysts polymerised 1-hexene and ethylene to produce polymers in good yields. In the case of palladium based catalysts, only the glyoxal derivatives managed to polymerise ethylene and in very low yields. The polymers produced were subjected to ^{1}H, ^{13}C and ^{13}C APT NMR for structural information and DSC, DTA, TGA for their thermal behaviour.

ABBREVIATIONS

AcacH	= acetylacetone
COD	= 1,5-cyclo-octadiene
Cp	= η^5-C_5H_5
D-(iPr)PI	= Diacetyl-bis(2,6-diisopropylphenyl)imine
D-MPI	= Diacetyl-bis(2,6-dimethylphenyl)imine
DME	= 1,2-dimethoxy ethane
DSC	= differential scanning calorimetry
DTA	= differential thermal analysis
G-(iPr)PI	= glyoxal-bis(2,6-diisopropylphenyl)imine
G-MPI	= glyoxal-bis(2,6-dimethylphenyl)imine
M	= transition metal
MAO	= methylalumoxane
MMAO	= modified methylalumoxane
NMR	= nuclear magnetic resonance
PE	= poly(ethylene)
PH	= poly(1-hexene)
R	= alkyl group
R-DAB	= 1,4-diaza-1,3-diene

RT	= room temperature
TGA	= thermogravimetric analysis
X	= halides

Table of contents

Chapter 1. Introduction

Chapter 2. Synthesis of diimine ligands and their transition metal complexes

Chapter 3: Polymerization of ethylene and 1-hexene by Ni(II) and Pd(II) based catalysts

Chapter One

Introduction

Chapter 1.

Introduction

Chapter 1.

1. Introduction

1.1. Review of recent developments in olefin polymerisation

Polymerization of a large variety of unsaturated hydrocarbons is catalysed by organometallic compounds. Polymerisation of olefin (such as ethene, propene, and other α-olefins) may be effected using homogeneous or heterogeneous catalysts. Both catalytic systems have their advantages and disadvantages. Homogeneously catalysed reactions are generally more efficient, stereoselective, specific, and reproducible than the heterogeneous ones.

However, heterogeneous catalysts are chemically and thermally more stable and also obviate the separation problem encountered in homogeneous catalytic systems[1,2,3]. The stimulus in the polymerisation of ethylene was provided by pioneering studies of Ziegler in the early 1950s[4]. Ziegler explored the use of organometallic compounds which consisted of transition metals in combination with reducing agent or Lewis acid (such as $TiCl_3.Et_2AlCl$), in the polymerisation of ethylene. G.Natta who was a

consultant for Montecatini extended Ziegler's work to polymerisation of propene and higher α-olefins.

In 1955, Natta announced the preparation and equally important, the characterisation of stereoregular polymers of α-olefins produced using a Ziegler type of catalyst based on titanium[5,6]. Since the pioneering days of Ziegler-Natta catalysis, the thrust of catalyst development in propene polymerisation was aimed almost exclusively at improving the catalyst productivities reflected by low content of transition metal in the polymer, and high stereoselectivity with respect to exclusive formation of highly stereoregular polypropylene, reflected by low content of extractable low stereoregular fractions[7].

In 1997, Randall pointed out that, despite very high stereoselectivities, polypropylene macromolecules are seldom 100% isotactic, but posses long isotactic sequences interrupted by stereo and regio-irregularities[8]. However, many conventional supported Ti-based catalysts gave mixtures of highly isotactic, high molecular mass polypropylene with low stereoregular polypropylene exhibiting much lower molecular masses.

This was associated with the presence of multiple catalytic active sites, which exhibit different stereoselectivities[9]. The advantage of the modern metallocene catalysts, often referred to as single site catalysts, is the presence of exclusively one type of catalytic active site.

This means that variation of catalyst structure gives control of stereoselectivity and translate into controlled variation of the contents of stereo-irregularities in the polypropylene backbone. As a consequence, metallocene catalysts can be designed to tailor polypropylene molecular architectures[10-18].

Conventional multi-site catalysts failed to produce ethene copolymers over the ethene/propene/octene range of comonomer. With modern metallocene catalysts such as rac-dimethylsilenylbis(2-methylbenz[e]indenyl) zirconium dichloride(MBI) (see Figure 1), excellent control of comonomer incorporation over the entire range was achieved[19-23], including homopolymers of polyethylene as well as isotactic polypropylene. Also the stereoblock polypropylene, consisting of alternating isotactic and low stereoregular segments was obtained with special metalloecene catalysts such as MAO-activated {HMe(Ind)Me_4Cp}$TiCl_2$, reported by Chien and

coworkes[24] and MAO-activated (2-Ph-Ind)$_2$ZrCl$_2$, reported by Waymouth and coworkers[25,26]. These copolymerisation metallocene catalysts are displayed in Figure 1.1 below.

Figure 1.1 Comparison of various metallocenes in ethene/oct-ene copolymerisation

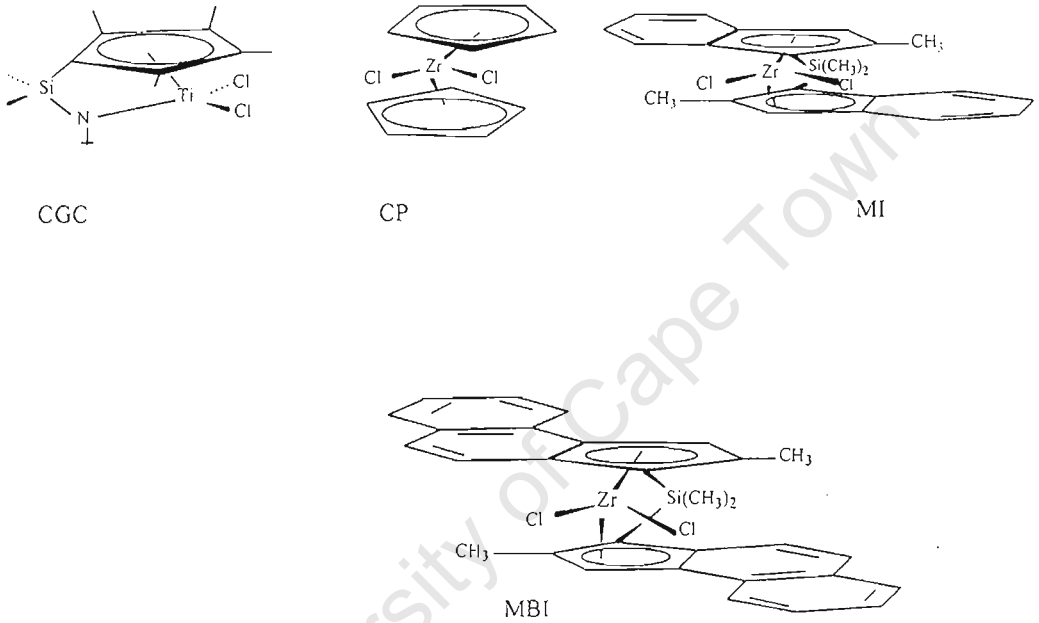

[CGC = dimethylsilenyl(tetramethylcyclopentadienyl)-(N-tert-butylamido)titanium(IV)dichloride].
[CP = zirconocene dichloride].[MI = rac-dimethylsilenylbis-(2-methylindenyl)zirconium dichloride].
[MBI = rac-dimethylsilenylbis-(2- methylbenz[e]indenyl)zirconium dichloride].

These single site metallocene catalysts were used to achieve short branched polyethylenes, by two strategies (i) copolymerisation of ethylene with 1-alkene such as oct-1-ene using the single site metallocene catalysts and (ii) migration insertion polymerisation producing methyl- and alkyl-branched

polyethylene. Similar to the formation of regio-irregularities, β-hydride transfer combined with rotation and migration insertion can account for the formation of methyl branches during ethene polymerisation. When insertion takes place exclusively at the chain ends, methyl-branched or linear polyethenes are formed[27-31](see Scheme 1.)

Scheme.1 Migratory insertion polymerisation of ethene to produce polymers

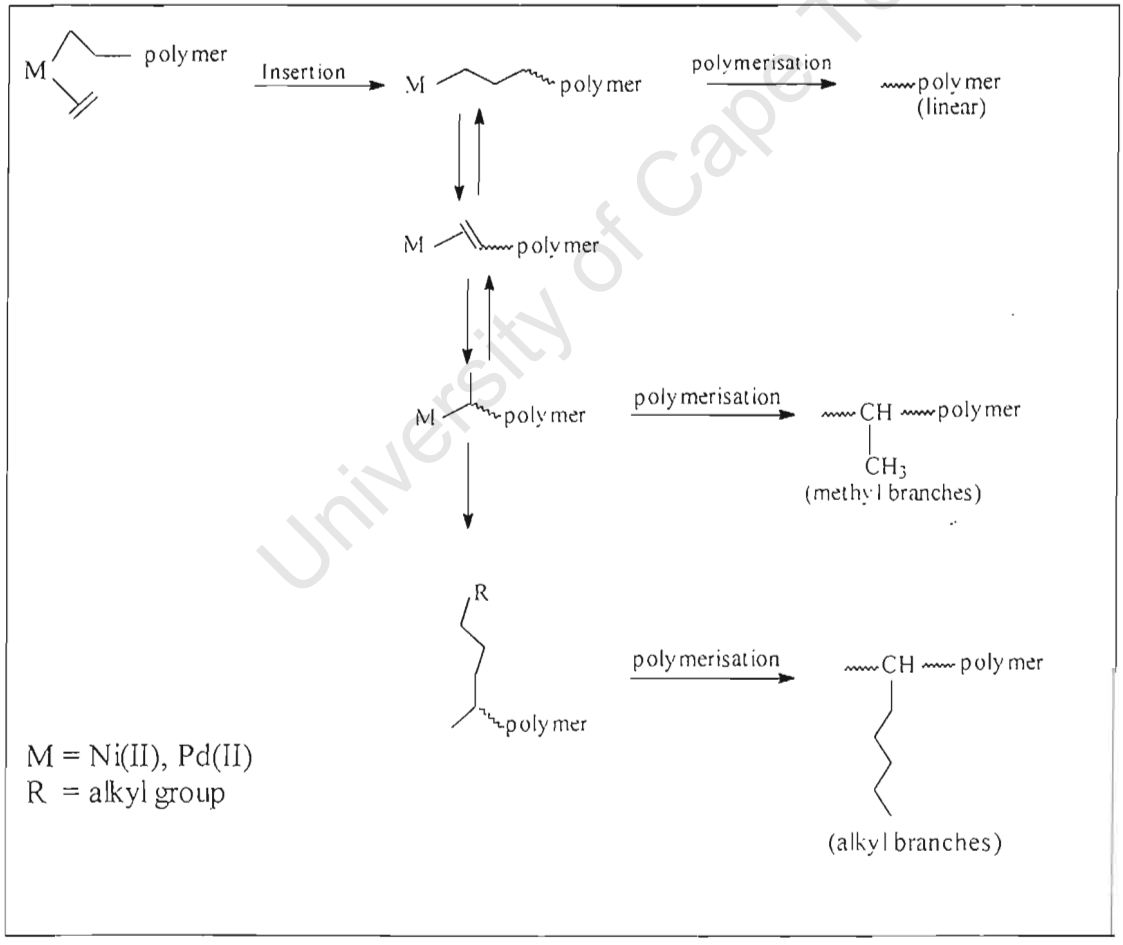

Insertion of transition metal alkyl, located somewhere in the polymer chain, gives short alkyl and alkyl side chains. This rather unusual behaviour was observed by Brookhart and coworkers[32], when he introduced bisimine co-ordinated nickel or palladium catalysts which are activated with MAO or borane to form cationic transition metal alkyl bonds as catalytically active intermediates.

After Brookhart's breakthrough in late transition metal (such as Pd(II), Ni(II)) catalysis, Gibson came up with a new strikingly active family of ethylene polymerisation catalysts based on iron and cobalt bearing 2,6-bis(imino)pyridyl ligands[33,34](see Figure.1.2)

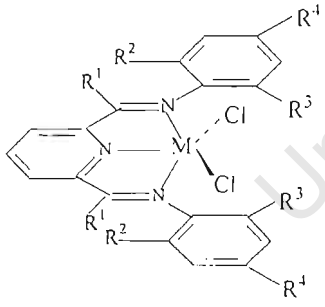

R^1 = Me, H

R^2 = iPr, Me

R^3 = iPr, Me

R^4 = H, Me

M = Fe, Co

Figure.1.2 The general structure of bis(imino)pyridyl

For these new late transition metal catalysts simple variation of pressure temperature and ligand substituents allows access to ethylene homopolymers with a structure that vary from highly branched, completely amorphous to linear , semicrytalline high density materials[35,36].

The Brookhart catalysts are cationic metal complexes that incorporate bulky aryl diimine ligands. Once these complexes are activated and exposed to ethylene, propylene or 1-hexene, they produce high molecular weight polymers that are isolated as amorphous materials (Scheme 2.)[37].

Scheme.2 Ni(II) and Pd(II) based catalysts used olefin polymerisation

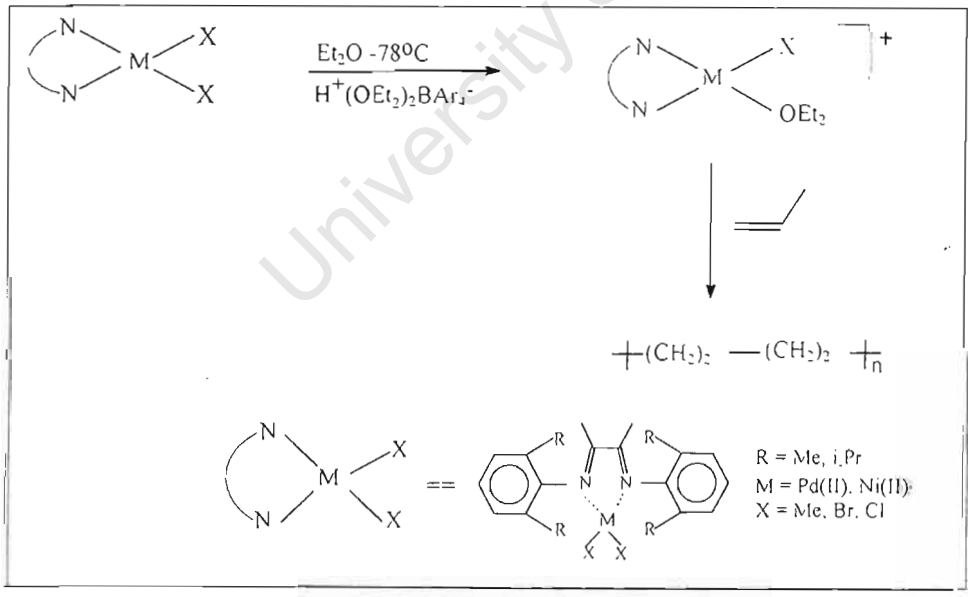

The fact that these complexes produce high molecular weight polymer is a consequence of slow chain transfer relative to chain propagation. In these d^8

square planar systems(Ni(II) ,Pd(II)), chain transfer is proposed to occur by associative olefin displacement (Scheme 3) and is hindered by the axial bulk provided by the ortho-substituents of the aryl ring (Scheme 3.)[38].

Scheme.3 Mechanism for olefin polymerisation/oligomerisation

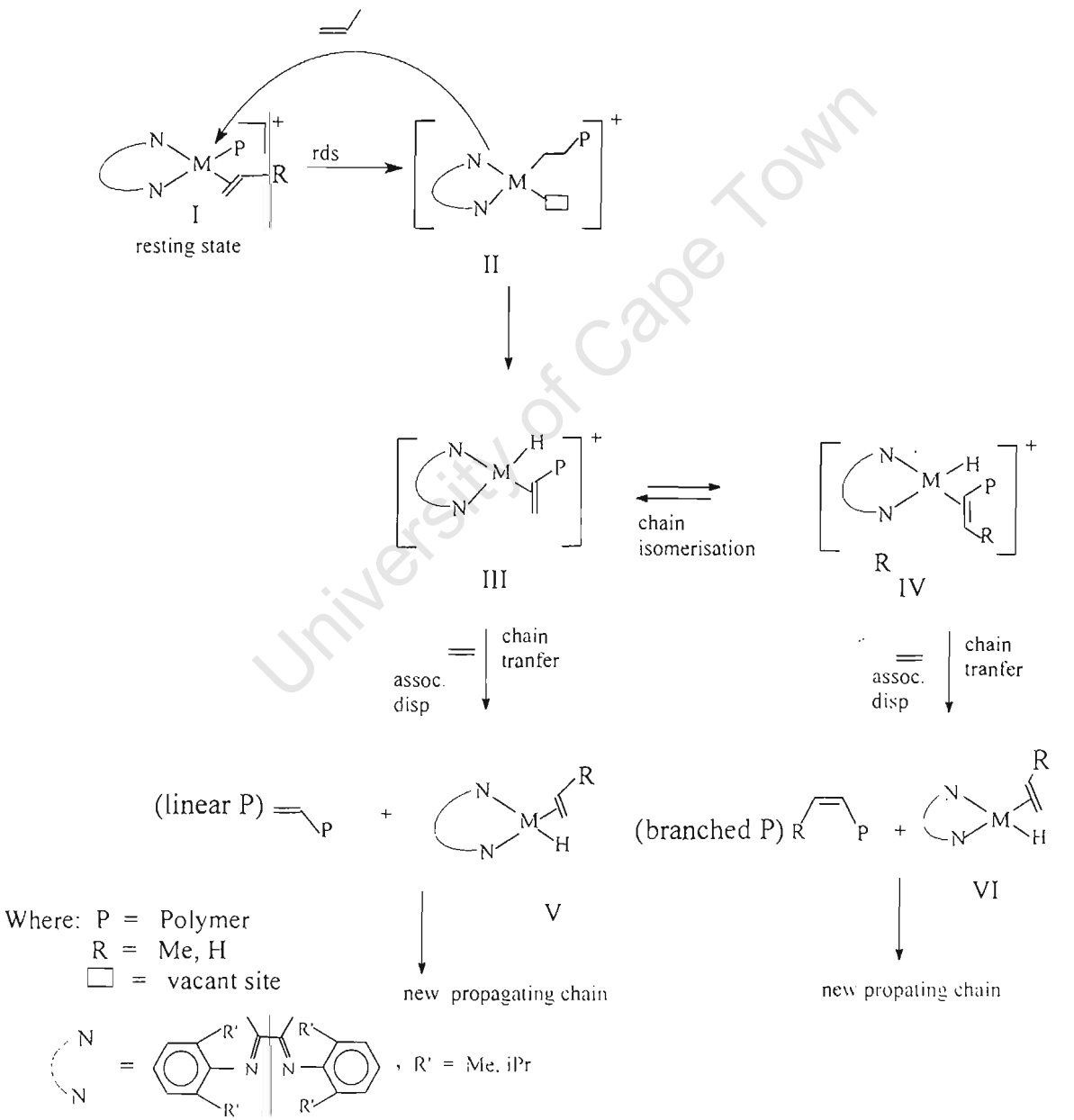

In 1997, it was shown that by eliminating the ortho-substituents of the aryl rings, rates of associative chain transfer should be substantially increased, resulting in oligomerisation rather than polymerization reaction (scheme.4)[39].

Scheme 4. Catalyst systems for ethylene oligomerisation

1-3

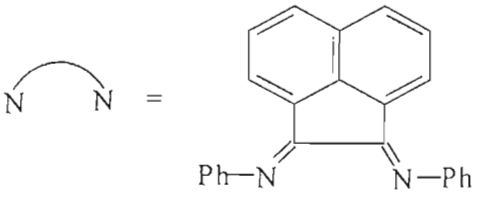

1.

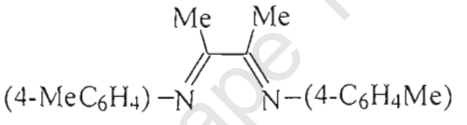

2.

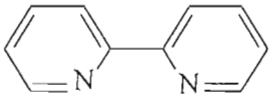

3.

Where: R = CH_3
X = Cl
MMAO = Modified Methyl alumoxane

1.2. The chemistry of diimine compounds

This section deals with the background chemistry and properties of diimine ligands. Diimine compounds have attracted much interest because of both their versatile co-ordination behaviour and the properties of their metal complexes. They are particularly fascinating since they have a flexible

N=C-C=N skeleton, whose flexibility is attributed to the ability of the C-C sigma bond to rotate . These molecules appear to have unusual donor and acceptor properties and they can potentially act in a variety of co-ordination modes. These co-ordination modes do not only involve nitrogen lone pairs but also the pi-C=N bonds[40].A few of the bonding modes are displayed below:

Scheme 4. Bonding modes of 1,4-diaza-1,3-diene and number of electrons donated

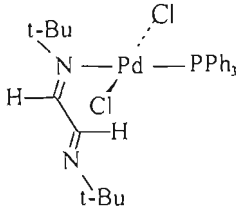

2e donated to the metal

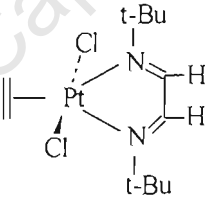

4e donated to the metal

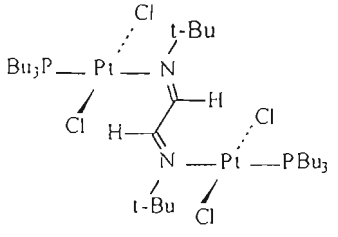

2e donated to each metal

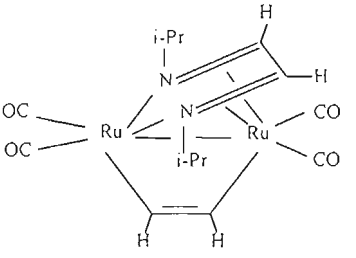

8e donated to two metals

1.3. Properties of Ni and Pd complexes with diimine as ligand

Some diimine compounds are either not known as free molecules or have only a very limited stability. The metal complexes of 1,4-diaza-1,3-butadiene show unusual stability and a characteristic colour being ascribed to the presence of pi-bonding between the metal and nitrogen atom[41].

A consistent structural feature of these diimine metal complexes appear to be the chelate system of diimine ligands. Since the free 1,4-diaza-1,3-butadiene exists in the trans conformation, this implies that upon co-ordination to the metal center, rotation around C-C has to take place to give the cis-conformation.

1.4 Scope of this thesis

The work described in this thesis deals with synthesis of Ni(II) and Pd(II) complexes bearing diimine ligands. Most of the complexes have been prepared before and few of them are new complexes. The complexes were fully characterised by ^{1}H NMR and melting points were determined. The metal complexes were tested in the polymerisation of 1-hexene and ethylene at room temperature and MAO was used as cocatalyst. The ^{13}C and ^{1}H NMR and thermal analysis(DSC, DTA and TGA) of the polymers are reported.

Chapter Two

Synthesis of diimine ligands and their transition metal complexes

Chapter 2.

Chapter 2: Synthesis of diimine ligands and their metal complexes

2.1. Introduction

2.1.1 Diimine ligands

The diimine ligands are molecules containing 1,4-diaza-1,3-butadiene(R-DAB)[42] in their backbone. They have general formulae of the form R-N=CR'-CR'=N-R. These ligands may be prepared by condensation reactions involving either diacetyl or gloxal with a primary aromatic amines as displayed in Scheme 2.1:

Scheme 2.1 Synthesis of dimine ligands(R-DAB) by condensation reactions

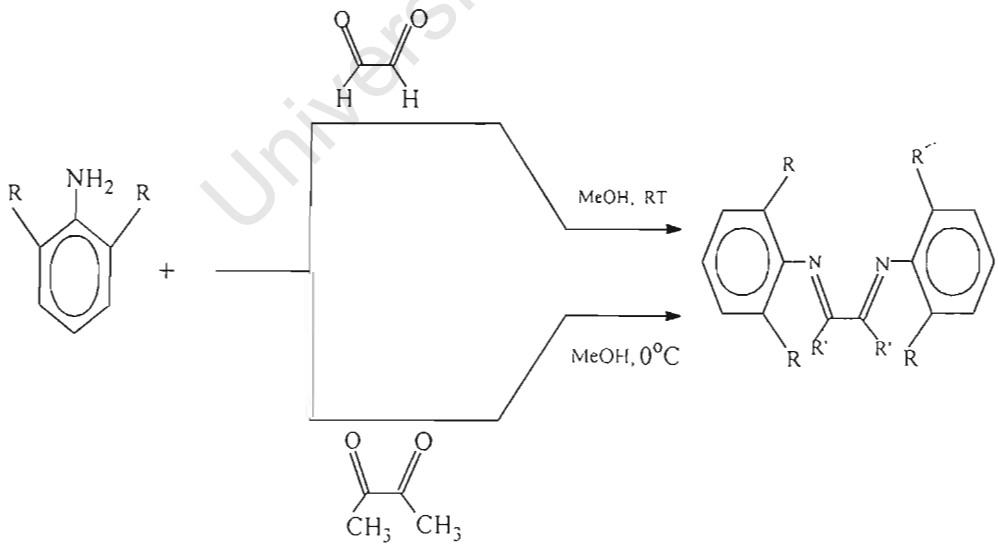

R = Me, iPr

R' = Me, H

2.1.2 Metal complexes

Some diimine ligands are unstable as free ligands but more stable as metal complexes. In most cases they are synthesised by an *in situ* preparation as illustrated in Scheme 2.2:

Scheme. 2.2 : The *in situ* preparation of diimine complexes

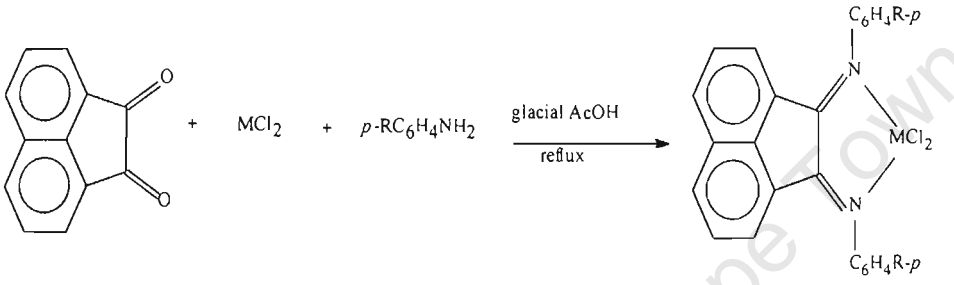

The stability and the characteristic colour of diimine metal complexes are attributed to the presence of pi-bonding between the metal and the nitrogen atoms[43-45]. In this thesis we report on very stable diimine compounds which can be obtained as free ligands and they are also obtained as very stable metal complexes. The focus of this thesis will only be on nickel and palladium complexes of these diimine compounds.

Starting with nickel complexes, there are three synthetic routes that can be followed to synthesize nickel complexes bearing the diimine ligands: (i) ligand substitution route where the starting material is $Ni(CO)_4$, this reaction occurs at elevated temperatures and it can not be used for thermally

unstable compounds like diimines and it sometimes stops at the stage of $Ni(CO)_2L$[46-48] as showed in Scheme 2.3:

Scheme 2.3 Synthesis of nickel complexes by ligand substitution

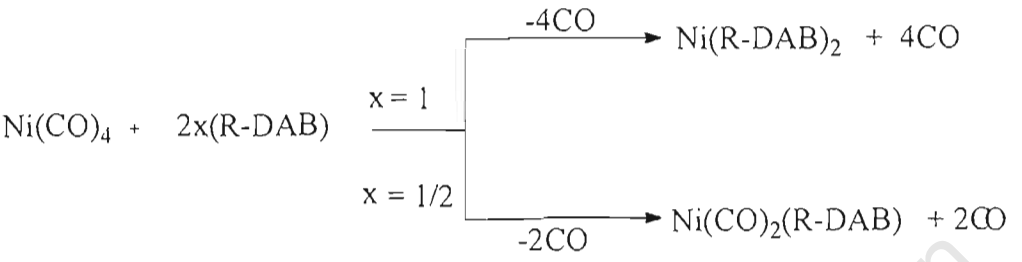

Where R-DAB = dimine ligand

(ii) reductive route, starts with $Ni(acac)_2$ as a source of nickel. The $Ni(acac)_2$ is reacted with the diimine ligand and RMgX or R_2Mg at -78°C in an *in situ* reaction. We attempted this reaction but was unsuccessful. The physical response in terms of colour was positive till the stage of separation of the product where it decomposed to form a black substance instead of a greenish material according to the literature[49,50]. The reaction equation is illustrated below in equation (A).

$$Ni(acac)_2 + R\text{-}DAB + 2MeMgI \xrightarrow[N_2]{\text{diethyl ether } -78\ ^0C} (R\text{-}DAB)Ni(Me)_2 + 2Mg(acac)I \quad \textbf{(A)}$$

(iii) ligand substitution route, it starts with $(DME)NiBr_2$ reacted which was with diimine ligand to produce $(R\text{-}DAB)NiBr_2$ according to the reaction equation below:

Scheme 2.4 Synthesis of diimine ligands by substitution reaction

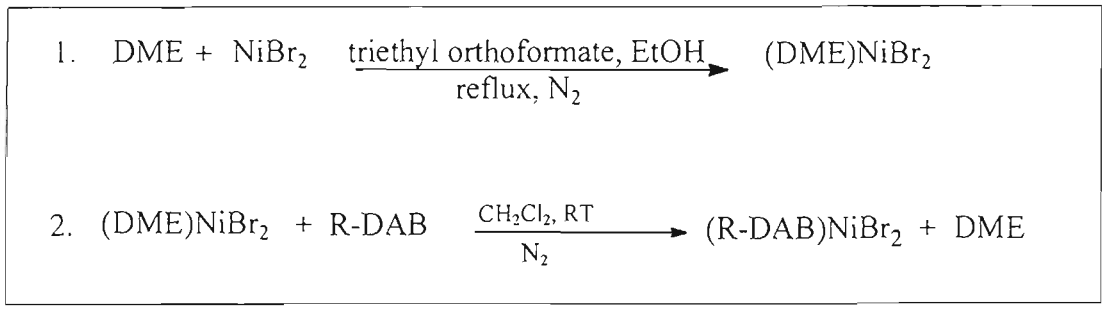

The synthesis of palladium complexes bearing diimine ligands occurred by ligand substitution reactions. The substitution reaction occurred via a three step process. The first step involved the reaction of COD with Na_2PdCl_4 to produce $(COD)PdCl_2$[51], which was then methylated by reaction with one equivalent of methyllithium at –78°C to give (COD)PdMeCl[52-54] this was then reacted with diimine ligands to produce (R-DAB)PdMeCl as illustrated in Scheme.2.5:

Scheme 2.5 Synthesis of palladium complexes bearing diimine ligands

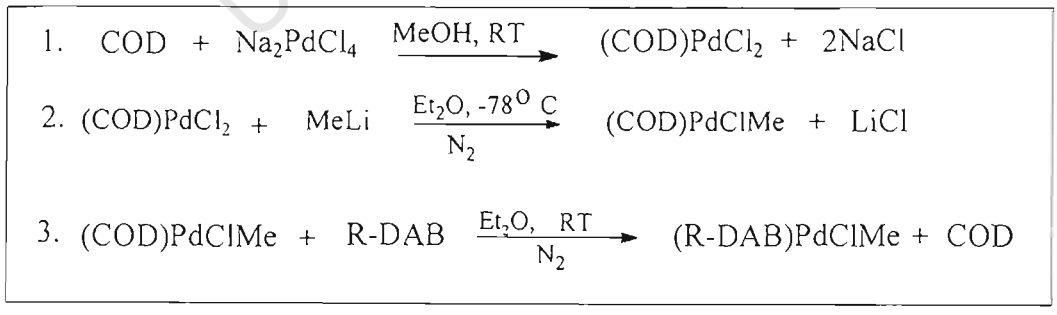

2.2 Results and discussion

2.2.1 Diimine compounds

All the diimine ligands reported in this thesis were synthesised according to the methods outlined by tom Dieck and coworkers[49] . The ligands were fully characterised by ^{13}C and ^{1}H NMR and their melting points were observed under a hotstage microscope. The ^{1}H NMR spectroscopy results of the diimine ligands correlated very well with those reported in the literature. The ^{13}C NMR spectra and the melting points of the diimine compounds were not reported in the literature[49]. All their details will be reported in the next sections. The experimental methods for the synthesis of these ligands will be reported in Chapter 4.

This present chapter will deal with discussion of ^{13}C and ^{1}H NMR spectra results of the diimine ligands.

2.2.1.1. Glyoxal-bis(2,6-diisopropylphenylimine)[G-(iPr)PI]

The [G-(iPr)PI] compound was obtained as a yellow powder stable in air and at room temperature with a melting point in the range 100-104°C. Another glyoxal derivative, i.e glyoxal-bis(2,6-dimethylphenyl)imine [G-MPI] was obtained as a pale yellow powder with melting point with range of 115-120°C. These compounds differ as result of having different substituents on the aryl ring. G-(iPr)PI has isopropyl substituents on the aryl rings whereas G-MPI has methyl substituents on the aryl ring. These compounds were both subjected to NMR spectrometry to obtain structural information. The schematic representation of G-(iPr)PI structure is shown in Figure 2.1 with assignation **a,b,c,d,e**, for the protons and **1,2,3,4,5,6,7** for the carbon atoms.

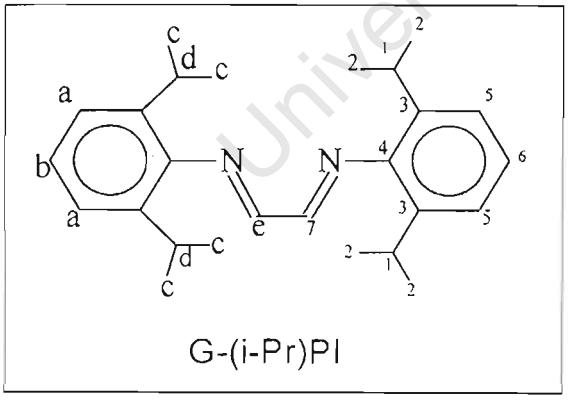

Figure 2.1 Structure of glyoxal-bis(2,6-diisopropylphenylimine)[G-(iPr)PI]

^{1}H NMR of G-(iPr)PI and G-MPI

The correlation of the protons **a,b,c,d,e** in Figure 2.1 with corresponding ^{1}H NMR chemical shifts are given in Table 2.1 below. The ^{1}H NMR spectra for the two ligands is shown in Figure 2.2.

Table 2.1: The ^{1}H NMR spectrum designations

Proton	Chemical shifts(ppm) for G-(i-Pr)PI
a,b	7.12-7.16 (m)
c	1.15-1.19 (d) J = 8.22 Hz
d	3.00 (sept)
e	8.18 (s)

Discussion

The ^{1}H NMR spectrum (Figure 2.2(a)) and chemical the shifts in Table 2.1, both give the structural information of G-(iPr)PI (see Figure 2.1). The peak that appears at δ = 7.26 ppm is $CDCl_3$ peak. The peaks in the region δ = 7.12-7.16ppm arise from hydrogens **a,b** of the aryl ring. The peak at δ = 8.18ppm is associated with of hydrogen **e** attached to the carbon of the C=N group. The doublet peak in region δ = 1.15-1.19ppm is associated with hydrogen **c** of the methyl group of the isopropyl group. And the septet peak at δ =3.00ppm is associated with hydrogen **d** attached to the tertiary carbon

of the isopropyl group. In the case of G-MPI, the spectrum is similar to the one of G-(iPr)PI except for the absence of the septet at δ = 3.00 ppm and the doublet at δ = 1.15-1.19 ppm because those peaks were due to the isopropyl groups on the aryl rings of G-(iPr)PI. In the place of isopropyl group, G-MPI has methyl groups attached on the rings which appear at δ = 2.10ppm in the ^{1}H NMR spectrum (see Figure 2.2(b)).

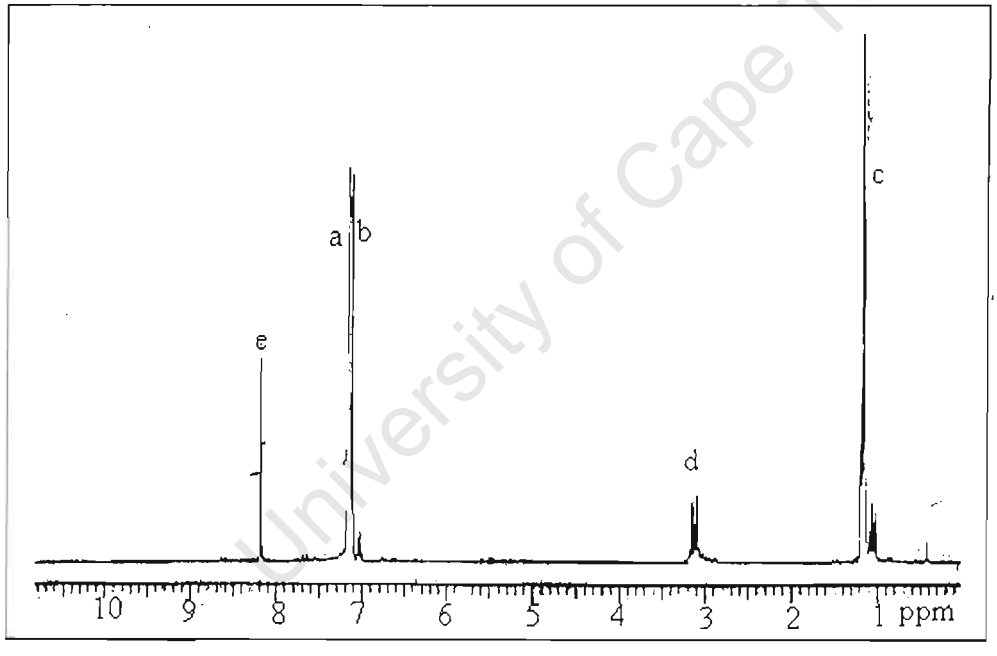

Figure 2.2(a) ^{1}H NMR spectrum (in $CDCl_3$) of G-(i-Pr)PI
(see Figure 2.1 for atom lettering scheme)

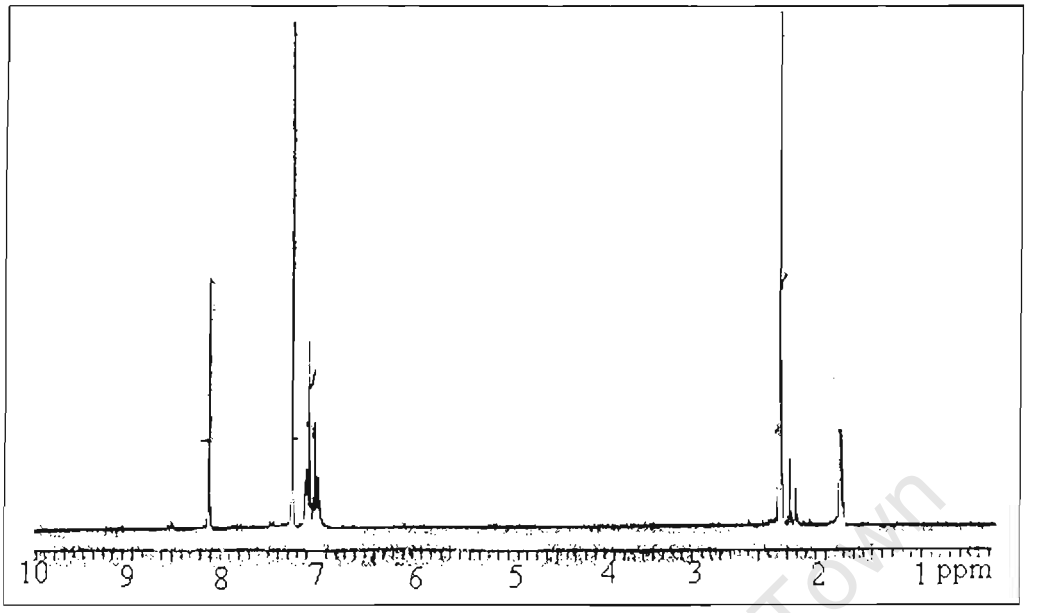

Figure 2.2(b) ^{1}H NMR spectrum (in $CDCl_3$) of G-MPI

^{13}C NMR of G-(iPr)PI and G-MPI

The chemical shifts corresponding to the assignments of carbon atoms labelled **1,2,3,4,5,6,7** (see Figure 2.1) are displayed in Table 2.2 below. The ^{13}C NMR spectra of the two ligands is shown Figure 2.3.

Table 2.2. ^{13}C NMR Chemical shifts

Carbon	Chemical shifts(ppm) for G-(i-Pr)PI
1	28.05
2	23.99
3,4	136.75-148.18
5,6	123.18-125.11
7	163.10

Discussion

The ^{13}C NMR spectrum of G-(iPr)PI (Figure 2.3(a)) and the chemical shifts listed in Table 2.2 confirm the structural information obtained from the ^{1}H NMR spectrum for G-(i-Pr)PI. The peaks that appear in the region δ = 76-77.6ppm is a $CDCl_3$ peak. The peak at δ = 28.05ppm is attributable to the response of carbon **1,** the tertiary carbon of the isopropyl group. The peak at δ = 22.99ppm is associated with carbon **2** of the methyls of the isopropyl groups. The peaks in the region δ = (135.05-146.18)ppm are associated carbon atoms **3,4** of the aryl ring with no hydrogen attached to them. The peaks in the region δ = (122.98 –123.72)ppm are associated with carbon atoms **5,6** of the aryl ring carbon with one hydrogen per carbon. The peak at δ = 168.17ppm is attributable to carbon 7 of the C=N group. In the case of G-MPI spectrum, the peaks at δ = 28.04ppm and 22.99ppm for carbon **1** and **2** respectively do not appear because they are due to the isopropyl groups on the aryl rings of G-(iPr)PI. For G-MPI, in the place of those peaks there are peaks at δ = 18.19ppm for methyl groups on the aryl rings(see Figure 2.3(b)).

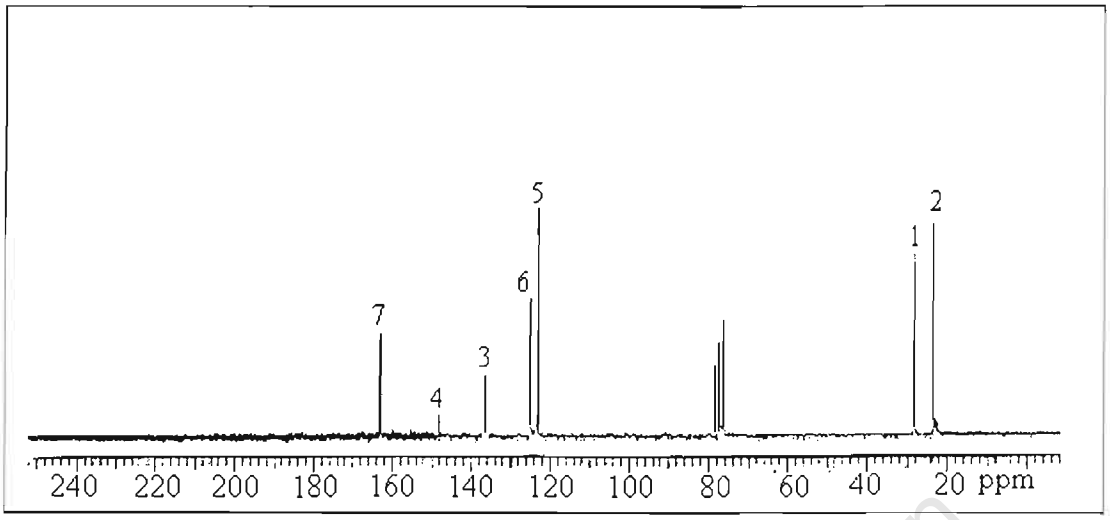

Figure 2.3(a) ^{13}C NMR spectrum (in $CDCl_3$) of G-(iPr)PI
(see Figure 2.1 for atom numbering scheme)

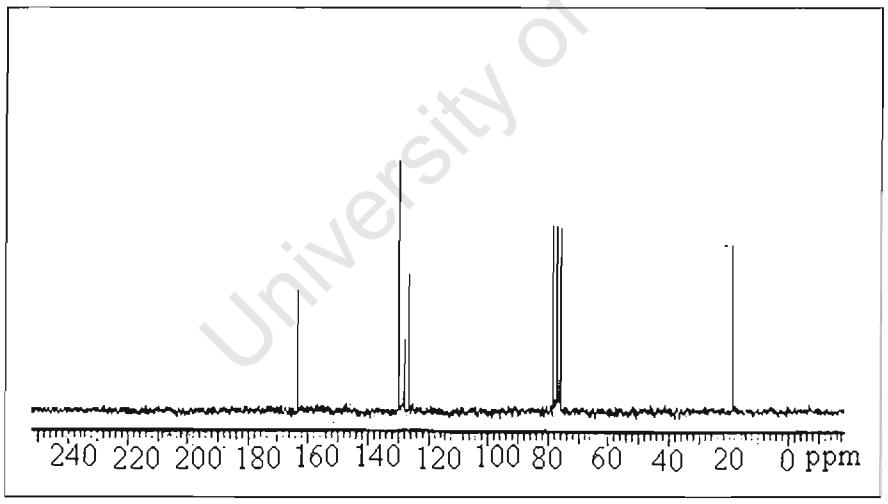

Figure 2.3(b) ^{13}C NMR spectrum (in $CDCl_3$) of G-MPI

2.2.1.2. Diacetyl-bis(2,6-diisopropylphenylimine)[D-(i-Pr)PI]

The D-(i-Pr)PI compound was obtained as a light yellow crystalline material. It is stable in air and at room temperature with a melting point in the range 90°C- 92°C. Another diacetyl derivative, i.e diacetyl-bis(2,6-dimethylphenyl)imine [D-MPI], a dimethyl substituted diimine compound

was obtained as a pale yellow crystalline material with a melting point range of 90°C-93°C. The NMR spectra of both compounds will be displayed but only one spectrum will be fully discussed. A schematic representation of the structure of D-(i-Pr)PI is displayed in Figure 2.4 with assignments **a,b,c,d,e** for protons and **1,2,3,4,5,6,7,8** for carbon atoms.

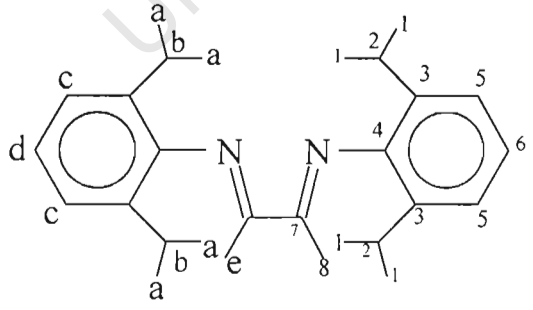

D-(i-Pr)PI

Figure 2.4 Structure of diacetyl-bis(2,6-diipropylphenylimine) [D-(iPr)PI]

^{1}H NMR of D-(iPr)PI and D-MPI

The chemical shifts corresponding to the designations **a,b,c,d,e**(see Figure 2.4) are displayed in Table 2.3. The ^{1}H NMR spectrum D-(iPr)PI is displayed in Figure 2.5(a).

Table 2.3 ^{1}H NMR chemical shifts

Proton	Chemical shift(ppm) for D-(i-P)PI
a	1.17-1.20(d) J = 6.80 Hz
b	2.80-2.95 sept
c,d	7.16 m
e	2.15 s

Discussion

The ^{1}H NMR spectrum (Figure 2.5(a)) below and the corresponding chemical shifts of D-(i-Pr)PI are listed in Table 2.3. The peak at δ = 7.26ppm for $CDCl_3$. The peak in the region δ =(2.88-2.95)ppm is associated with proton **b** of the tertiary carbon of the isopropyl group. The peak at δ =

1.17-1.20ppm is associated with proton **a** of the methyl groups of the isopropyl substituents. The singlet peak at δ = 2.15ppm is attributable to the response of proton **e** of the methyl group bonded to the C=N group. In the case of D-MPI spectrum, For D-MPI, the methyl protons attached to the aryl ring are observed at δ = 2.04ppm (see Figure 2.5(b)) and the septet peaks and doublet peaks at δ = 2.80-2.95ppm and δ = 1.19ppm due to the isopropyl protons do not appear.

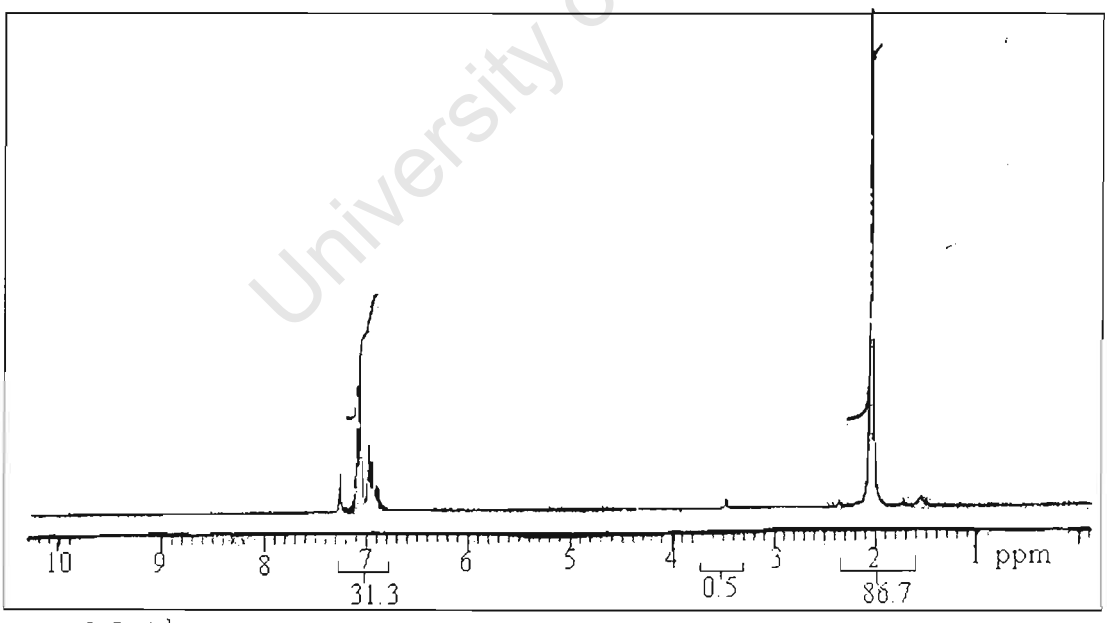

Figure 2.5(b) ^{1}H NMR spectrum (in $CDCl_3$) of D-MPI

^{13}C NMR of D-(iPr)PI and D-MPI

The designations **1,2,3,4,5,6,7,8** (Figure 2.4) and the corresponding chemical shifts in Table 2.4 below refer to the ^{13}C NMR spectrum of D-(i-Pr)PI in Figure 2.6(a).

Table 1.4 Chemical shifts of ^{13}C NMR spectrum

Carbon	Chemical shifts(ppm) for D-(i-Pr)PI
1	22.99
2	28.50
4,3	146.18 and 153.10
5,6	123.70 and 122.98
7	168.17
8	16.55

Discussion

The ^{13}C NMR spectrum (Figure 2.6) can be correlated with the structural assignments for D-(iPr)PI (see Figure 2.4). The peaks in the region δ = (76.36-77.63)ppm are due to $CDCl_3$ peak. The peak in the region δ = (22.67-22.99)ppm is associated with the response of carbon **1** of the methyl of the isopropyl group. The peak at δ = 28.50 is attributable to the response of carbon **2** , the tertiary carbon of the isopropyl group with one hydrogen attached to it. The peaks in the region δ = (146.18 and 153.50)ppm are associated with the response of carbon **4** and **3** of the aryl ring with no hydrogen attached to them. The peaks in the region δ = (123.70and 122.90)ppm are associated with the response of carbon **5** and **6** of the aryl ring with one hydrogen attached to each of them. The peak at δ = 168.18ppm is attributed to the response of carbon **7** of the N=C group and the peak at δ = 16. 55ppm is associated with carbon **8** of the methyl groups attached to C=N group. In the case of D-MPI, the peak at δ = 17.75ppm is due to methyl carbons on the aryl ring (see Figure 2.6(b))and the peaks at δ = 22.67 and 22.99ppm and at δ = 28.50ppm due to the isopropyl substituents do not appear.

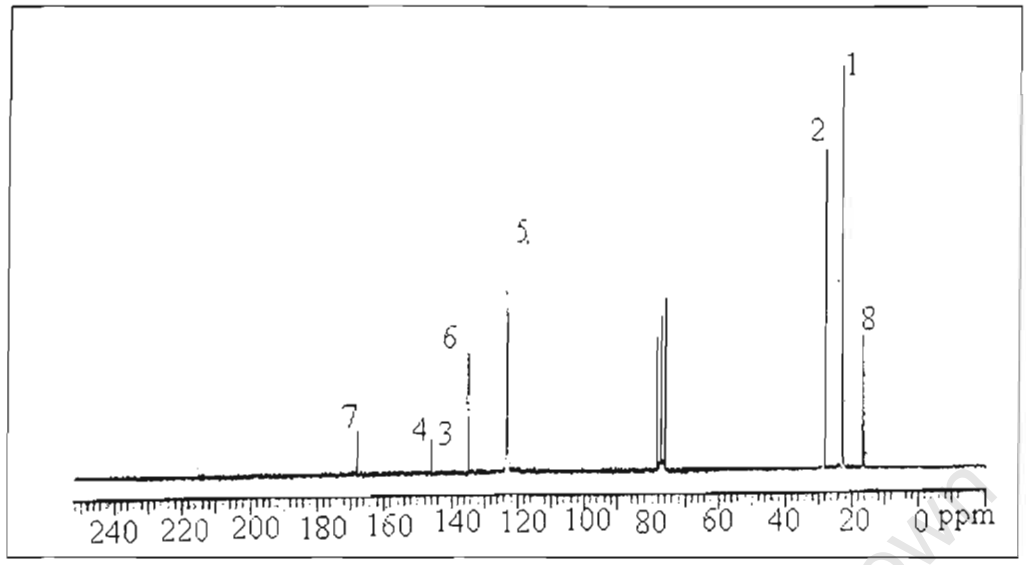

Figure 2.6(a) ^{13}C NMR spectrum (in $CDCl_3$) of D-(i-Pr)PI
(see Figure 2.4 for atom numbering scheme)

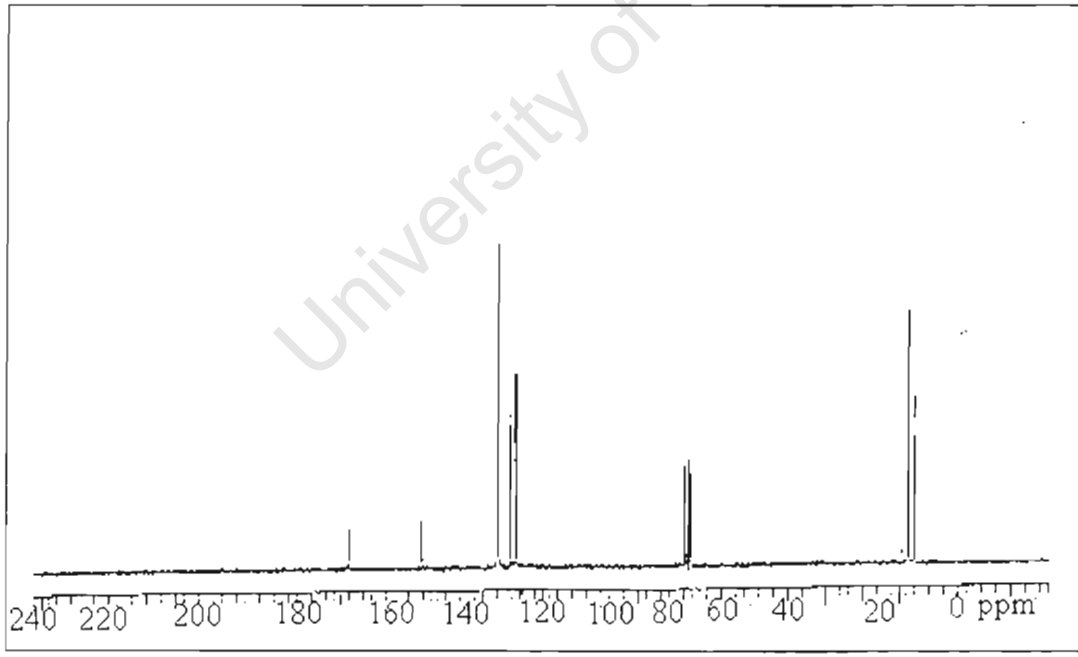

Figure 2.6(b) ^{13}C NMR spectrum (in $CDCl_3$) of D-MPI

2.2.2. Ni(II) and Pd(II) metal complexes

The nickel and palladium complexes are strongly coloured complexes, a property that helps to confirm the formation of that particular complex during the synthesis process.

2.2.2.1 Ni(II) complexes

Synthesis of nickel complexes bearing diimine ligands have been reported but no full characterisation of nickel diimine dihalides have been reported. In this thesis, nickel complexes are fully characterised and modified methods of their synthesis are reported. The full experimental details are reported in Chapter 4 of this thesis. These nickel complexes have been prepared via a ligand substitution route which involved the reaction of $(DME)NiBr_2$ with a diimine (R-DAB) to produce $(R\text{-}DAB)NiBr_2$ under nitrogen atmosphere. Reported methods[32,94,95] of their synthesis were difficult to reproduce ,hence it necessary to modify them in order to obtain the required products in good yields.

2.2.2.1.1. (1,2-Dimethoxyethane)nickeldibromide

This compound was obtained as a salmon pink powder, stable at room temperature but very sensitive to moisture. It has to be stored under an inert

atmosphere. This compound was synthesised by modifying the methods outlined in two different references[94,95]. The ^{1}H NMR spectral results are reported below. This complex was used as a starting material for ligand substitution reactions in the synthesis of nickel diimine dihalide complexes. The structural representation of this complex is displayed in Figure 2.7

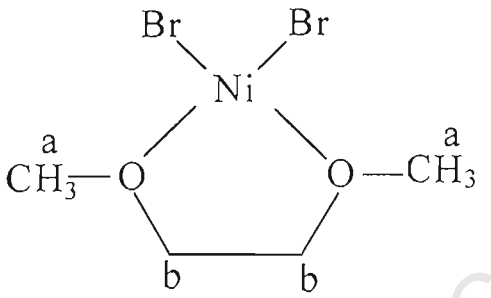

(DME)$NiBr_2$

Figure 2.7 Structure of (1,2-dimethoxyethane)$NiBr_2$

^{1}H NMR spectrum of (DME)$NiBr_2$

The chemical shifts corresponding to the assignations **a** and **b** in Figure 2.7 are displayed in Table 2.8. The ^{1}H NMR spectrum of this complex is displayed in Figure 2.8

Table 2.8 ^{1}H NMR chemical shifts for $(DME)NiBr_2$

Proton	Chemical shifts(ppm)
a	3.53s
b	3.38s

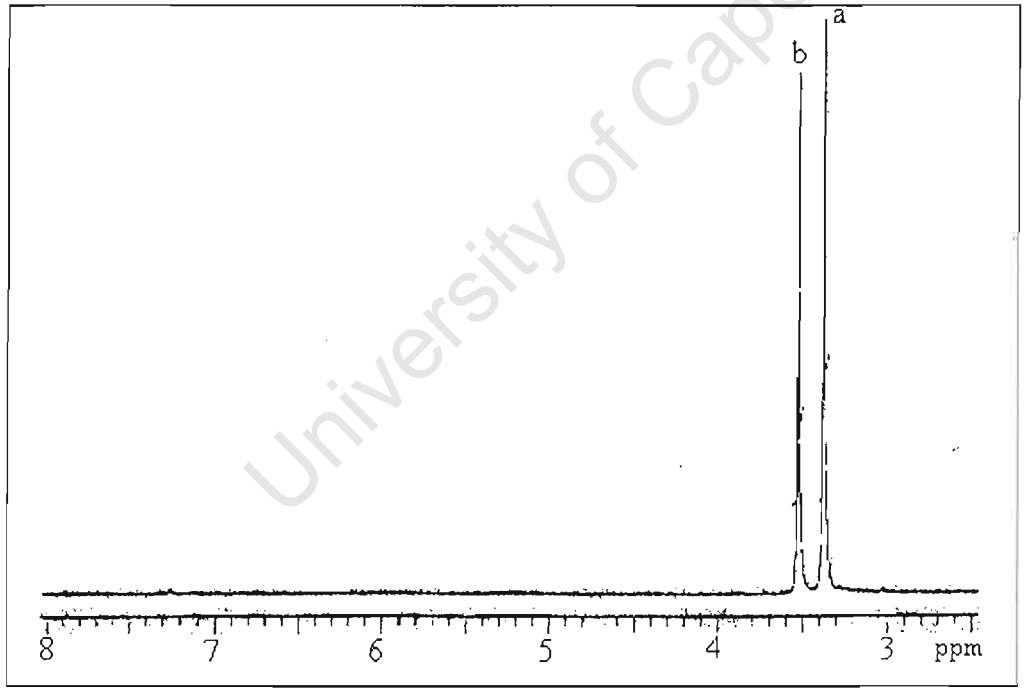

Figure 2.8 ^{1}H NMR spectrum(in $CDCl_3$) of $(DME)NiBr_2$

Discussion

The assignations in Figure 2.7 and the corresponding chemical shifts in Table 2.8 both refer to the ^{1}H NMR spectrum in Figure 2.8. The peak at δ = 3.53ppm arises from proton **a** of the methoxy groups and the peak at δ = 3.38ppm is associated with proton **b** attached to the carbon of the ethane backbone. The influence of $NiBr_2$ to the NMR spectrum is only observed as a broadening of the peaks.

2.2.2.1.2 Glyoxal-bis(2,5-diisopropylphenylimine)nickeldibromide [(G-(I-Pr)PI)NiBr$_2$]

This nickel diimine dihalide complex was obtained as a red-brown powder, which decomposed at 175°C when observed under a hotstage microscope. The dimethyl substituted diimine nickel complex (G-MPI)$NiBr_2$ was also obtained as a red-brown powder with a decomposition point of 170°C. Both complexes are very air sensitive. They have to be stored under a nitrogen atmosphere. The ^{1}H NMR spectra of these complexes are very similar to

the spectra of the free ligand but show broader peaks compared to those of the free ligand. The NMR spectra for both compounds will displayed because of their similarity only one will be discussed. The structural representation of (G-(iPr)PI)$NiBr_2$ is displayed in Figure 2.9 below with proton designations and interpertation of the ^1H NMR spectrum.

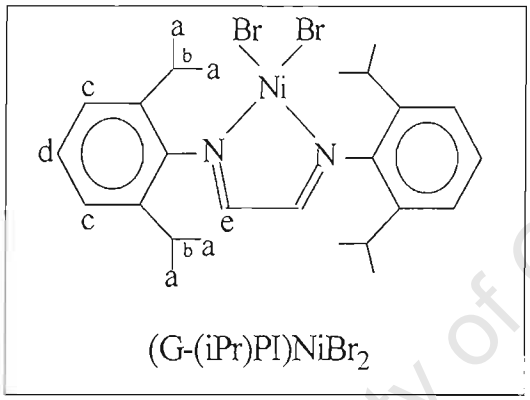

(G-(iPr)PI)$NiBr_2$

Figure 2.9 Structural representation of (G-(iPr)PI)$NiBr_2$

^1H NMR of (G-(iPr)PI)$NiBr_2$ and (G-MPI)$NiBr_2$

The chemical shifts corresponding to the designations **a,b,c,d,e** in Figure 2.9 are given in Table 2.9 below. The ^1H NMR spectrum is displayed in Figure 2.10.

Table 2.9 ^{1}H NMR chemical shifts

Proton	Chemical shift(ppm) for (G-(i-Pr)PI)$NiBr_2$
a	1.19-1.22(d) J = 6.00Hz
b	2.85-3.09(sept)
c,d	7.01-7.32(m)
e	8.01(s)

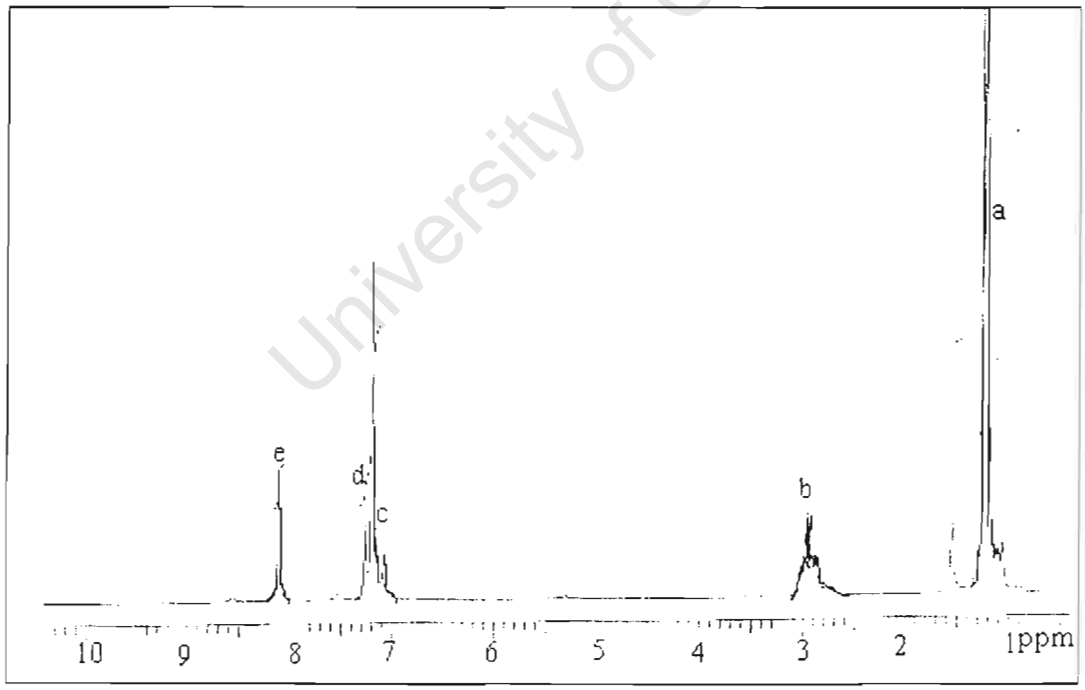

Figure 2.10(a) ^{1}H NMR spectrum (in $CDCl_3$) of (G-(i-Pr)PI)$NiBr_2$

(see Figure 2.9 for atom lettering scheme)

Discussion

The designations in Figure 2.9 and the corresponding chemical shifts in Table 2.9 both refer to the spectrum in Figure 2.10(a) above. The peak in the region δ = (1.19 – 1.22)ppm arises from the response of proton **a** of the methyls of the isopropyl group. The septet peak in the region δ = (2.85 – 3.09) ppm is associated with proton **b** attached to the tertiary carbon of the isopropyl group. The peaks at δ = 7.01ppm to δ = 7. 32ppm are associated with proton **c** and **d** of the aryl ring . The singlet peak at δ = 8.10ppm is associated with proton **e** attached to the carbon of C=N group. In the (G-MPI)$NiBr_2$ ^1H NMR spectrum, the septet peak and the doublets at δ = 2.85-3.09ppm and at δ = 1.19-1.22ppm do not appear because there are no isopropyl substituents. The complex has methyl substituents attached to the aryl rings that give the resonance at δ = 2.10ppm (see Figure 2.10(b). The spectrum is very similar to the obtained for the free ligand except for the broadening of the peaks due to the presence of nickel(II) bromide.

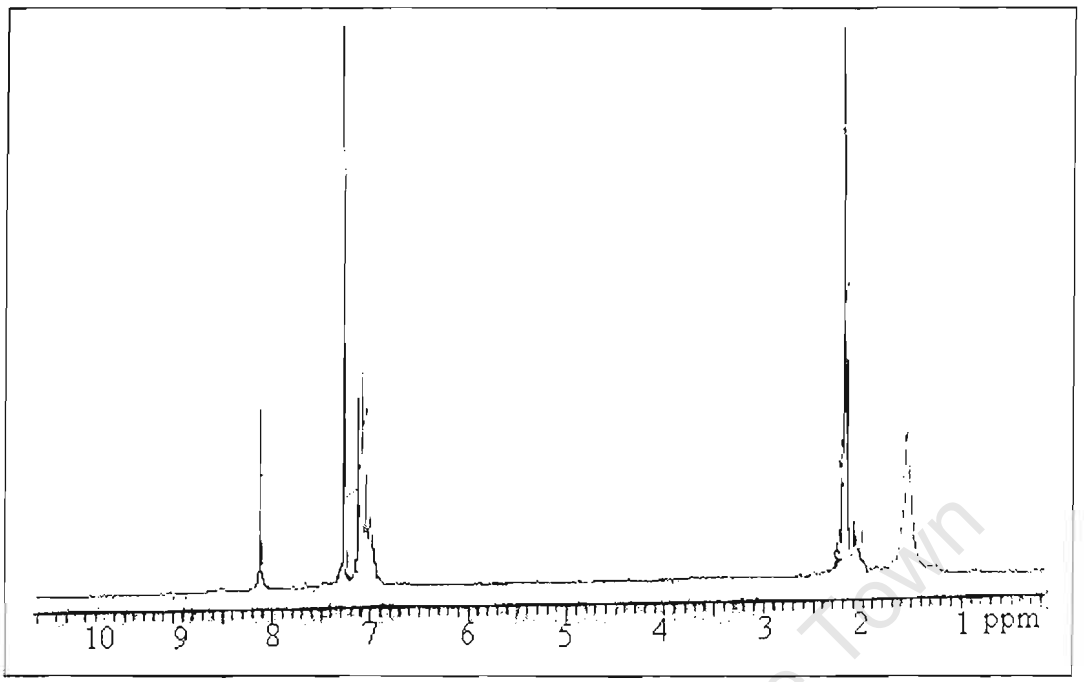

Figure 2.10(b) ^{1}H NMR spectrum (in $CDCl_3$) of (G-MPI)$NiBr_2$

2.2.2.1.3. Diacetyl-bis(2,6-diisopropylphenylimine)nickeldibromide

(D-(i-Pr)PI)$NiBr_2$

The nickel diimine dihalide complex (D-(iPr)PI)$NiBr_2$ was obtained as an orange-brown powder, stable in air and at room temperature with a decomposition temperature at 300°C. The dimethyl substituted nickel diimine dihalide (D-MPI)$NiBr_2$ was also obtained as a greenish brown powder stable in air and with a decomposition temperature at 295°C. Similar to the glyoxal nickel derivatives, the NMR spectra of these complexes

showed broad peaks when compared to those of the free ligands. The ^{1}H NMR spectra for both complexes will be displayed below but only one will be discussed. The structural representation of the complex is displayed in Figure 2.11.

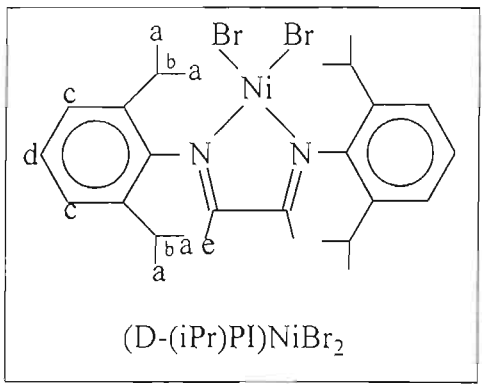

Figure 2.11 Structural representation of (D-(iPr)PI)$NiBr_2$

^{1}H NMR of (D-(iPr)PI)$NiBr_2$ and (D-MPI)$NiBr_2$

The chemical shifts corresponding to the designations in Figure 2.11 are displayed in Table 2.10 below. The proton NMR of the ligands is shown in Figure 2.12.

Table 2.10 ^{1}H NMR chemical shifts

Proton	Chemical shifts(ppm) for (D-(i-Pr)PI)$NiBr_2$
a	1.17-1.19(d) J= 6.24Hz
b	2.59-2.89(sept)
c,d	7.15(m)
e	2.06(s)

Discussion

The designations in Figure 2.11 and the corresponding chemical shifts in Table 2.10 refer to ^{1}H NMR spectra shown in Figure 2.12. The peak at δ = 7.26ppm is a $CDCl_3$ peak. The peak in the region δ = (1.17-1.19)ppm arise from proton **a** of the methyl groups of the isopropyl groups. The septet peak in the region δ = (2.59-2.89)ppm is associated with proton **b** of the tertairy carbon of the isopropyl group. The peaks at δ = 7.15ppm are associated with the protons **c** and **d** of the aryl ring. The singlet peak at δ = 2.04ppm is attributable to proton **e** of the methyl attached to the carbon of C=N group.

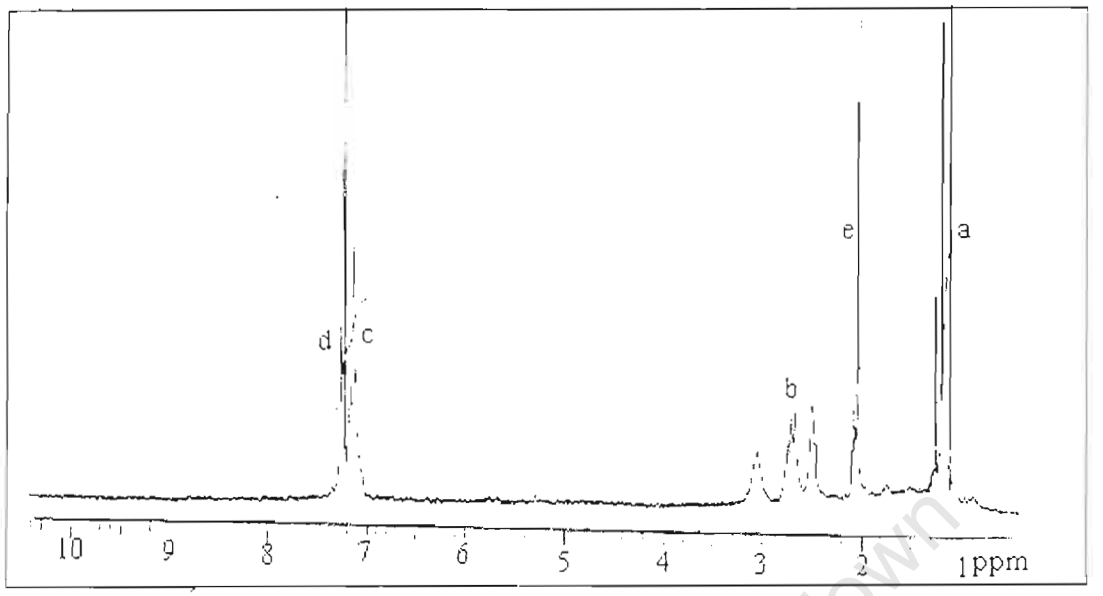

Figure 2.12(a) ^{1}H NMR spectrum (in $CDCl_3$) of (D-(i-Pr)PI)$NiBr_2$
(see Figure 2.11 for atom letttering scheme)

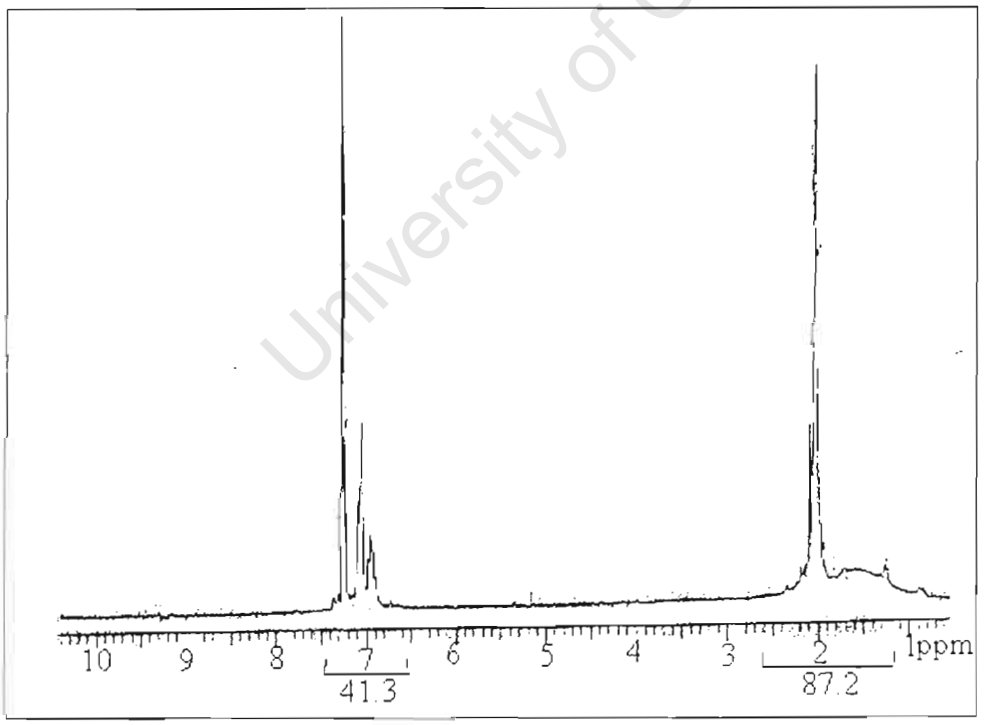

Figure 2.12(b) ^{1}H NMR spectrum (in $CDCl_3$) of (D-MPI)$NiBr_2$

2.2.2.2. Pd(II) complexes

The synthesis of palladium complexes bearing diisopropyl substituted diimine ligands is reported in the literature[32] but the synthesis of palladium complexes bearing dimethyl substituted diimine ligands is not reported in the literature . To synthesize dimethyl substituted diimine palladium complexes, the procedure[32] similar to the one used for diisopropyl substituted diimine palladium complexes was followed. In this thesis, these complexes were synthesised and fully characterised by NMR spectroscopy and their decomposition temperatures are also observed under a hotstage microscope. These complexes were synthesised by ligand substitution route, starting with (COD)PdMeCl as a source of palladium methyl chloride.

2.2.2.2.1 . (1,5-Cyclo-octadiene)palladiumdichloride [(COD)PdCl$_2$]

This complex was obtained as a yellow powder which is very stable in air and at room temperature. It was synthesised according to the method outlined by Chatt, Vallarino and Venanzi[51]. These authors started with Na_2PdCl_4 which was reacted with cyclo-octadiene in methanol at room temparature. It was a very simply and convenient reaction to reproduce and gain product in a 90% yield. The schematic representation of this complex is

displayed below and the elemental analysis results are reported in experimental section.

Figure 2.13 Structural representation of (1,5-cyclo-octadiene)$PdCl_2$

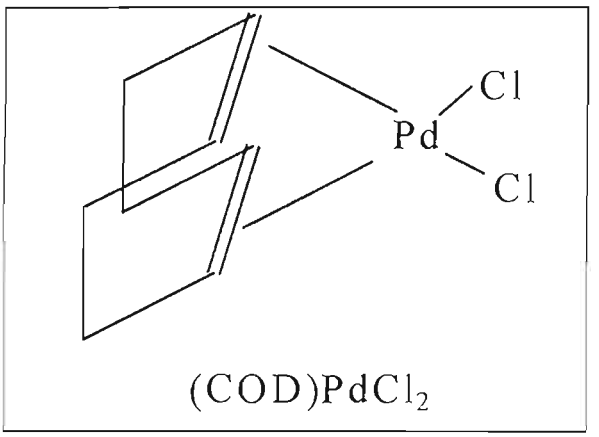

(COD)$PdCl_2$

Table 2.11 (COD)$PdCl_2$ elemental analysis

		C%	H%
(COD)$PdCl_2$	calculated	33.81	4.30
	Experimental 1.	33.92	4.44

2.2.2.2.2 (1,5-Cyclo-octa-diene)palladiummethylchloride[(COD)PdMeCl]

This compound was synthesised by Rulke *et al*[52-54] starting with (COD)$PdCl_2$ (prepared as described above) and using tetramethyltin as a methyllating agent. It was obtained by the above authors as an off-white powder stable in air but no further characterisation information was reported. The method outlined by Rudle-Chauvin and Rudler[52] was attempted but it failed. A method similar to the one reported by Calvin and Coates[53] in 1960 for synthesis of (COD)$PdMe_2$ was followed successfully.

The ^{1}H NMR spectral data obtained for (COD)PdMeCl were compared with the results reported by Rudler-Chauvin and Rudler. The data compared very well, except for the colour which was greyish instead of an off-white colour reported. The greyish colour was due to the decomposition of (COD)$PdMe_2$ which was in competition with our product. The (COD)$PdMe_2$ is only stable at temperatures below $-10^{\circ}C$ and is very air sensitive, whereas (COD)PdMeCl is stable in air and at room temperature (for a short time). The proton NMR spectrum for this complex is discussed below. The structural representation of this complex is displayed Figure 2.14.

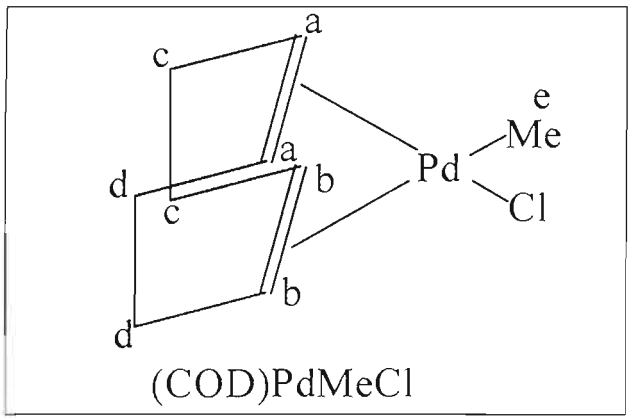

Figure 2.14 Structural representation of (1,5-cyclo-octadiene)PdMeCl

^{1}H NMR of (COD)PdMeCl

The chemical shifts corresponding to the assignations in Figure 2.14 are displayed in Table 2.11. The ^{1}H NMR spectrum of the compound is also displayed in Figure 2.15.

Table 2.11 ^{1}H NMR chemical shifts for (COD)PdMeCl

Proton	Chemical shift (ppm)
a	(5.94-5.90)(m)
b	(5.16- 5.10)(m)
c,d	(2.64-2.45) (m)
e	1.18(s)

Discussion

The chemical shifts in Table 2.11 and the corresponding designations in Figure 2.14 both refer to the ^{1}H NMR spectrum shown in Figure 2.15. The resonances in the region δ = (5.94- 5.90)ppm are associated with proton **a** , the two hydrogens attached to alkene carbons. The peaks the region δ = (5.16-5.10)ppm are associated with proton **b** , the two hydrogens attached to two carbon of the the alkene group. The multiplets in the region δ = (2.64-2.45)ppm are associated with protons **c** and **d,** the hydrogens attached to the alkyl carbons. The singlet peak at δ = 1.18ppm arises from proton **e,** the hydrogens of the methyl group attached to palladium.

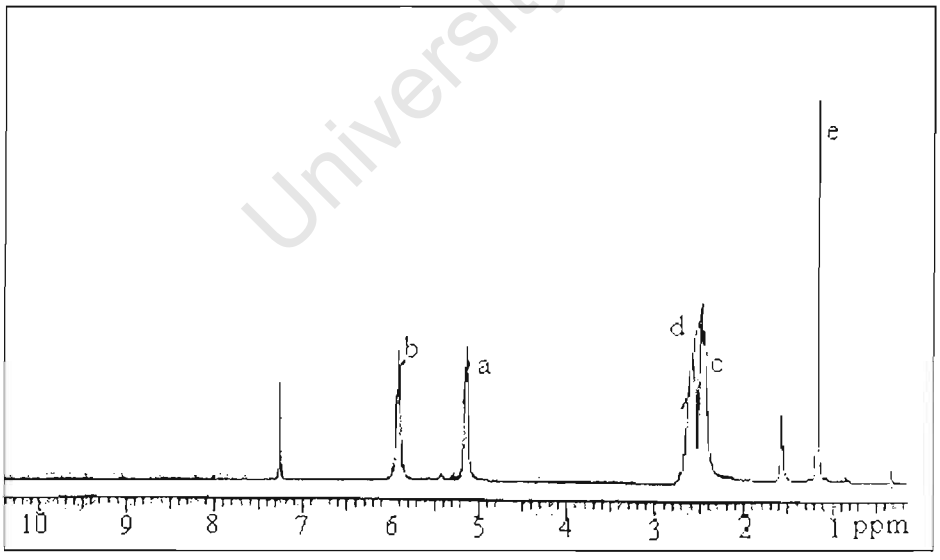

Figure 2.15 ^{1}H NMR spectrum (in $CDCl_3$)of (COD)PdMeCl

(see Figure 2.14 for atom lettering scheme)

2.2.2.2.3 Glyoxal-bis(2,6-diisopropylphenylimne)Palladiummethylchloride

[(G-(iPr)PI)PdMeCl]

This (G-(iPr)PI)PdMeCl complex was obtained as a pale orange-brown powder, which was found to be very stable in air and at room temperature with a decomposition temperature at 230°C. The dimethyl substituted palladium complex (G-MPI)PdMeCl was obtained as a pale orange-brown powder with decomposition temperature of 210°C also stable in air. The free ligand of these complexes is a symmetric molecule. The co-ordination of palladium methylchloride to the ligand created a non-equivalent environment for which resulted to changes in the proton NMR chemical shifts compared to the proton NMR spectrum of the free ligand. The ^{1}H NMR spectra of these complexes will be displayed but only one will be discussed. The structural representation of this complex is displayed in Figure 2.16 below.

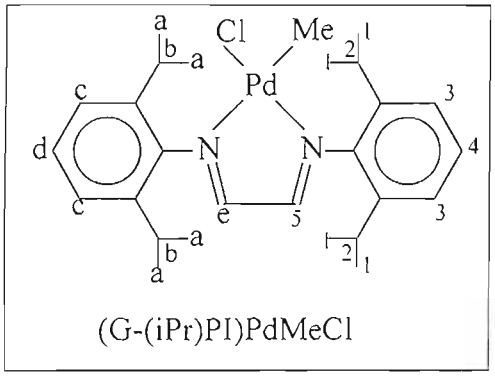

(G-(iPr)PI)PdMeCl

Figure 2.16 Structural representation of (G-(i-Pr)PI)PdMeCl

^{1}H NMR of (G-(iPr)PI)PdMeCl and (G-MPI)PdMeCl

The chemical shifts corresponding to the designations in Figure 2.16 above are given in Table 2.12. The ^{1}H NMR spectra for these complexes are displayed in Figure 2.17.

Table 2.12 ^{1}H NMR chemical shifts

Proton	Chemical shifts(ppm) for (G-(iPr)PI)PdMeCl
a,1	(1.16-1.19)(d)J = 6.00Hz, (1.34-1.37)(d)J = 6.75Hz
b,2	(3.17-3.33),(3.46-3.49)(sept)
c,d,3,4	(7.20-7.45)(m)
e,5	(8.09-8.29)(s)
f	0.85(s)

Discussion

The designations in Figure 2.16 below and the corresponding chemical shift in Table 2.12 both refer to the proton NMR spectrum in Figure 2.17(a) below. The resonance peaks in the region δ = (1.16-1.19)ppm and δ = (1.34-1.37)ppm arise from protons **a,1** both of methyls of the isopropyl group but in a slightly different environment because of the influence of palladiummethylchloride group. The septet peaks in the region δ = (3.17-3.33)ppm and δ = (3.46-3.49)ppm are associated with proton **b, 2** both of the tertiary carbon of the isopropyl group but experiencing the influence of palladiummethylchloride group. The multiplet peaks at δ = (7.20-7.45)ppm are associated with proton **c,d,3** and **4** of the aryl ring. The singlet peaks at δ = 8.09ppm and δ = 8.29ppm both arise from proton **5** and **e** attached to the of C=N but experiencing the influence of palladium methylchloride. The singlet peak at δ = 0.85ppm arise from proton **f** of the methyl of palladium methylchloride group. The results correspond very well with literature results[32]. A similar ^{1}H NMR spectrum was obtained for (G-MPI)PdMeCl except for absence of isopropyl substituents. The spectrum of (G-

MPI)PdMeCl show peaks at δ = 22.29ppm and δ =2.24ppm that are due to the presence of methyl protons on the aryl rings (see Figure 2.17(b)).

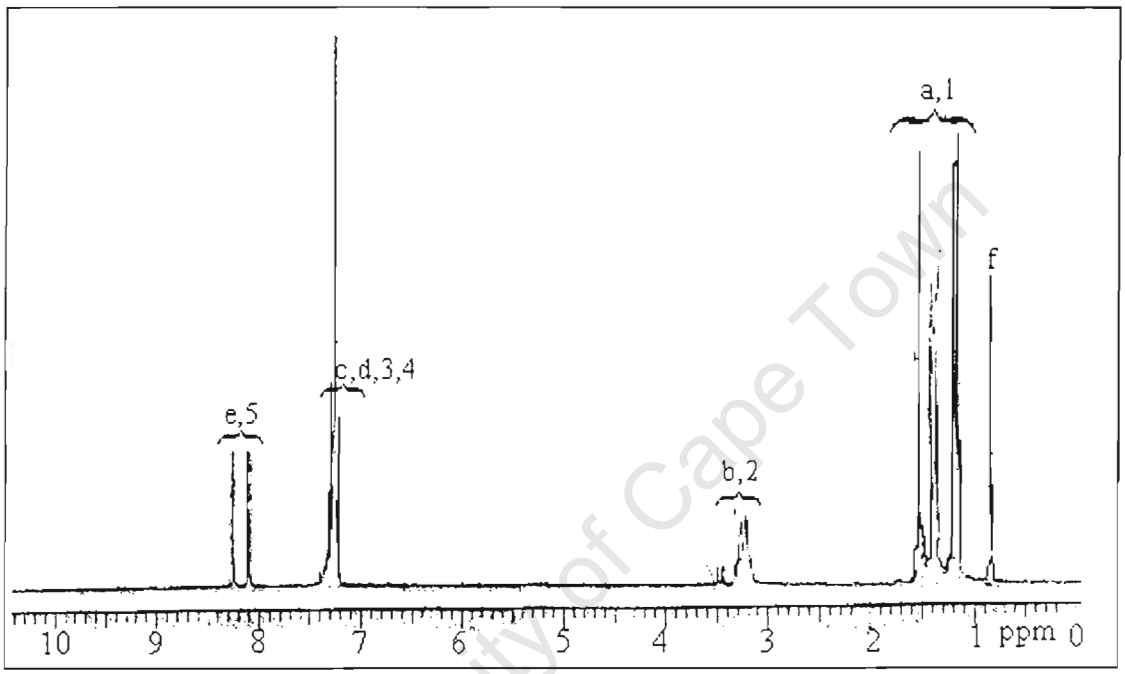

Figure 2.17(a) ^{1}H NMR spectrum (in $CDCl_3$) of (G-(i-Pr)PI)PdMeCl (see Figure 2.16 for atom lettering scheme)

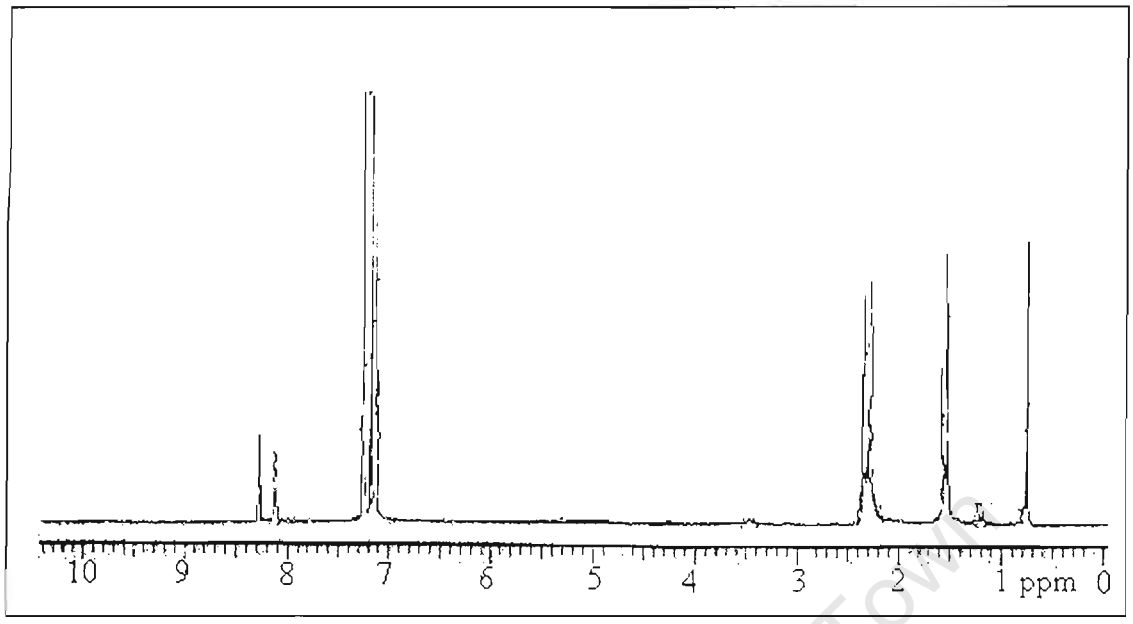

Figure 2.17(b) ^{1}H NMR spectrum (in $CDCl_3$) of (G-MPI)PdMeCl

2.2.2.2.4 Diacetyl-bis(2,6-diisopropylphenylimne)palladiummethylchloride [(D-(i-Pr)PI)PdMeCl]

The (D-(iPr)PI)PdMeCl complex was obtained as a yellow brown powder, stable in air and at room temperature with decomposition temperature of 245°C. The dimethyl substituted palladium complex (D-MPI)PdMeCl was obtained as greenish brown powder with a decomposition temperature of 248°C. Similar to glyoxal derivatives, the free ligands of these complexes are symmetric molecules but co-ordination of palladium methylchloride to the ligand created a non-equivalent environment for which resulted to

changes in the proton NMR chemical shifts compared to the proton NMR spectrum of the free ligand. The structural representation of (D-(iPr)PI)PdMeCl complex is displayed in Figure 2.18 below.

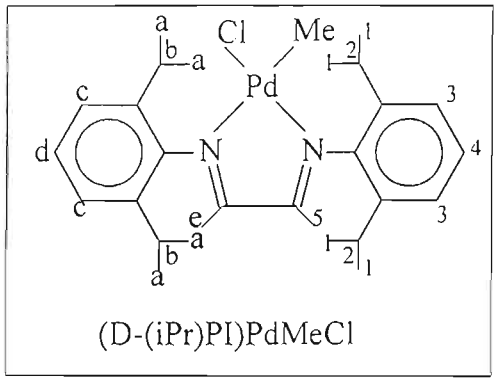

(D-(iPr)PI)PdMeCl

Figure 2.18 Structure of (D-(i-Pr)PI)PdMeCl

^{1}H NMR of (D-(iPr)PI)PdMeCl and (D-MPI)PdMeCl

The chemical shifts corresponding to the designations in Figure 2.18 are displayed in Table 2.13 below. The ^{1}H NMR spectrum is displayed in Figure 2.19.

Table 2.13 ^{1}H NMR chemical shifts

proton	Chemical shifts (ppm) for (D-(i-Pr)PI)PdMeCl
1,a	(1.15-1.19)(d) J = 6.50Hz, (1.33-1.37)(d) J = 6.70Hz
2,b	2.98-3.15(sept)

4,3,c,d	7.24-7.28(m)
5,e	2.05-2.02(s)
f	0.52(s)

Discussion

The chemical shifts in Table 2.13 and the corresponding designations in Figure 3.8 both refer to the ^{1}H NMR spectrum in Figure 3.9(a) below. The doublet peaks in the regions δ = (1.15-1.19)ppm and δ =(1.33-1.37)ppm are associated with proton **a, 1** both from the methyls of the isopropyl groups but experiencing the influence of palladiummethylchloride. The septet peak in the region δ =(2.97-3.15)ppm is associated with proton **b, 2** of the tertiary carbon of the isopropyl group. The multiplets at δ = (7.24-7.28)ppm arise from proton **c,d,3** and **4** of the aryl ring. The singlet peaks in the regions δ =(2.05-2.02)ppm is associated with proton **e** and **5** both from the methyl group attached to the carbon of C=N group. The singlet peak at δ = 0.52ppm arises from proton **f** of the methyl group attached to palladium of palladium methylchloride. The (D-MPI)PdMeCl ^{1}H NMR spectrum is very to that of (D-(iPr)PI)PdMeCl except for the absence of the septet peaks at δ = 2.98-

3.15ppm that were associated with the isopropyl group. In the of these isopropyl protons the (D-MPI)PdMeCl spectrum showed peaks at δ =1.54ppm and δ = 2.29ppm that are attributed to the methyl groups on the aryl rings of (D-MPI)PdMeCl.

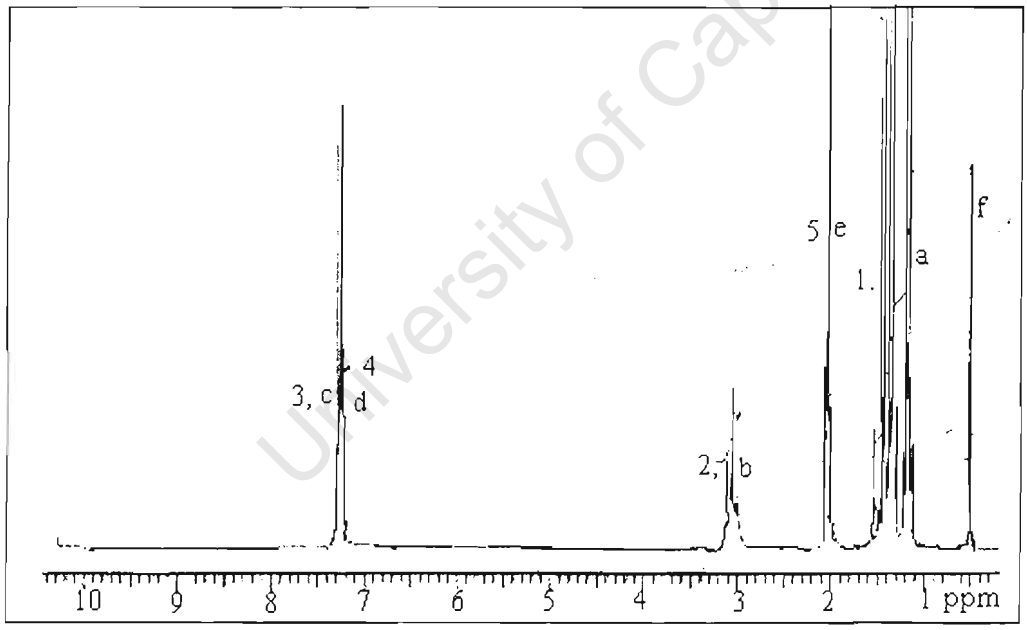

Figure 2.19(a) ^{1}H NMR spectrum (in $CDCl_3$) of (D-(i-Pr)PI)PdMeCl (see Figure 2.18 for atom lettering scheme)

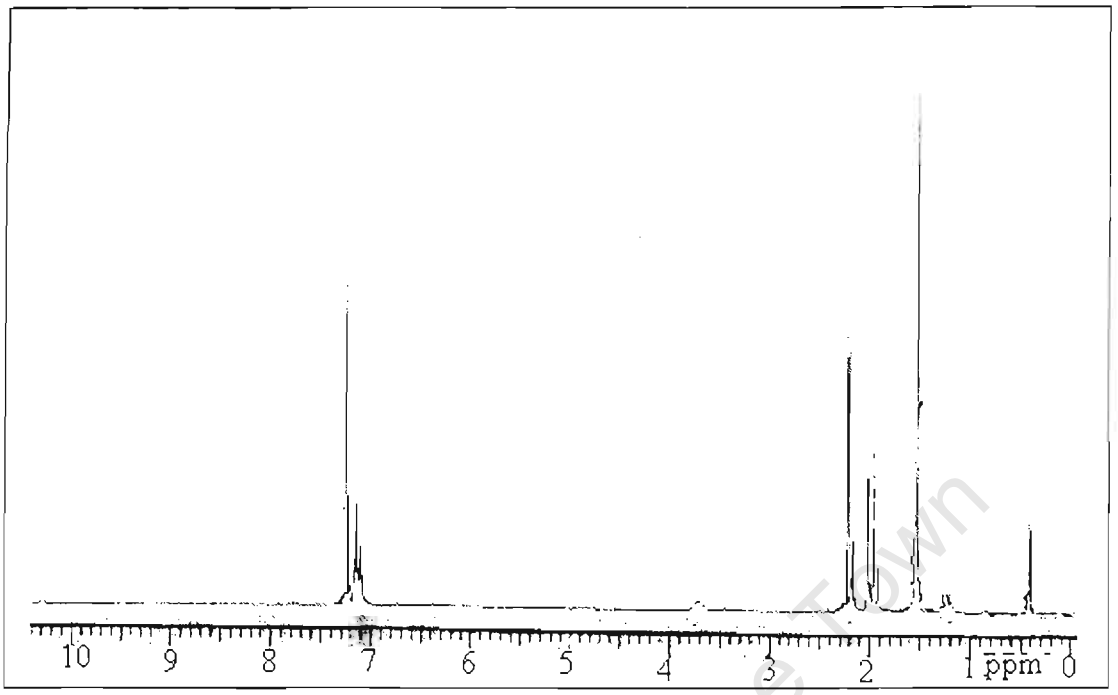

Figure 2.19(b) ^{1}H NMR spectrum (in $CDCl_3$) of (D-MPI)PdMeCl

Conclusions

All diimine ligands were prepared and stored at room temperature and they are very in stable in air. The diisopropyl substituted diimine ligands were obtained in good yields compared that is attributed to impurities to the starting material. All the yields are reported in the experimental chapter. Palladium complexes bearing diimine ligands showed better stabilities in air and at room temperature than nickel complexes. Both nickel and palladium complexes bearing diimine ligands gave good yields even better than the yields reported in the literature. The preparation of palladium complexes bearing dimethyl substituted diimine ligands was not reported in literature,

so they were prepared similarly to the methods used to prepared palladium complexes bearing diisopropyl substituted diimine ligands. Their preparation produced good yileds and also gave convincing ^{1}H NMR results and a colour similar to the diisopropyl substituted palladium complexes. In the next chapter all complexes including these palladium complexes bearing dimethyl substituted diimine ligands will be tested(used as catalysts) in homopolymerisation reactions of ethylene and 1-hexene. All the polymerisation results will be discussed in the next chapter.

Chapter Three

Polymerization of ethylene and 1-hexene by Ni(II) and Pd(II) based catalysts

Chapter 3: Polymerization of ethylene and 1-hexene by Ni(II) and Pd(II) based catalysts

Contents

3.1. Introduction

3.1.1. Polymerization of α-olefins by metallocenes

Olefin polymerization by metallocene catalysts is a co-ordination polymerization. Co-ordination polymerization is a chain addition reaction that usually involves a propagation step in which an olefin monomer is held in a co-ordinated way on the active site of the metallocene catalyst. The catalytic activity of the metallocene catalysts can only be exploited when a Lewis base cocatalyst such as methylalumoxane(MAO) or a borate compound such as $B(C_6F_5)^-_4$ is used[55,56].

There are two main classes of activated metallocene catalyst :

(i). a bicomponent catalyst system consisting of a metallocene and methylalumoxane(cocatalyst) , e.g. bicyclopentadienyl zirconium dichloride (Cp_2ZrCl_2/MAO)[57].

(ii). and a single component catalyst system such as { $[Cp_2MR]^+B(C_6F_5)_4$}[58]

.

In this chapter, we will be investigating catalytic polymerisation using Pd(II) and Ni(II) based catalysts bearing diimine ligands and methylalumoxane (MAO) as cocatalyst.

3.1.2. Mechanisms in olefin polymerization

There are four general mechanisms that have been proposed for the insertion the olefin monomer into a catalyst[59-63]:

(i) The first mechanism proposed by Rooney *et al*[64], involves the oxidative 1,2-hydrogen shift from the α-carbon of the polymer chain to generate a metal-alkylidene hydride complex. This species then reacts with an olefin to generate a metallacyclobutane, and reductive elimination completes the propagation sequence.

(ii) The second mechanism involves the transfer of the long alkyl chain to the coordinated olefin(monomer). This results in the formation of a new transition metal carbon bond. This mechanism is known as Cossee-Arlman mechanism[65-67](Scheme 1).

(iii) The third mechanism proposed by Green *et al*[68] involves a hydrogen on the α-carbon of the growing chain interacts with the metal center during the catalytic cycle. This three-centered system is termed an

agostic interaction when the hydrogen is simultaneously bonded to both a carbon and a metal atom.

(iv) The last mechanism involves the olefin insertion, in which an α-hydrogen interacts with the metal center only during the transition state of the C-C bond forming step.

Scheme 1. Cossee mechanism for Ziegler-Natta polymerization

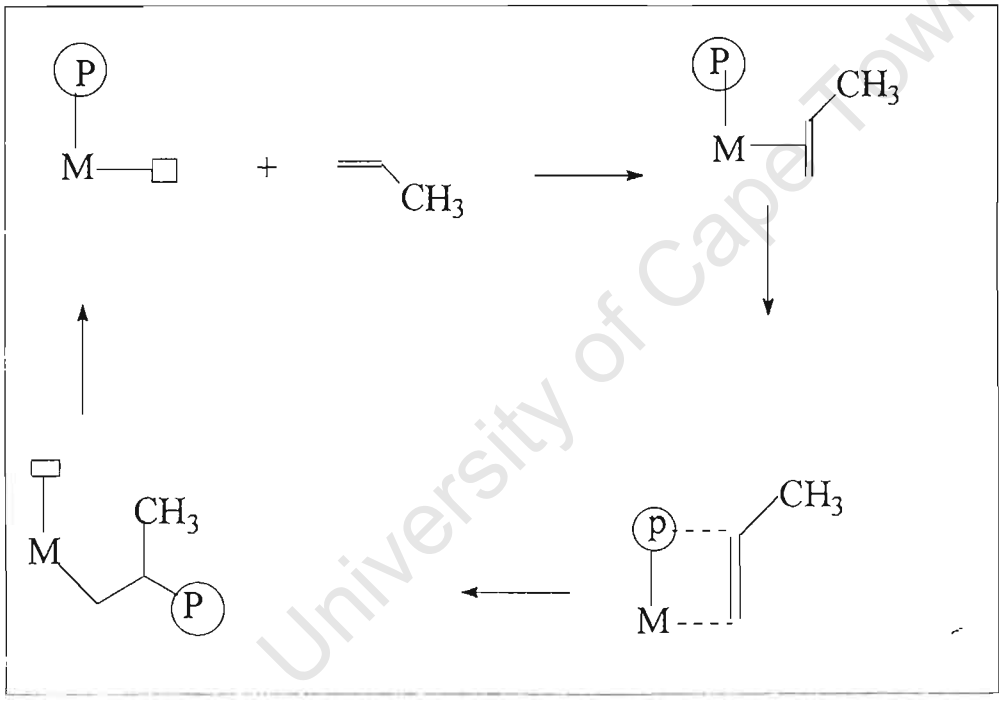

The mechanisms above indicate that at some point in the catalytic cycle, the metal atom will be coordinated to a π-ligand and the alkyl group of the growing chain. During polymerization, the monomer will coordinate with the metal center of the cationic complex followed by insertion of a monomer in the metal-carbon bond to extend the polymer chain. The migration of

polymer chain and the formation of the metal-carbon bond occur simultaneously, through a four centered transition state. This result in the creation of a vacant coordination site, at site originally occupied by the polymer chain. This process continues until the polymer chain is terminated.

Furthermore, in metallocene catalyzed olefin polymerization, the termination of the propagating polymer chain occurs through a chain transfer involving both β-H elimination[69-71] and β-CH_3 elimination[72,73]. The termination of the polymer chain propagation may also occur due to the chain transfer to aluminium, or the monomer[74,75].

In our of polymerization process, the chain termination is proposed to occur by β-H elimination chain transfer, but this type of chain transfer is hindered by the presence of bulky groups in metallocene catalysts which leads to slower rate of chain transfer than chain propagation[32].

3.1.3. MAO and its role in olefin polymerization

Methylalumoxane, normally called MAO, is a poorly characterized, glassy polymeric substance, usually of molecular weight 900-1200 and composition of $\{MeAlO\}_n$ and consists of linear cyclic and crosslinked compounds[76.77].

This compound is readily dissolved in hydrocarbon solvents such as toluene, in which, due to the facile ligand exchange in aluminium complexes it establishes a solution equilibria.

This MAO and other alumoxane compounds are synthesized by controlled reaction of trimethylaluminium with water molecules contained in the hydrated salts such as $CuSO_4.5H_2O$ and $Al(SO_4)_3.6H_2O$[78,79]. The role played by this compound in the polymerization can be describe as follows:

(i). In the metallocene dihalide system, the function of MAO is to complex and alkylate the metallocene halide complex, replacing one halide atom with an alkyl group removing the second halide creating a co-ordinatively unsaturated cationic complex. This gives rise to the catalytically active species and propagation ensues.

(ii). MAO helps to maintain the catalyst complex in a cationic state by acting as a non-co-ordinating anion.

(iii). MAO can also help to scavenge impurities that may poison the catalyst.

The main role of these MAO cocatalysts, in summary, is generally thought to be facilitated by the formation of electron-deficient /coordinatively unsaturated cationic metallocene species (see eq 1) which are the actual catalysts[80].

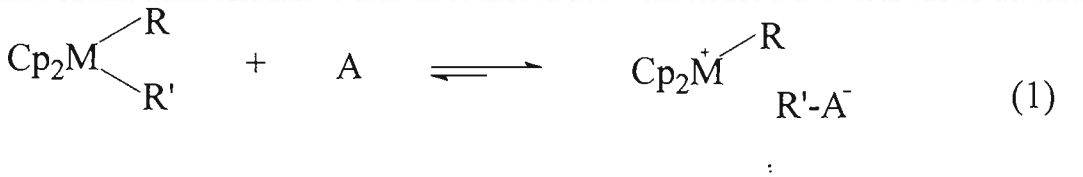

(1)

M = Pd,Ni,Zr,Ti, or Hf

A = cocatalyst

R' = alkyl or halide

Cp = cyclopentadienyl-type ligand

R = alkyl

3.1.3. Characterization methods

This section briefly describes the main methods used in characterization of the polymers formed in this study.

Differential Scanning Calorimetry(DSC)

Melting point determinations on the polymers were obtained from a Perkin-elmer Differential Scanning Calorimetry(DSC) interfaced to a PC7 Series Thermal analysis system. The DSC traces were recorded at a scan rate of 10°C/min. This machine collects energy flow rate data as a function of temperature and time. The energy response of the DSC was calibrated using the enthalpy of fusion of indium and the temperature measurement was calibrated using the melting point of ultra-pure metals (indium, tin or lead).

The sample was place in an aluminum pan and an empty pan was used a reference.

Thermogravimetric analysis (TGA) and Differential thermal analysis (DTA)

The study of the degradation of linear macromolecules is of major interest since in many cases it determines the upper temperature limit of use of a polymeric material. Thermogravimetric analysis (TGA) is a system whereby the thermal stability of a polymeric material is measured. In this process the weight loss of the polymer is measured as a function of temperature. TGA can be used with DTA in order to understand if the polymer melts before degradation or the melting of a polymer is accompanied by degradation[81-85].

The TGA trace and DTA trace of our polymers were recorded on a STA409C DTA/TG machine at a heating rate of 20°C/min under an argon purge. For TGA measurement the sample was placed in an aluminium pan and an empty pan was used as a reference.

^{1}H, ^{13}C, and ^{13}C APT NMR spectroscopy

The NMR spectra were recorded on a Varian XR200 or 400 Unity spectrometer using tetramethylsilane as an internal standard.

The ^{13}C APT NMR spectroscopy is a J-modulated spin echo method that can be used as an aid to signal assignment, as it enables one to quickly determine from a single experiment whether the number of hydrogen atoms attached to each carbon is odd (1or 3) or even (0 or 2).

3.2. Results and discussion

All nickel complexes were activated by MAO before they were used as catalysts in the homopolymerization of 1-hexene and ethylene. The homopolymers produced were subjected to ^{1}H , ^{13}C and ^{13}C APT NMR spectroscopy studies to determine structural information and DTA/TG and DSC studies were used to investigate the thermal stability and melting points of the polymers. Interestingly, both homopolymers of ethylene and 1-hexene exhibited very similar ^{1}H ,^{13}C and ^{13}C APT NMR results. The similarity of the NMR spectral results might be an indication of the same pattern of branching in these homopolymers. The DSC and DTA/TG results showed different behaviour for each polymer made. This can be ascribed to a

difference in the degree of branching, chain length and chain packing. The characterization results of these polymers is discussed below.

The synthesis and characterization of these polymers were reported in the literature.

3.2.1. Poly(1-hexene)(PH) polymers

A schematic representation of a general structure of 1-hexene unit of a poly(1-hexene) polymer is displayed in Figure 3.1 below with assigments **1,2,3,4,5** and **6** for the protons and carbon atoms.

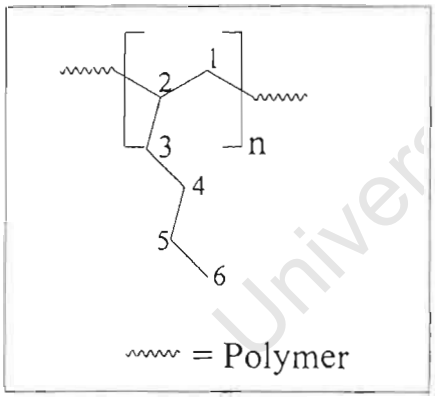

Figure 3.1 A general structure of 1-hexene unit in poly(1-hexene)

3.2.1.1. Poly(1-hexene) polymers by nickel catalysts

The polymer PH1 obtained from the polymerisation catalyzed by (D-(iPr)PI)$NiBr_2$ /MAO from a 10ml of 1-hexene monomer was a colourless

plastic like polymer produced in the yield of 1.70g . This polymer showed a melting point of 65-69°C when observed under a hotstage microscope. Similar to the polymer PH2, produced from the reaction catalyzed by (G-(iPr)PI)$NiBr_2$, showed a melting of 68-79°C. Polymer PH2 was produced as an amorphous colourless material with in a yield of 3,70g. Both polymers exhibited similar ^{1}H, ^{13}C and ^{13}C APT NMR results as expected. Polymer PH1 results will be discussed. The TGA results will be displayed for both polymers.

3.2.1.1.1 ^{1}H NMR of nickel catalysed poly(1-hexene) polymers

The chemical shifts corresponding to the assignments in the general structure of poly(1-hexene)(Figure 3.1) are displayed in Table 3.1 below and the ^{1}H NMR spectrum is shown is Figure 3.2 below.

Table 3.1 The ^{1}H NMR chemical shifts for PH1 measured in $CDCl_3$

Proton	Chemical shifts(ppm)
6	0.82-0.91
5,4,3,1	1.22-1.25
2	1.55

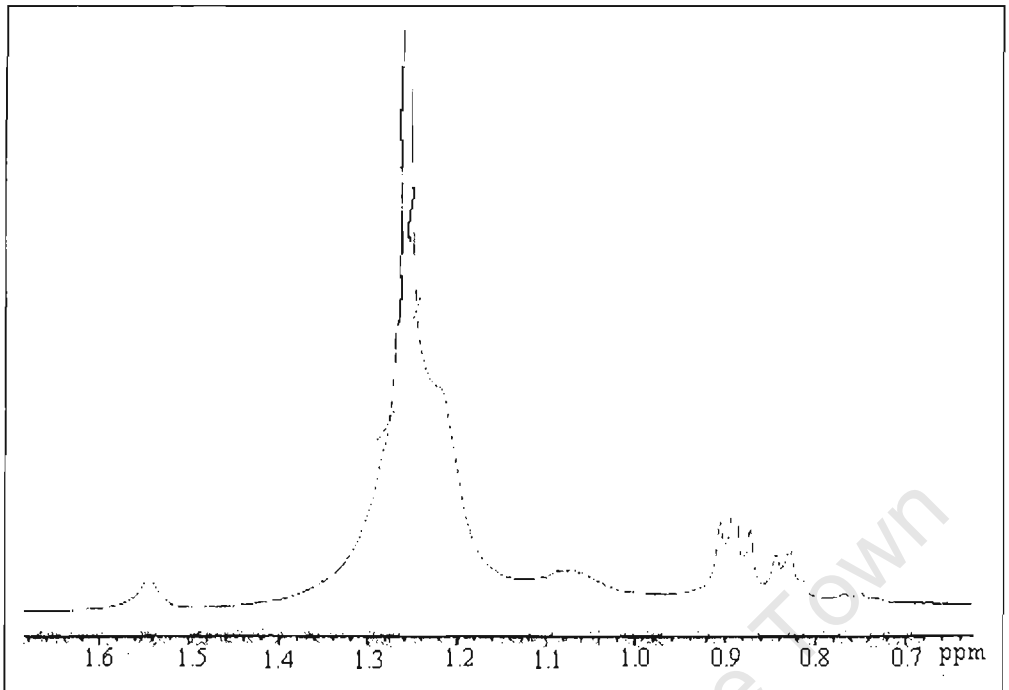

Figure 3.2 ^{1}H NMR spectrum for PH1 (in $CDCl_3$) at room temperature

Discussion

The ^{1}H NMR spectrum of PH1 (Figure 3.2) was recorded at room temperature in $CDCl_3$ as a solvent. The spectrum shows a small broad peak at δ = 1.55ppm which is associated with the methine proton **2**. The broad peak at δ = (1.22-1.25)ppm arises from the methylene protons(**3,4,5 and 1**) which are α, β and γ to the methyl group of the chain branch and the in-chain methylene protons.

^{13}C NMR spectra of poly(1-hexene) polymers from nickel catalysed reactions

To determine the structure of the PH1 polymer ^{13}C NMR and ^{13}C APT NMR spectra were recorded. The results are displayed in Figure 3.3(a) and (b). The peaks at δ = (23.13-30.13)ppm are associated with methylene carbons ($\underline{C}H_2$) of butyl or longer chain branches such as octyl branches. The peaks at δ = 33.67ppm are associated with in-chain methylene carbons(carbon **1,** α to the tertiary carbon **2** (see Figure 3.1)) . The peak at δ = 37.08ppm is associated with methine carbon atoms, i.e the tertiary carbon at the branching point of the chains(carbon **2** in the general structure). The peaks at 14.11ppm and 19.65ppm are attributed to methyl carbon atoms at main chain end or methyl carbon atoms at the end of long chain branches such as octyl branchs. The peaks at 32.48ppm and 34.69ppm are associated with methyl carbon atoms of short branches such as ethyl branches. These methyl carbons were further confirmed by ^{13}C APT NMR spectrum shown in Figure 3.3(b) where the methyl carbon atoms are pointing down (-) while other carbons pointing in the normal direction (+). The same type of NMR response was obtained for other polymer as expected because they are also poly(1-hexene)s and they should have at least same pattern of micro-

structural make up in terms of chain branching but the degree of branching should differ resulting to different properties.

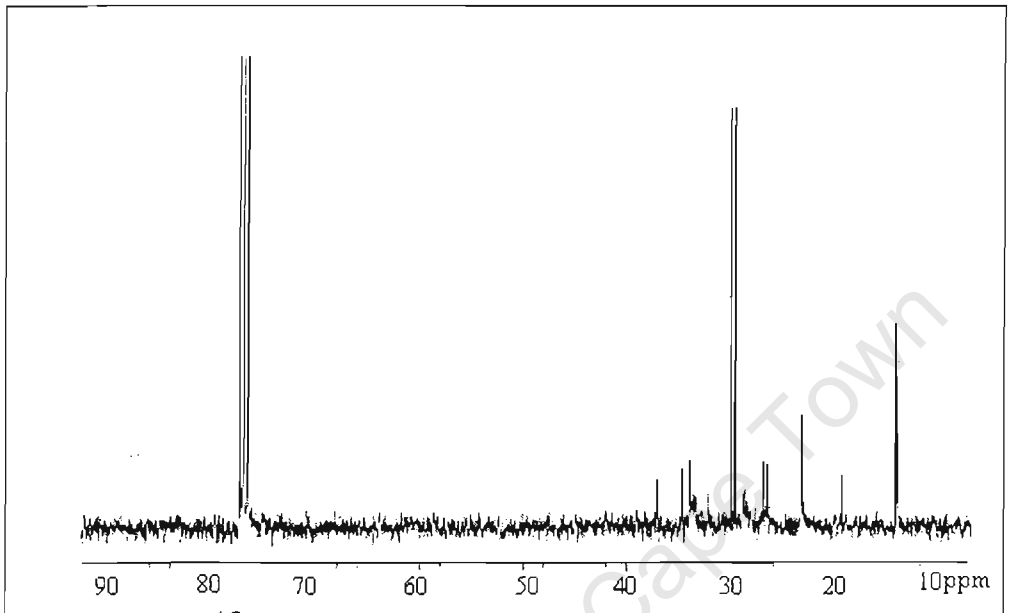

Figure 3.3(a) ^{13}C NMR spectrum for PH1(in $CDCl_3$) at room temperature

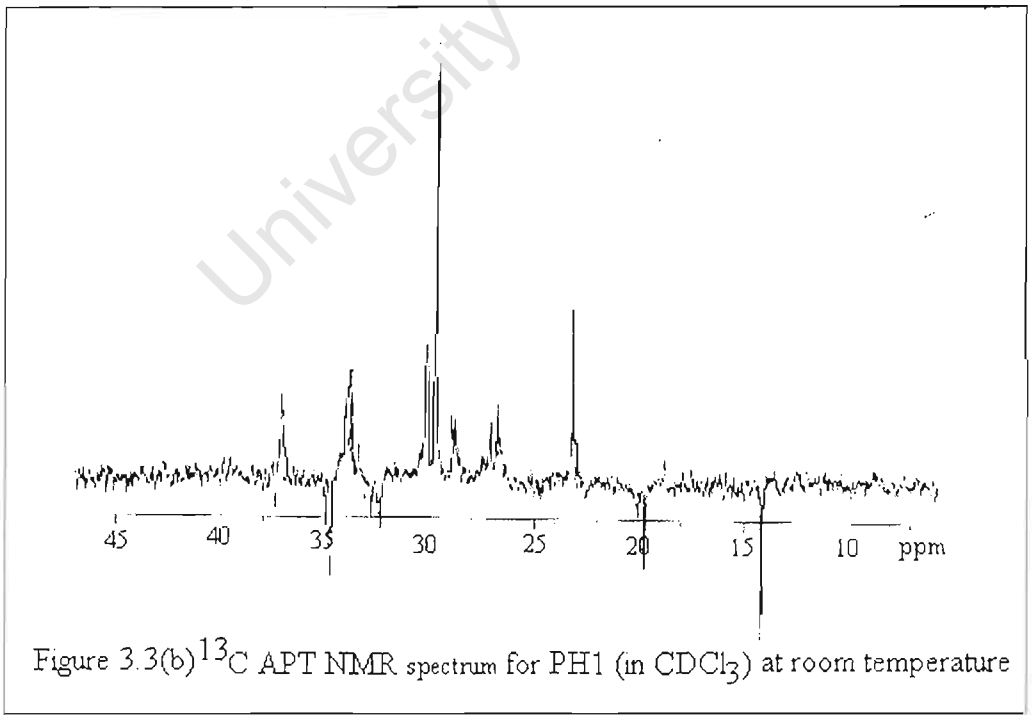

Figure 3.3(b) ^{13}C APT NMR spectrum for PH1 (in $CDCl_3$) at room temperature

3.2.1.1.2 Thermal behaviour of poly(1-hexene) polymers from nickel catalysed reactions

These polymers showed very low melting points and poor thermal stabilities as already mentioned above. The TGA trace shows that, the polymers started to lose mass at a temperature and the mass loss continued until the total decomposition (see Figure 3.4 and 3.5).

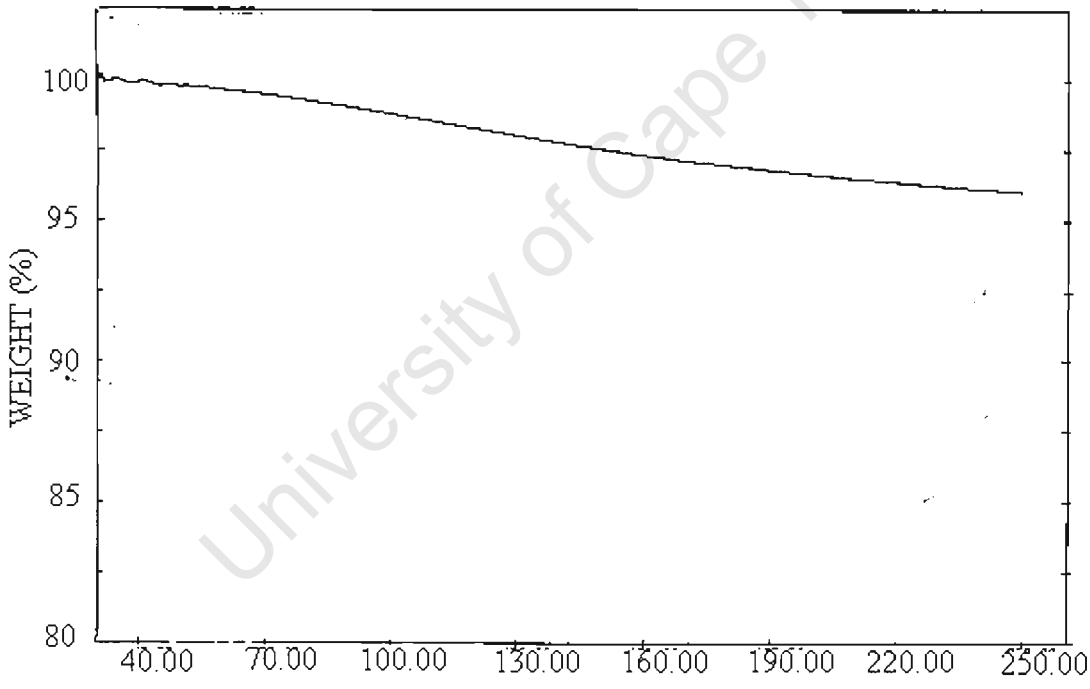

Figure 3.4 TGA for PH1

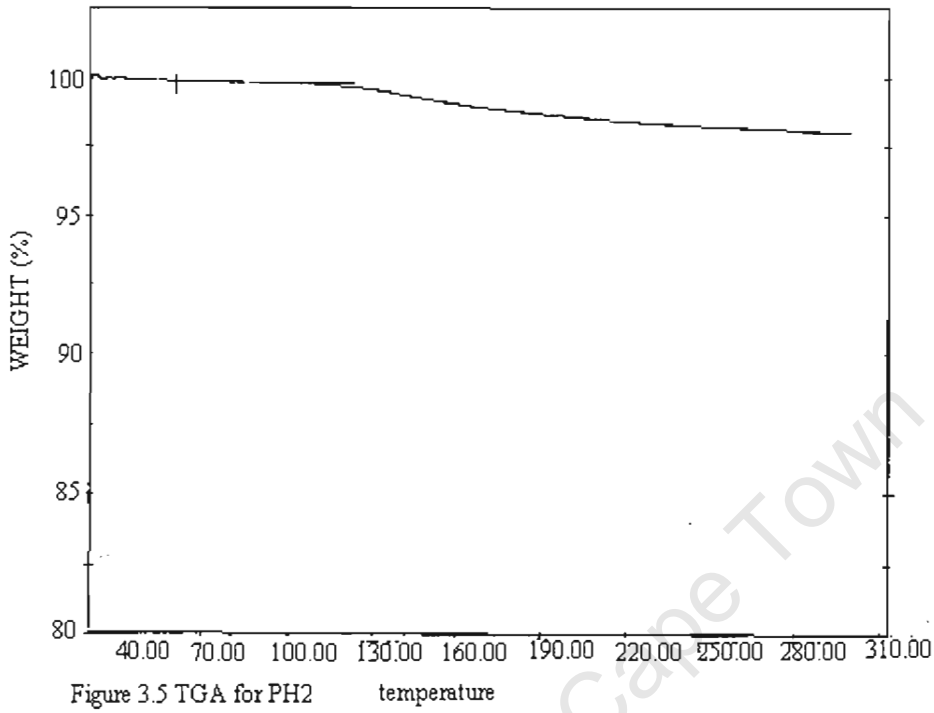

Figure 3.5 TGA for PH2

3.2.1.2. Poly(1-hexene) polymers obtained using palladium catalysts

The poly(1-hexene) polymers PH3 and PH4 were obtained from the reaction catalysed by (G-(iPr)PI)PdMeCl and (D-(iPr)PI)PdMeCl respectively. Both polymers were obtained as greyish powders (0.24g of PH3 and 0.13g of PH4). The poly(1-hexene) polymer PH4 was the only that showed a melting point of 98°C from (DSC measurement). Thermal analysis results will be discussed below. The NMR spectra of these polymer were very similar to the NMR spectra of 1-hexene polymers obtained from nickel catalysts as

expected. The only difference that will be expected for all polymers is the degree of branching and the molecular weights that will be reflected by thermal stabilities of each polymer.

3.2.1.2.1 The NMR spectral data: for palladium catalysed poly(1-hexene) polymers

The ^{1}H NMR spectrum of PH3 shown in Figure 3.6, was recorded at room temperature in deuterated chloroform. The small(low intensity) singlet peak at δ = 1.54ppm is associated with methine protons(C<u>H</u>). The peak at δ = 1.25ppm arise from the in chain methylene protons(C<u>H</u>$_2$) and also methylene protons at the chain branches included. The small broad peak at δ = (1.06 – 1.09)ppm are associated with methyl protons at methyl or ethyl chain branches. The peaks at δ = (0.82-0.87)ppm arise from the methyl protons at the butyl branches or main chain ends. The spectrum is exactly the same as those of poly(1-hexene)s from nickel catalysed reactions above and also for ^{13}C NMR and ^{13}C APT NMR the same results as those polymers were obtained (see Figure 3.7(a) and (b) below).

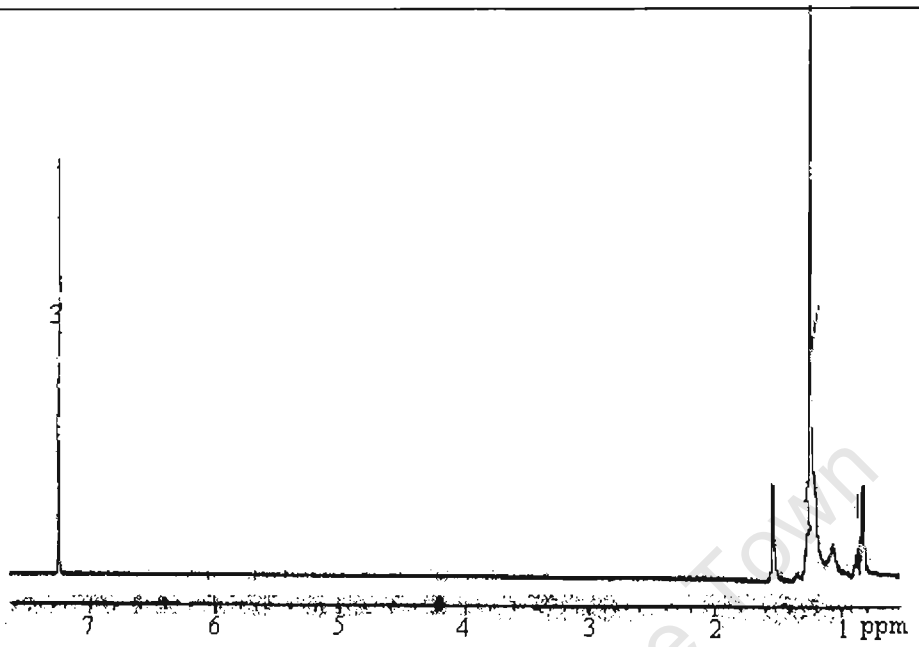

Figure 3.6 ^{1}H NMR spectrum for PH3 (in $CDCl_3$) at room temperature

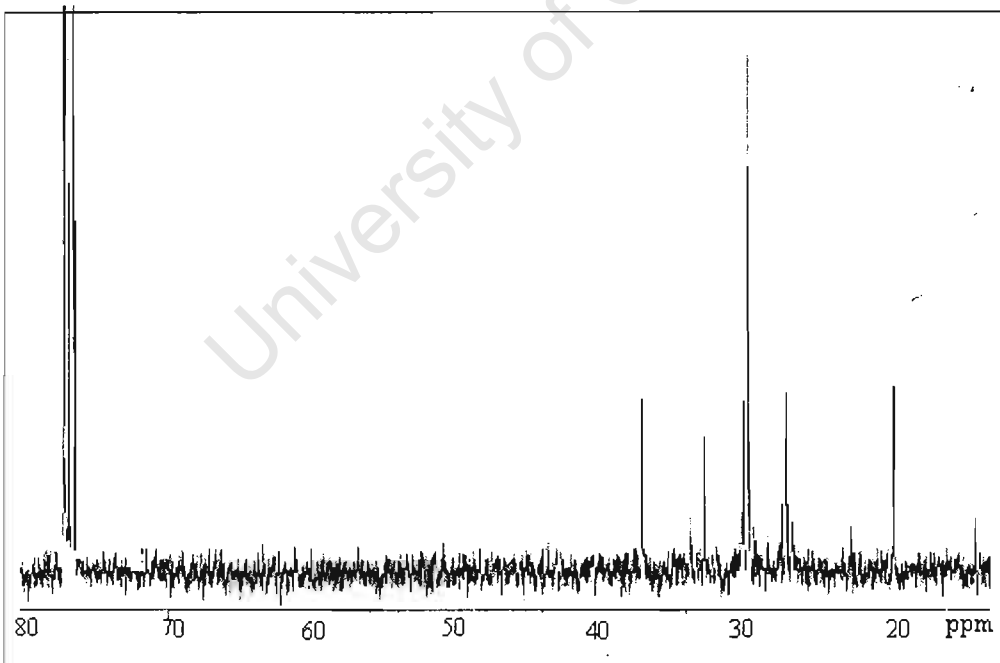

Figure 3.7(a) ^{13}C NMR spectrum for PH3(in $CDCl_3$) at room temperature

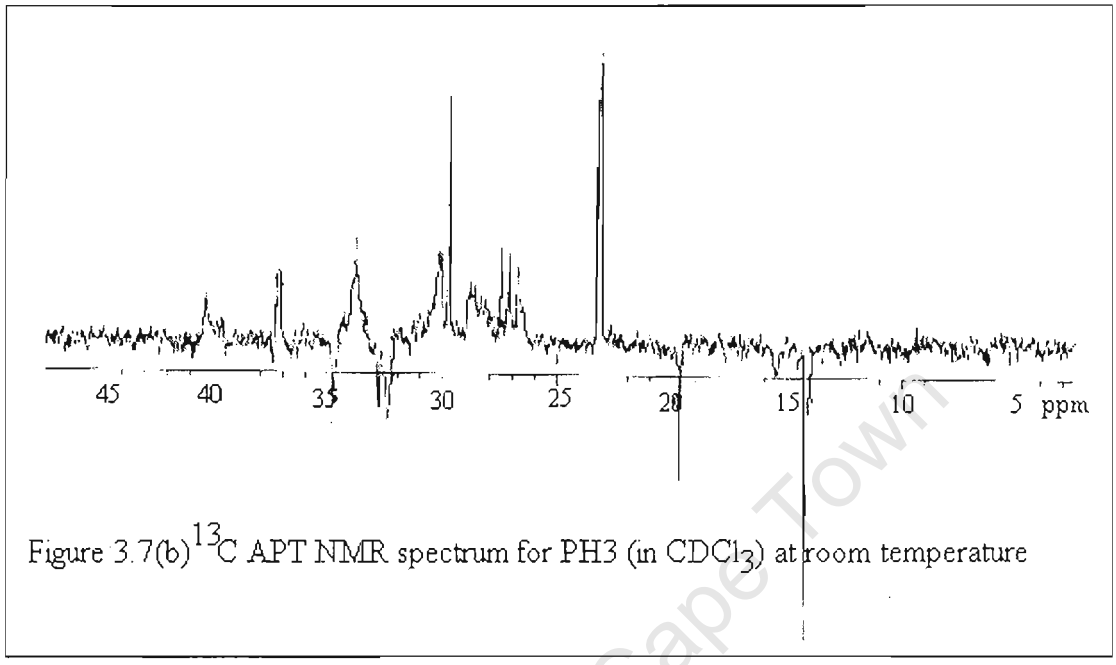

Figure 3.7(b) ^{13}C APT NMR spectrum for PH3 (in $CDCl_3$) at room temperature

3.2.1.2.2 Thermal behaviour of the palladium catalysed pol(1-hexene) polymers

These polymers showed poor thermal stabilities when compared to the polymer obtained from the nickel catalysed reactions. For both polymers from the nickel catalysed reactions DSC information could not be recorded . The polymer PH4 from palladium catalysed reactions was the only poly(1-hexene) polymer that showed a melting point of 98 °C. However, the polymer exhibited early weight loss, starting before the melting point as

shown Figure 3.8(b). The polymer PH3 could not give DSC results and the TGA in Figure 3.9 showed very early decomposition. The DSC and TGA thermograms are displayed below in Figures 3.8(a) and (b) and Figure 3.9 below:

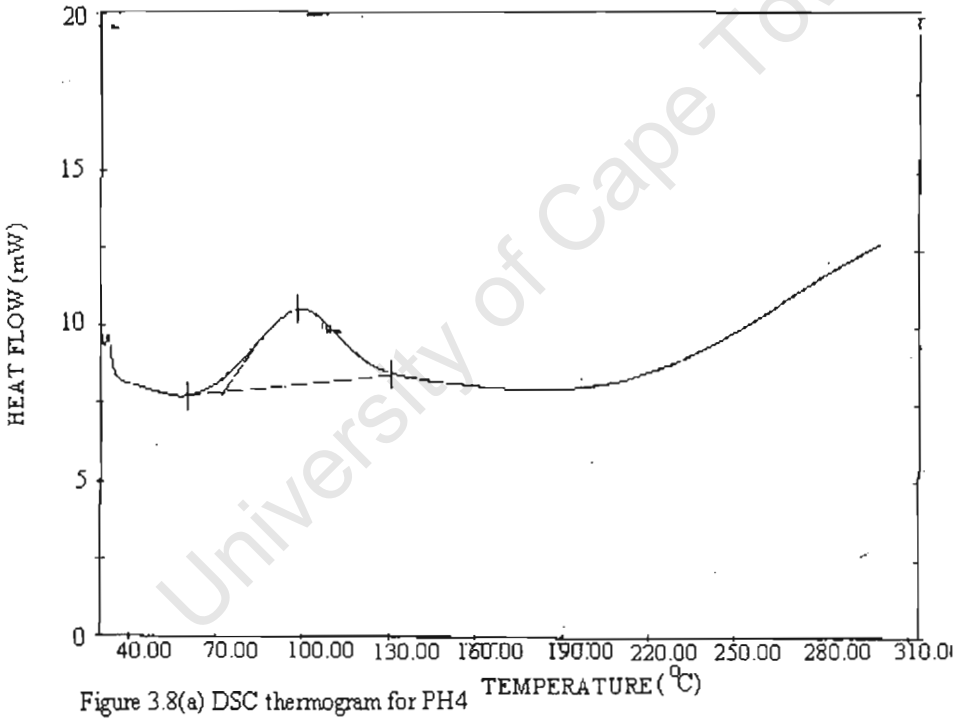

Figure 3.8(a) DSC thermogram for PH4

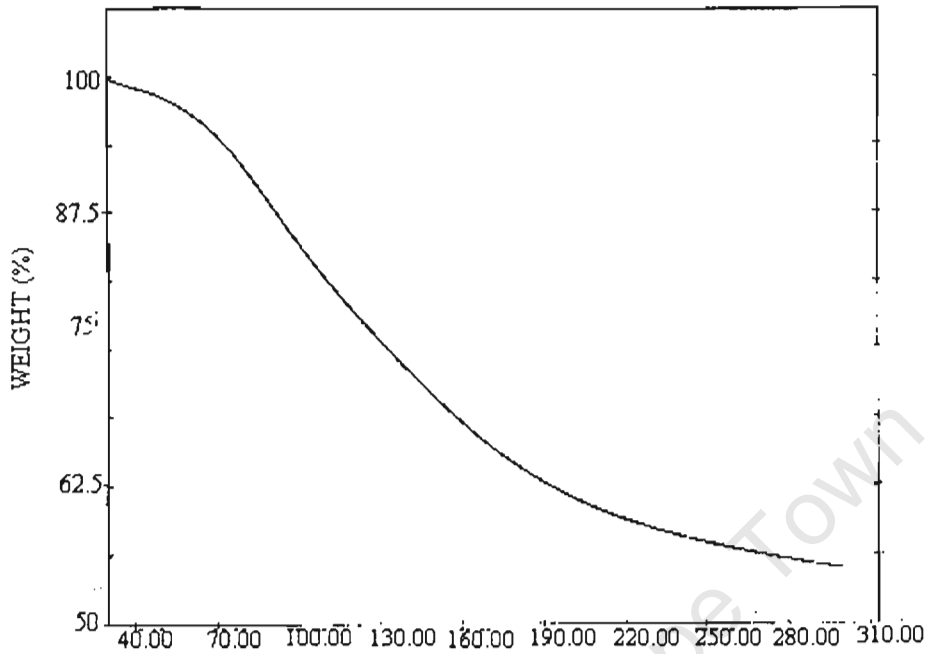

Figure 3.8(b) TGA for PH4

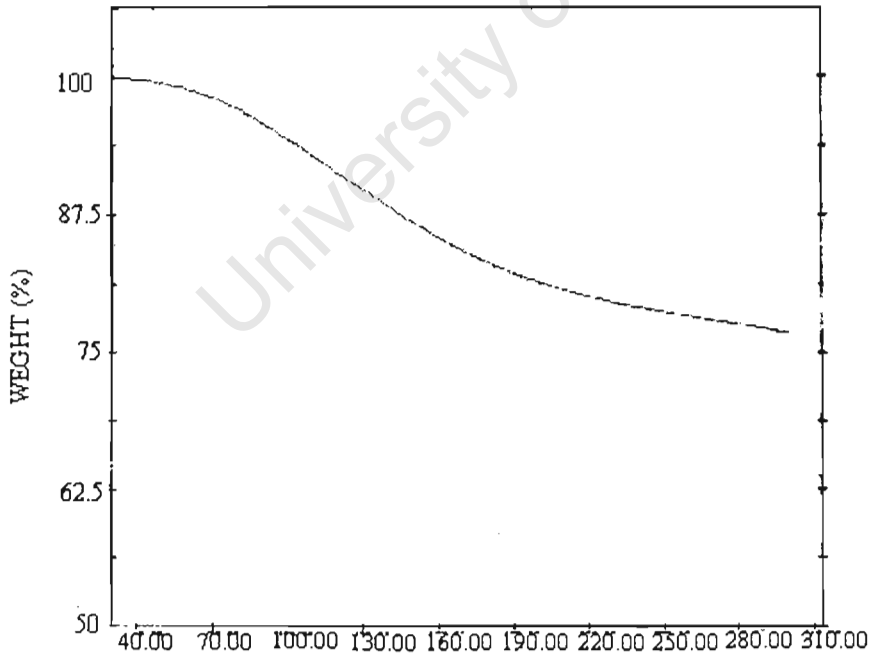

Figure 3.9 TGA for PH3

3.2.2. Poly(ethylene) polymers

A schematic representation of a general structure of poly(ethylene) homopolymers with assignment **1** for proton and carbon atoms is displayed in Figure 3.10 below:

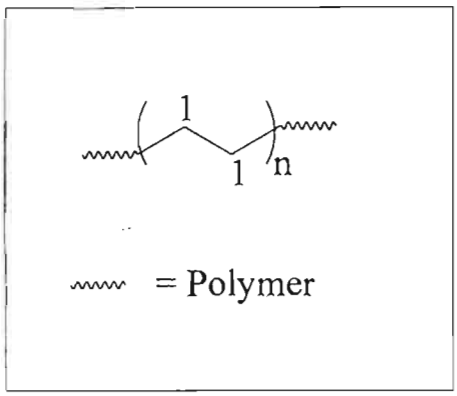

Figure 3.10 A structure of an ethylene unit in poly(ethylene) polymer

The structure in Figure 3.10 above shows that poly(ethylene) homo polymers are made up of mainly linear chains composed of methylene units (CH_2) in the chain backbone and with methyl groups at the chain ends. According to this suggested view, polyethylene homopolymers should be crystalline polymers.

However, the ethylene homopolymers that are experimentally produced are branched and amorphous polymers. The degree of branching of these

polymers is inversely proportional to the crytallinity of the polymeric material[26,27], and differs for each polymer depending on the methods and conditions of synthesis.

This difference in degree of branching in ethylene homopolymers leads to different types of polymers with different applications. There are four main different types of polyethylene polymers that are available commercially. These are :

(i). Ultra-pure poly(ethylene) polymers

(ii). High density poly(ethylene) (HDPE)

(iii). Low linear density poly(ethylene) LLDPE and

(iv). Low density poly(ethylene) LDPE.

All these types of polymers above differ according to the methods and conditions of synthesis. This can give rise to the degree of branching and crystallinity[85-87]. In this thesis, we produced polymers from reactions catalysed by diimine complexes at room temperature under 1 atm pressure of ethylene monomer.

The polymers produce were characterized by ^{1}H and ^{13}C NMR spectroscopy supported by ^{13}C APT NMR spectra for structural information and they were subjected to DSC and DTA/TG thermal studies.

3.2.2.1. Poly(ethylene) polymers produced by nickel catalysts

The polymer PE1 was obtained from the reaction catalysed by (D-(iPR)PI)$NiBr_2$/MAO at room temperature under 1atm pressure of ethylene monomer as a colourless amorphous polymer in yield of 2.43g . The polymer PE2, obtained from the reaction catalysed by (G-(iPr)PI)$NiBr_2$/MAO under the same conditions as PE1, was a white powder in yield of 0.253g. The polymer PE2 exhibited better thermal stability than PE1 as determined by TGA . Both polymers showed very similar NMR spectra and the NMR results corresponded very well with that reported by Brookhart and his coworkers[32]. The polymer PE3 obtained from the reaction catalysed by (D-MPI)$NiBr_2$/MAO under the same same condition as the other two polymer mentioned above was a colourless amorphous polymer in 2.10g. The polymer PE4 from the reaction catalysed from by (G-MPI)$NiBr_2$/MAO under the same conditions as the other polymers was above obtained as a milky solid polymer. PE4 showed better thermal stability than PE3. With both PE3 and PE4 more thermally stable than PE1 and PE2. All these polymers showed very similar NMR spectra although other polymers such as PE3, PE2 and PE4 showed very poor solubility in

many solvents such as 1,2 dichlorobenzene, benzene, dichloromethane and slightly soluble in chloroform.

3.2.2.1.1 ^{1}H NMR for nickel catalysed poly(ethylene) polymers

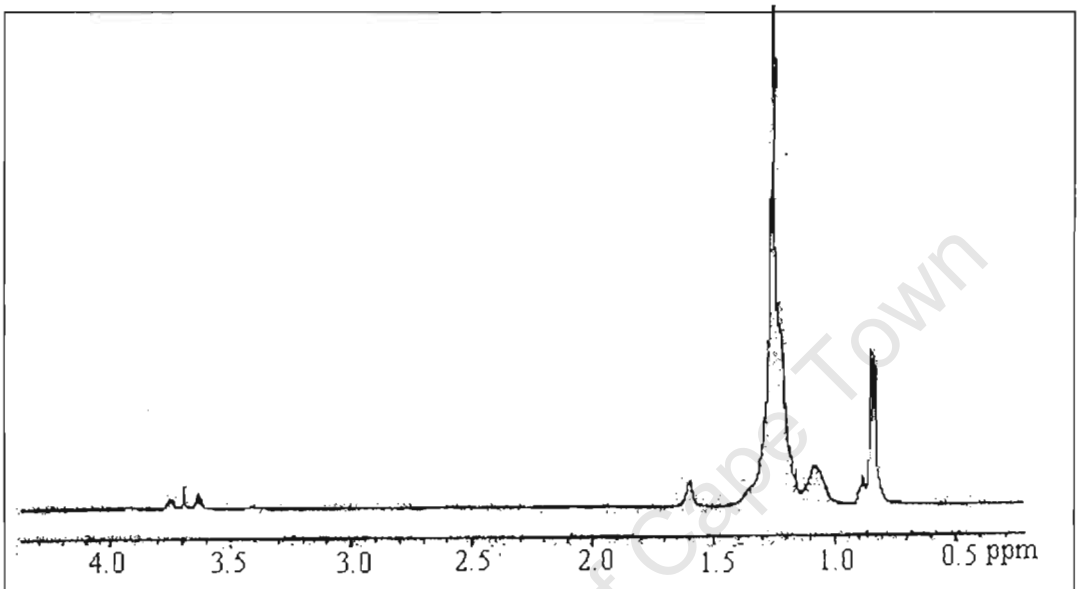

Figure 3.11 ^{1}HNMR for PE1(in $CDCl_3$) at room temperature

Discussion

In Figure 3.11, the ^{1}H NMR spectrum of PE1 shows a small peak at δ = 1.52 ppm which is associated with a methine (C<u>H</u>) proton, the proton attached to the tertiary carbon at the chain branch. There is a broad peak at δ = (1.19-1.26)ppm arising from the in chain methylene protons(C<u>H</u>$_2$) The resonance peaks at δ = (0.83 – 0.84)ppm are associated with methyl protons at the

chain ends. Similar spectra were obtained for other polymers such as PE3(see Figure 3.12), to avoid repetition, other spectra are not displayed

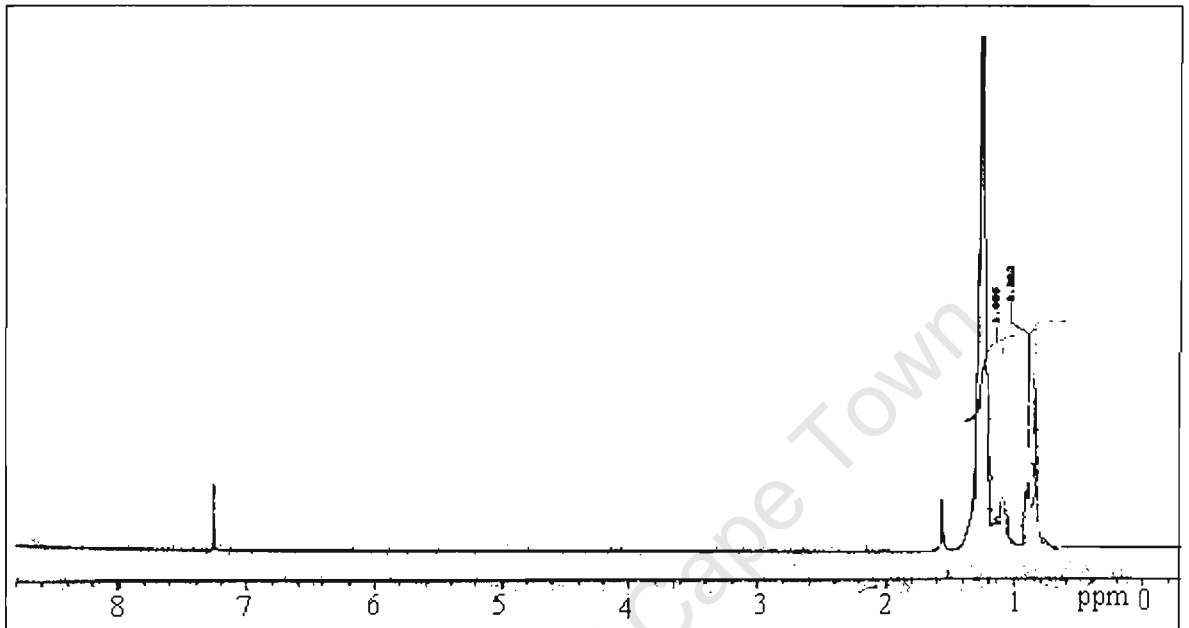

Figure 3.12 ^{1}H NMR for PE3(in$CDCl_3$) at room temperature

3.2.2.1.2 ^{13}C and ^{13}C APT NMR spectra for poly(ethylene) polymers produced from nickel catalysed reactions

The ^{13}C NMR and ^{13}C APT NMR spectra for PE3 were recorded at room temperature. The results are displayed in Figure 3.13(a) and (b) below. The peaks at 19.72ppm and 19.86ppm are associated with methyl carbons on the chain and also at the chain ends of long branches such as butyl or hexyl branches. The peaks at 32.78ppm to 33.07ppm are associated with methyl carbons on the shortest branches such as methyl branches (that means

carbons α or β to the tertiary carbons in the main chain). These peaks can also be observed in the ^{13}C APT NMR spectra in the same region but pointing down. The peaks at 26.73ppm to 30.18ppm are associated with methylene carbons on the long chain branches and on the chain backbone. But the peaks at 33.13ppm to 34.78ppm are associated with in chain methylene carbons α to the tertiary carbon(or in between the two tertiary carbon in the chain backbone). The peak at 37.25ppm is associated with methine peak (the 3°carbon at the branching point). Looking at the intensities of the peaks especially in ^{13}C APT NMR it can be observed as expected that the peak at 37.25ppm and the peak 19.72ppm for 1° carbon are in a 1:1 ratio which means for every methine (3° carbon) there is one methyl carbon(1° carbon)

at the chain end. And also the methylene peaks (2° carbon) at 34.38ppm have low intensities compared to the methylene peaks at

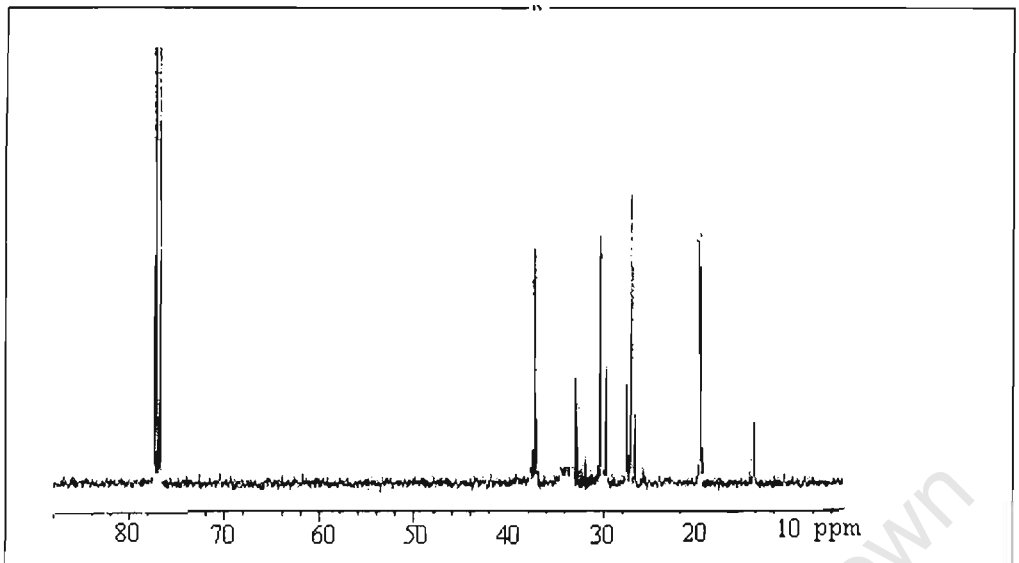

Figure 3.13(a) ^{13}C NMR spectrum for PE1(in $CDCl_3$) at room temperature

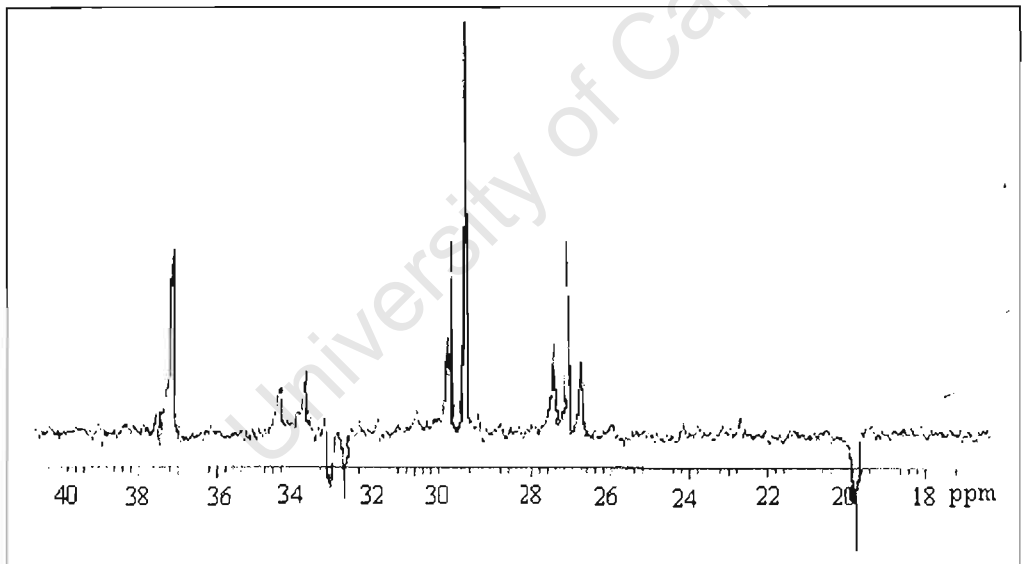

Figure 3.13(b)^{13}C APT NMR spectrum for PE1(in $CDCl_3$) at room temperature

26.72ppm to 30.18ppm meaning that there is low population of the methylene groups at the α position to tertiary carbon of the branching point. The same discussion holds for other polymers because these have very similar NMR spectrum as explained in the sections above.

3.2.2.1.3 Thermal behaviour of nickel catalysed poly(ethylene) polymers

(i) Differential Scanning calorimetry (DSC)

Melting points

The melting points of poly(ethylene) homopolymers produced using different Ni(II) catalysts with the same concentration and synthesized under the same reaction conditions are displayed below.

Table 3.2 DSC melting point endotherms for poly(ethylene) polymers

Polymer	Catalyst/MAO	Melting points determined by DSC
PE1	(D-(iPr)PI)$NiBr_2$	70°C
PE2	(G-(iPr)PI)$NiBr_2$	92 °C
PE3	(G-MPI)$NiBr_2$	129°C
PE4	(D-MPI)$NiBr_2$	116°C

Discussion

The Figures 3.14, 3.15 and 3.16 below show the DSC thermograms of the poly(ethylene) polymers mentioned in Table 3.2. These DSC thermograms are characterized by broad peaks which is the indication either (i) of the amorphous nature of these polymers or (ii) of the degree of branching of the polymer. The DSC trace for PE2 in Figure 3.14 show a broad endotherm centered at 92 °C, associated with the melting of the polymer.

There is also an exothermic peak at 245°C which is attributed to the structural rearrangements before decomposition. The DSC thermograms of PE3 in Figure 3.15 shows a peak centered at 129°C which is associated with melting point of the polymer. The thermogram of PE4 in Figure 3.16 shows an endotherm centered at 116°C which is attributed to the melting of polymer. In order to see if the melting of the polymer was accompanied by decomposition these results were further confirmed by DTA/TG in the next section.

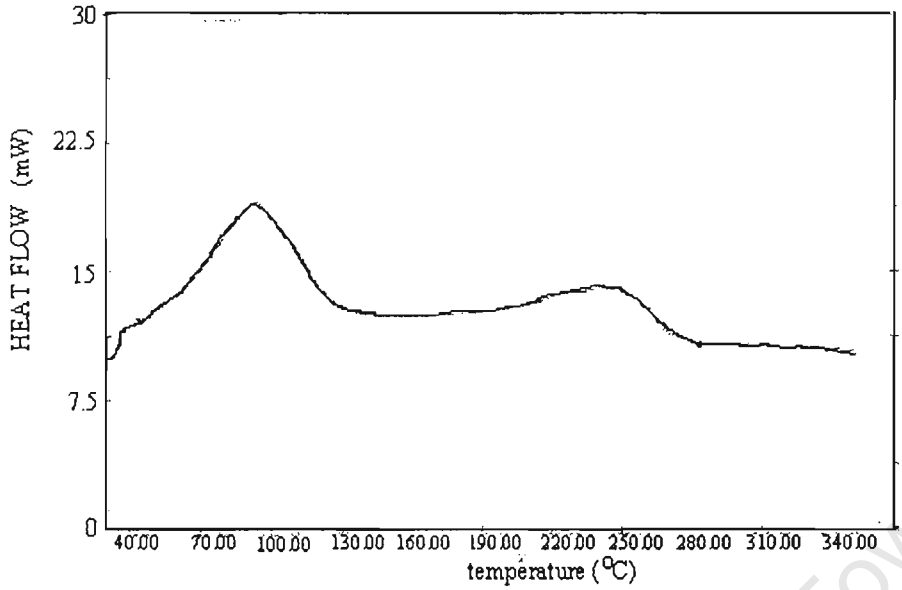

Figure 3.14 DSC thermogram for PE2

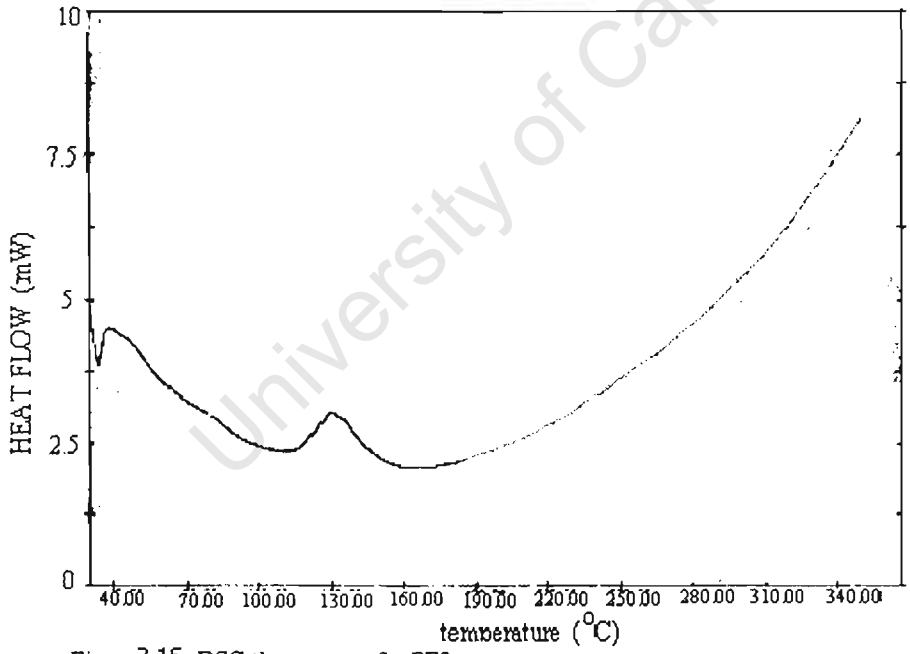

Figure 3.15 DSC thermogram for PE3

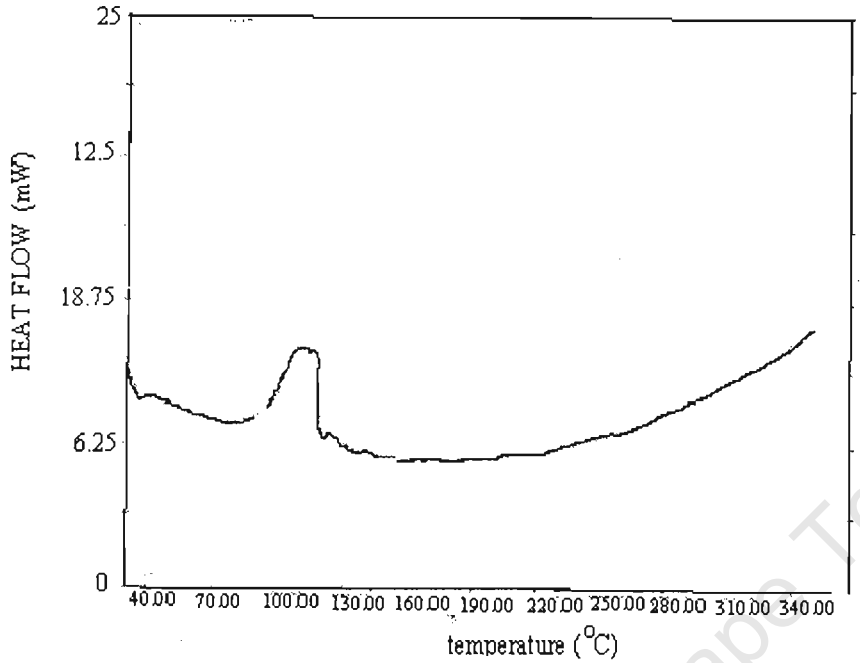

Figure 3.16 DSC thermogram for PE4

(ii) Thermogravimetric analysis(TGA) and Differential Thermal Analysis(DTA)

The TGA and DTA trace of the polymers were recorded on a STD409C DTA/TG machine at the heating rate of 20°C/min under an argon purge. All the polymers were heated up to 600°C. The overlays of DTA/TG thermograms for all polymers are displayed after the discussion section.

Discussion

DTA interfaced to TG thermograms will help us to see wheter the thermal events are accompanied by decomposition of the polymer during heating.

The DTA/TG traces for PE1 are shown in Figure 3.17(a). The polymer PE1 showed an onset weight loss at about 185°C after it has melted at 108.4°C and there was major offset degradation at 430°C. The polymer PE2 in Figure 3.18(a) and(b) showed a melting point centered at 112°C, higher than that of PE1 but immediately followed by gradual weight loss until the major offset decomposition at 426°C.

The DTA/TG and TG thermograms of PE3 shows the polymer melted at 127°C followed by onset decomposition at 149°C and a major degradation at 441°C whereas PE4 shows an onset weight loss at 236°C and major decomposition at 437°C.

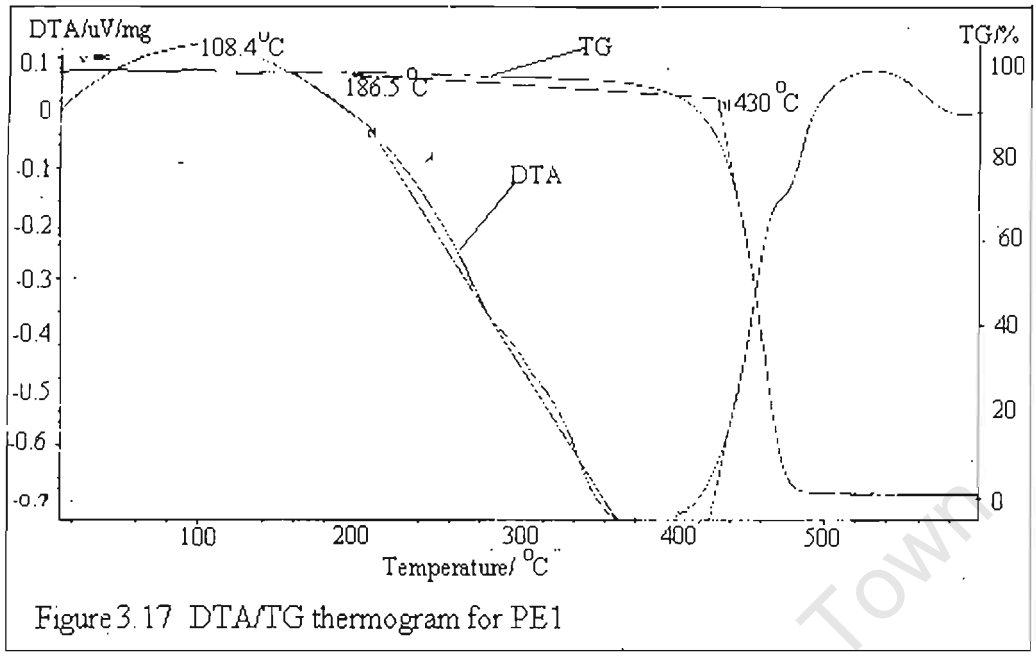

Figure 3.17 DTA/TG thermogram for PE1

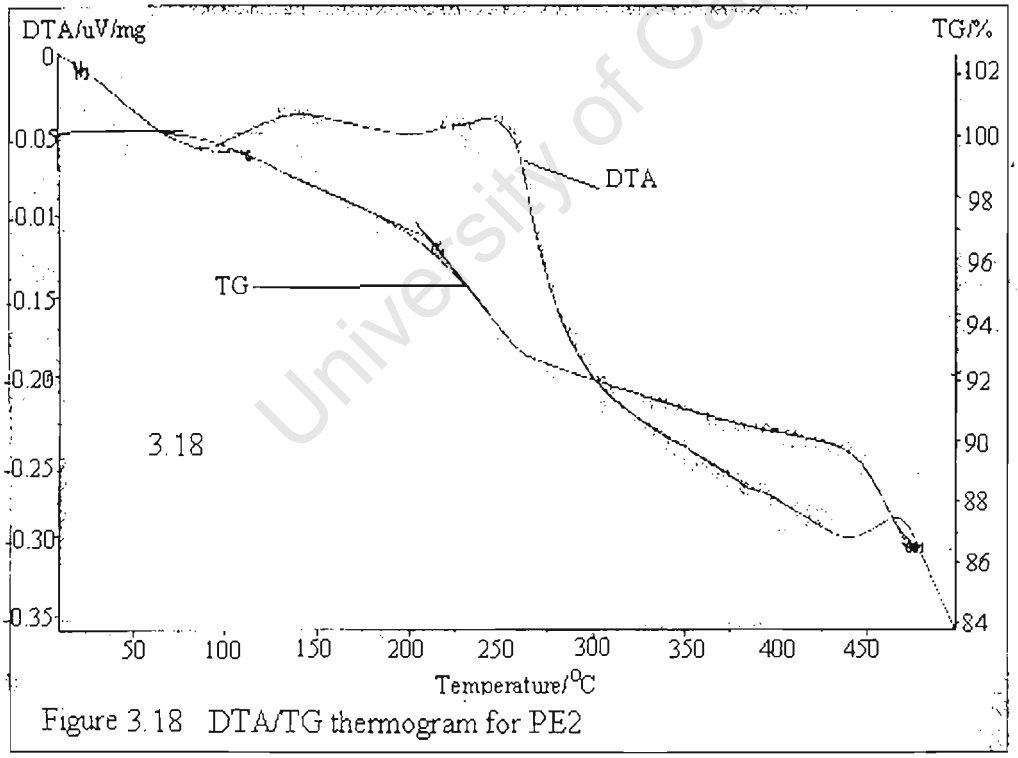

Figure 3.18 DTA/TG thermogram for PE2

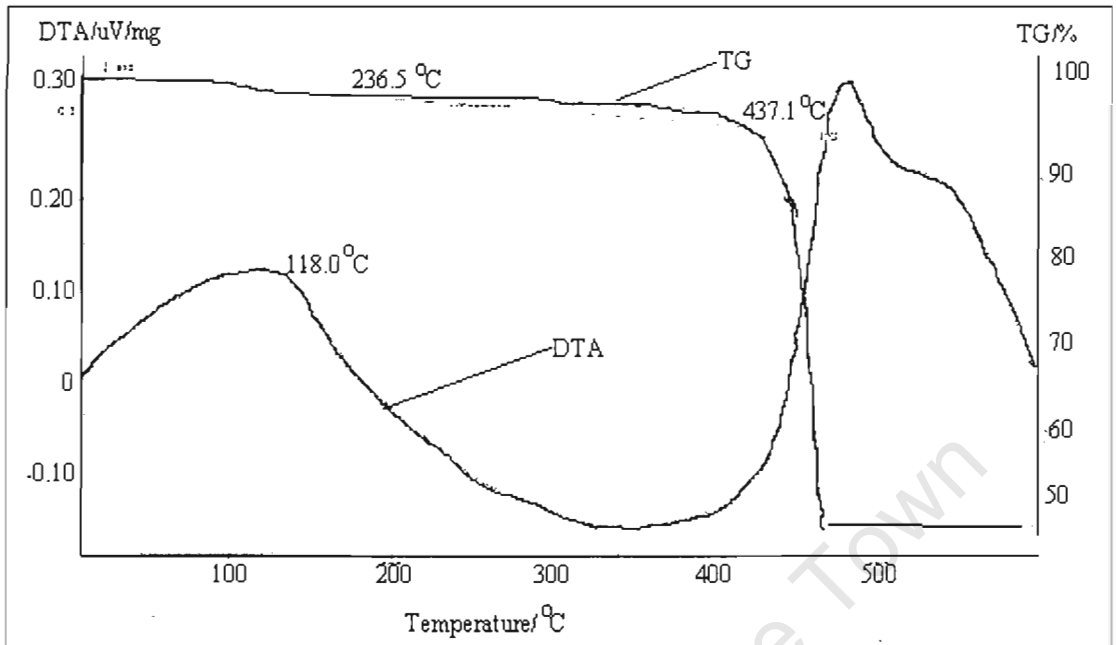

Figure 3.19 DTA/TG thermogram for PE3

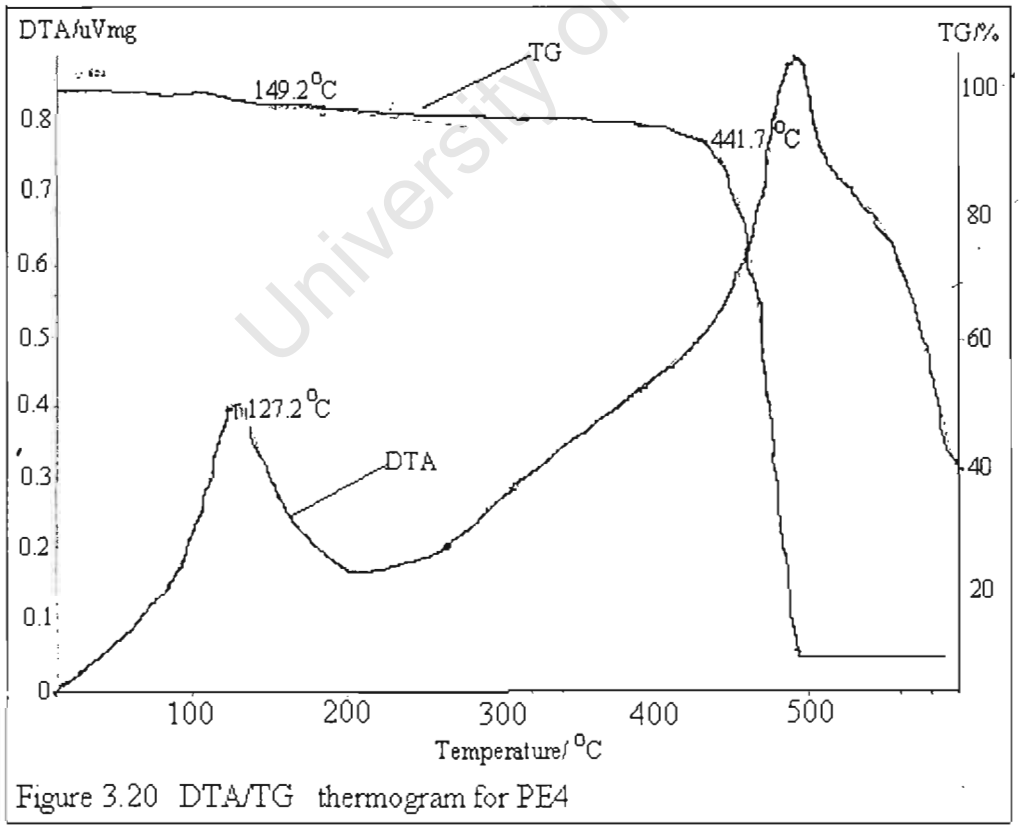

Figure 3.20 DTA/TG thermogram for PE4

From DSC and DTA/TG data, it can be observed that polymers PE3 and PE4 exhibit better thermal stability than PE1 and PE2. But polymer PE2 shows better thermal stability than PE1 same as PE4 shows better thermal stability than PE3. Polymers PE3 and PE4 are produced from dimethyl substituted diimine catalysts and polymers PE2 and PE1 are produced diisopropyl substituted diimine catalysts. This means that the substituents on the aryl rings of diimine catalysts had an effect on thermal of the polymer produced.

3.2.2.2. Poly(ethylene) polymers prepared using palladium catalysts

The palladium catalysts showed very poor catalylic activity. Four catalysts were used for polymerization studies and only two catalysts consistently produced polymers, in very low yields and the third catalyst produced a polymer(PE5) only in the first run. The NMR spectra of these polymers were very similar to poly(ethylene) polymers produced by the nickel catalysts. These polymers showed poorer thermal stability than polymers produced from nickel catalysed reactions. The polymer PE5 was obtained from the reaction catalysed by (D-(iPr)PI)PdMeCl under the same conditions as the nickel catalysed reactions, as a greyish powder in yield of 0.19g. The

polymers PE5 and PE6 were respectively produced from the reactions catalysed (G-(iPr)PI)PdMeCl and (G-MPI)PdMeCl .

^{1}H NMR results of poly(ethylene) polymers by palladium catalysts

As was mentioned above, the polymers gave very similar NMR results to polymers produced from the nickel catalysed reactions. To avoid repetition, one NMR spectrum for PE5 will be displayed in Figure 3.21.

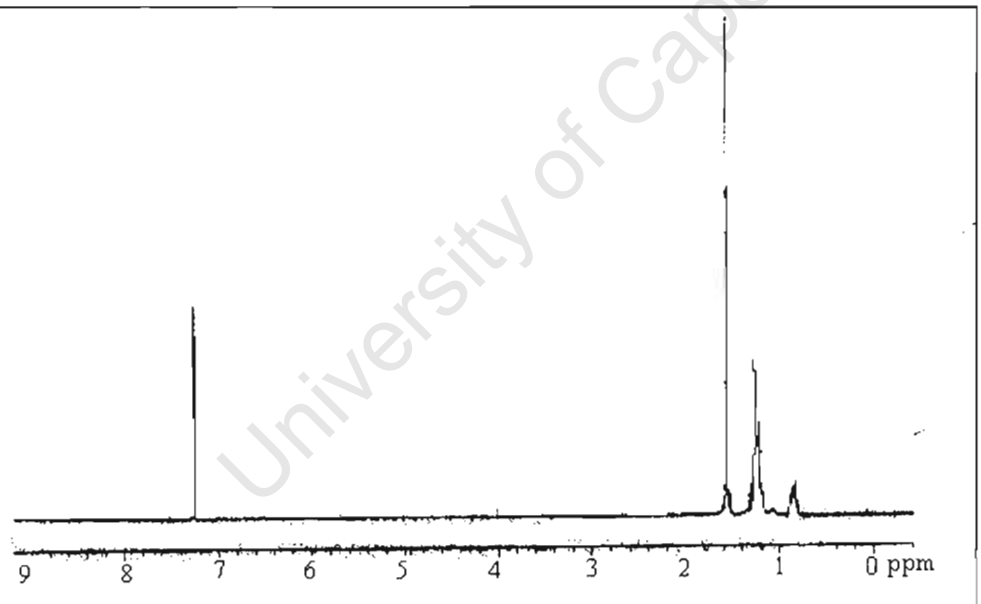

Figure 3.21 ^{1}H NMR of PE5(in $CDCl_3$) at room temperature

3.2.2.2 Thermal behaviour of palladium cataslyed poly(ethylene) polymers

The polymers from the palladium catalysed reaction were also subjected to DTA/TG analysis and spectra of the PE5 and PE6 are displayed in Figures 3.22 and 3.23 respectively. The DTA results shows that polymer PE5 melted at 103 °C and a TG thermogram showed that the melting of the polymer was accompanied by mass loss .

The DTA results for PE6 shows that this polymer has a melting point of 115°C which is higher than that of PE5 but that at the melting point of PE6 there was major decomposition. When comparing these results with DTA and TG results of the nickel catalysed poly(ethylene), it can be observed that although these polymers prepared from palladium catalysed reactions show high melting points they have poor thermal stability according to the TG analysis.

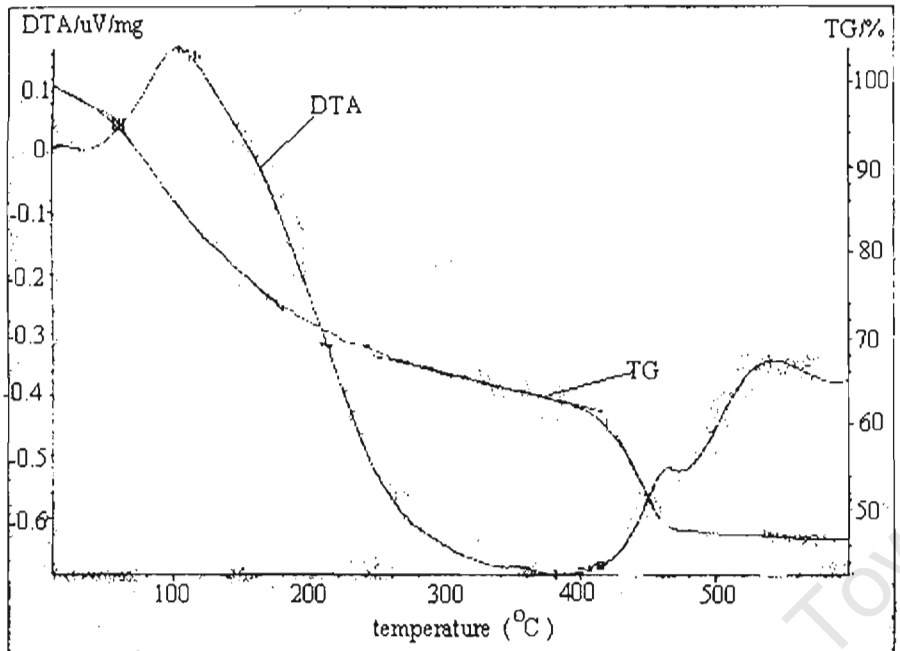

Figure 3.22 DTA/TG thermograms for PE5

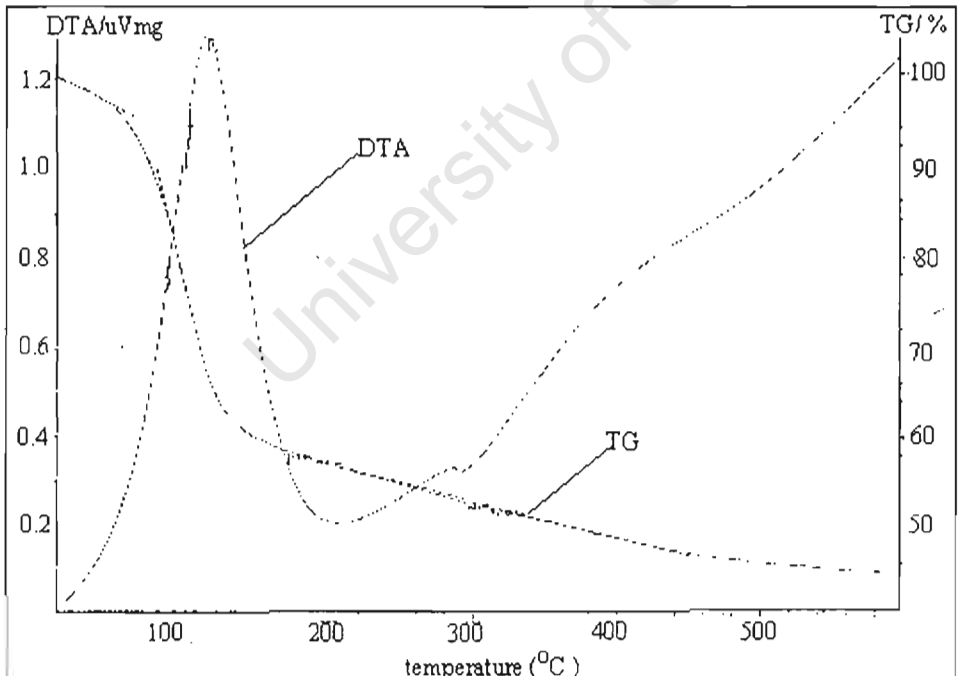

Figure 3.23 DTA/TG thermograms for PE6

3.2.3. Degree of crystallinity

Polymers are only partially crystalline but the degree of crystallinity,$\mathbf{X_c}$, reflects their history, i.e crystallisation temperature, time, annealing temperature[85,88]etc. Physical and mechanical properties vary markedly with X_c and can limit their commercial and technological exploitation. Most approaches to the measurement of crystallinity adopt a two phase model, made up of crystalline and amorphous regions. The Degree of crystallinity can be determined by many experimental procedures but each adopts different definitions of crystallinity and measure different values for X_c.

The DSC determines X_c from the ethalpies of fusion or crystallisation ,ΔH_x,, by measuring the area under the melting curves[82], i.e :

$Xc = \Delta H_x/\Delta H^o_x$

Where ΔH^o_x refers to the enthalpy of fusion or crystallisation of the totally crystalline polymer.

In our case, ΔH^o_x, will be that of 100% pure crystalline poly(ethylene), with a value of **293,13cal/g**[89-91]**.** All the values of the degree of crystallinity of our experimentally produced poly(ethylene) are displayed in Table 3.3.

Table 1.3 Degree of crystalliy of poly(ethylene) polymers

Catalyst/MAO	polymer	Enthalpy (ΔH_x)cal/g	Crystallinity(%)
(G-(iPr)PI)$NiBr_2$	PE2	134,3	50
(D-MPI)$NiBr_2$	PE3	8,8	3
(G-MPI)$NiBr_2$	PE4	73,3	25
(G-(iPr)PI)PdMeCl	PE5	79,0	27
(G-MPI)PdMeCl	PE6	143,6	49
pure crystalline poly(ethylene)	PE	**293,13**	**100%**

3.3 Conclusion

3.3.1 Poly(1-hexene) polymers

As it was mentioned in the discussion all these polymers gave very similar NMR spectra and these NMR results corresponded very well with the results obtained by Brookhart and the coworkers[32]. The only difference was observed when the polymers were subjected to thermal analysis. Each polymer exhibited different thermal behaviour. The nickel catalysed

polymers showed better thermal stability than the palladium catalysed polymers according to TG analysis.

3.3.2 Poly(ethylene) polymers

Similar to the poly(1-hexene) polymers these polymers gave very similar NMR spectra that can attributed to similar pattern of structural make up in terms of branching. They are all poly(ethylene)s but the degree of branching, molecular weight and the chain length will be different for each polymer. This can be reflected in the thermal behavior of the material. Looking at the thermal stabilities of these polymers especially the polymers produced from nickel catalysed reactions, it can be observed that each polymer shows independent thermal behaviour. There is however a pattern in their behaviour. That means the polymers produced from reaction catalysed by glyoxal derivatives of nickel diimine catalysts exhibited better thermal stability.The dimethyl substituted catalysts such as G-MPINiBr$_2$ also produced polymers of better thermal stability than the diisopropyl substituted catalysts such as (G-(iPr)PI)NiBr$_2$. This means that the overall structure of the ligand played a role in the thermal stability of these polymer. The activity of the catalysts served as a measured of the effect of the metal. The palladium catalysts showed very low activities observed also

from very low yields of polymers produced . As it was mentioned the results correlated very well with the results reported by Brookhart and coworkers[32]

Future work

These catalysts especially all the diimine nickel dihalide catalysts have a great potential in α-olefin polymerisation reactions. Thus there is scope for further research on them. The polymers produced by these catalysts, also need thorough investigation in terms of their application and processibility.

Chapter Four

Experimental

Chapter 4: Experimental

Materials

Formic acid, 2,6-dimethyl aniline, 2,6-diisopropyl aniline, Na_2PdCl_4, 1,5-cyclo-octadiene, triethyl orthoformate, 1,2-dimethoxy ethane, methyl lithium, and methyl alumoxane(MAO), were purchased from Sigma Aldrich. Glyoxal , diacetyl and 1-hexene were purchased from Merck N.T.

Nitrogen and ethylene gases purchased from Afrox.

Solvents: Toluene was purchased from Continental lab Suppliers, diethyl ether, methanol and dichloromethane were purchased from Merck N.T, hexane was purchased from B & M Scientific, acetone and ethanol were purchased from Kimix Chemicals

Purification of solvents and other reagents[92,93]

Diethyl ether:

Was purified by distillation over sodium benzophenone ketyl under nitrogen atmosphere.

Hexane:

Was purified by distillation over sodium benzophenone ketyl under nitrogen atmosphere

4.1. Diimine ligands

All products were air stable, reactions were conducted in the fumehood especially handling of 2,6-dimethyl aniline which is very toxic. The experimental detail follows in the sections below.

4.1.1. Synthesis of glyoxal-bis(2,6-diisopropylphenyl)imine[G-(iPr)PI]

A solution of 2,6-diisopropylaniline (1.00g, 5.64mmole) in methanol (20ml) was mixed with formic acid (1ml) as a catalyst and the mixture was stirred at 0°C for 5 minutes before the dropwise addition of glyoxal (0.16g 2.82mmol) solution. The reaction mixture was allowed to stir for 2.5 hours at 0°C and a yellow precipitate formed during stirring. The yellow precipitate was filtered-off, washed with cold methanol and dried. This product was purified by addition of hexane(just enough to dissolve the solid) and recrystallised from methanol. The product was isolated as a yellow powder stable in air and in 0.696g (60% yield).

4.1.2. Synthesis of Diacety-bis(2,6-diisopropylphenyl)imine[D-(iPr)PI]

A solution of 2,6-diisopropyl aniline (1.00g, 5.64mmol) in methanol (30ml) was mixed with formic acid (1ml) as catalyst and stirred at room temperature for 2 minutes before the slow addition of diacetyl (0.25g, 2.82mmol) solution. The reaction mixture was allowed to stir for 25hours at room temperature and the light yellow precipitate formed. The precipitate was filtered-off the solution and washed with methanol (2x10ml) then dried. The product was isolated as an air stable light yellow powder in 0.625g (50% yield).

4.1.3. Synthesis of glyoxal-bis(2,6-dimethylphenyl)imine[G-MPI]

A solution of 2,6-dimethyl aniline (3.00g, 0.02mol) in methanol (30ml) was mixed with formic as a catalyst and the mixture was stirred at 0°C for 5 minutes before the slow addition of glyoxal (0.71g, 0.01mol). The resulting mixture was stirred for 2.5 hours at 0°C and pale yellow crystalline precipitate was formed. The precipitate was filtered-off the solution and washed with cold methanol (3x10ml) then dried. The product was isolated as an air stable pale yellow crystalline powder in 1.93g (52% yield).

4.1.4. Synthesis of diacetyl-bis(2,6-dimethylphenyl)imine[D-MPI]

A solution of 2,6-diimethyl aniline (3.00g, 0.02mol) in methanol (35ml) was mixed with formic acid (1ml) as a catalyst and stirred at room temperature for 2 minutes before the dropwise addition of diacetyl (1.03g, 0.01mol). The reaction mixture was allowed to stir for 25 hours at room temperature and 1 day in the fridge before the light yellow crystals were formed. The crystals were filtered-off and washed with methanol (2x10ml) then dried. The product was isolated as light yellow crystals in 1.61g (40% yield).

4.2. Ni(II) and Pd(II) complexes bearing diimine ligands

The synthesis of these metal complexes involves very air sensitive steps and some steps were conducted at –78°C. Most of the products were air stable. All the manipulation of air sensitive compound were performed using standard schlenk techniques. All glassware were oven-dried at 150°C before use.

4.2.1. Synthesis of 1,2-dimethoxy ethane nickel(II) bromide[94,95] *[(DME)$NiBr_2$]*

A two necked round bottom flask equipped with a reflux condenser and a magnetic stirrer bar was charged with dehydrated nickel(II) bromide ($NiBr_2.3H_2O$) (5.26g, 0.20mol) salt in freshly distilled ethanol (10ml) and freshly distilled triethyl orthoformate (7.99g, 0.05mol). The mixture was stirred at reflux for 2 hours under nitrogen atmosphere and the solvent of the resulting mixture was evaporated to the stage of incipient crystallisation at the boiling point and then diluted with freshly distilled 1,2-dimethoxy ethane (0.16g, 0.4mol) . The resulting salmon pink solid was collected under nitrogen in a schlenk frit then rinsed with freshly distilled 1,2-dimethoxy ethane and dried in a current flow of nitrogen. The product was finally isolated as a salmon pink powder in 4.73g (90% yield).

4.2.2. Synthesis of glyoxal-bis(2,6-diisopropylphenyl)imine nickel(II) bromide [(G-(iPr)PI)$NiBr_2$]

A 150ml schlenk flask equipped with a magnetic stirrer bar was charged with (DME)$NiBr_2$(0.494g, 1.60mmol) suspended in a freshly distilled CH_2Cl_2 (20ml) and G-(iPr)PI (0.600g, 1.60mmol) dissolved in a freshly

distilled CH_2Cl_2 (10ml) under nitrogen atmosphere. The resulting red/brown mixture was stirred at room temperature for 20 hours under nitrgen atmosphere. After the solvent has been evaporated, the resulting red/brown powder was collected and washed with distilled hexane (3x10ml) then dried under reduced pressure. The product was isolated as a red/brown powder in 0.875g (80% yield) and stored under nitrogen.

4.2.3. Synthesis of diacetyl-bis(2,6-diisopropylphenyl)imine nickel(II) bromide [(D-(iPr)PI)NiBr$_2$]

In a two-necked round bottom flasks was placed a suspension of (DME)$NiBr_2$ (0.467g, 1.49mmol) in a freshly distilled CH_2Cl_2 (20ml) and a solution of D-(iPr)PI (0.610g, 1.49mmol) in CH_2Cl_2 (10ml) under nitrogen atmosphere. The resulting orange/ brown mixture was stirred at room temperature for 22hours under nitrogen atmosphere. After evaporating the solvent, the resulting orange/brown powder was collected and washed with distilled hexane (3x10ml) then dried under reduced pressure. The product was isolated as an air orange/brown powder in 0.249g (75% yield).

4.2.4. Synthesis of glyoxal-bis(2,6-dimethylphenyl)imine nickel(II) bromide[(G-MPI)$NiBr_2$]

A solution of G-MPI (0.23g, 0.870mmol) in a freshly distilled CH_2Cl_2(10ml) was added to a suspension of (DME)$NiBr_2$ (0.267g, 0.870mmol) in a freshly distilled CH_2Cl_2 (20ml) at room temperature under nitrogen atmosphere. The resulting solution reddish-brown mixture was stirred at room temperature for 20 hours. After the evaporating the solvent, the resulting reddish-brown powder was collected and washed with distilled hexane (3x10ml) then dried under reduced pressure. The product was isolated as a red-brown powder in 0.249g (50% yield) and stored under nitrogen.

4.2.5. Synthesis of diacetyl-bis(2,6-dimethylphenyl)imine nickel(II) bromide [(D-MPI)$NiBr_2$]

An oven dried two necked-round bottom flask fitted with a magnetic stirrer bar was charged with D-MPI (0.200g, 0.685mmol) and (DME)$NiBr_2$ (0.210g 0.685mmol) in their solid form followed by addition of freshly distilled CH_2Cl_2 (40ml) and stirred at room temperature under nitrogen atmosphere. The resulting greenish brown mixture was stirred for 20 hours at room temperature. The solvent was then evaporated and the resulting powder was collected and washed with distilled hexane (3x10ml) then dried under

reduced pressures. The product was isolated as an air stable greenish brown powder in 0.246 (60% yield).

4.2.6. Synthesis of 1,5-cyclo-octadiene palladium dichloride [(COD)$PdCl_2$]

A 250ml round bottom flask equipped with a magnetic stirrer bar was charged with a COD (0.24g, 2.23mmol)) and Na_2PdCl_4 (0.500g, 2.23mmol) in methanol (25ml). A yellow precipitate was formed almost at once and the reaction was allowed to stir for 1hour at room temperature. The yellow precipitate was filtered-off and washed with methanol (2x10ml) then dried. The product was isolated as an air stable yellow powder in 0.669g (90% yield).

4.2.7. Synthesis of 1,5-cyclo-octadiene palladium methylchloride [(COD)Pd MeCl]

A two necked-round bottom flask equipped with a magnetic stirrer bar was charged with (COD)$PdCl_2$ (0.300g, 1.05mmol) suspended in a freshly distilled diethyl ether and cooled to $-72^{\circ}C$ using CO_2/ethanol bath then stirred for 10 minutes at that temperature under nitrogen atmosphere before the addition of (1.6M)methyllithium (0.91ml, 1.05mmol) in diethyl ether. The resulting mixture was allowed to stir at $-72^{\circ}C$ for 1hour then warmed to $-15^{\circ}C$ using CO_2/CCl_4 bath and stirred for 20minutes. The solvent was

evaporated under reduced pressures and the resulting blackish material was dissolved in freshly distilled CH_2Cl_2 then filtered. The solvent was evaporated from the filtrate, the resulting greyish powder was washed with distilled hexane then dried under reduced pressures. The product was isolated as greyish powder in 0.099g (33% yield) and stored under nitrogen.

4.2.8. Synthesis of (glyoxal-bis(2,6-diisopropylphenyl)imine palladium methylchloride [(G-(iPr)PI)PdMeCl]

A Shlenck flask equipped with a magnetic stirrer bar was charged with (COD)PdMeCl (0.100g, 3.84mmol) suspended in a freshly distilled diethyl ether (15ml) and G-(iPr)PI (0.140g, 3.84mmol) in diethyl ether (10ml) at room temperature under nitrogen. The resulting orange brown mixture was stirred at room temperature for 18hours under nitrogen atmosphere. The solvent was evaporated and the resulting orange brown powder was washed with distilled diethyl ether (1x10ml) then with distilled hexane (1x10ml). The product was isolated as an air stable orange-brown powder in 0.216 (90% yield).

4.2.9. Synthesis of diacetyl-bis(2,6-diisopropylphenyl)imine palladium methychloride [(D-(iPr)PI)PdMeCl]

A Schlenk flask equipped with a magnetic stirrer bar was charged with (COD)PdMeCl (0.100g, 3.84gmmol) suspended in diethyl ether (15ml) and D-(iPr)PI (0.155g, 3.84mmol) in diethyl ether (10ml) at room temperature under nitrogen. The resulting yellowish brown mixture was stirred for 18 hours at room temperature under nitrogen. The solvent was evaporated the resulting a yellowish brown powder was washed with distilled diethyl ether (1x10ml) and then distilled hexane (1x10ml) then dried under reduced pressures. The product was isolated as yellowish brown powder in 0.217g (85% yield).

4.2.10. Synthesis of glyoxal-bis(2,6-dimethylphenyl)imine palladium methylchloride [(G-MPI)PdMeC]

A Schlenk tube equipped with a magnetic stirred bar was charged with (COD)PdMeCl (0.080g, 0.308mmol) suspended in a freshly distilled diethyl ether (20ml) and G-MPI (0.081g, 0.308mmol) in freshly distilled diethyl ether (10ml). The resulting reddish brown mixture was stirred at room temperature under nitrogen atmosphere. The solvent was evaporated and the resulting reddish brown was washed with distilled diethyl ether (1x10ml)

and then distilled hexane (1x10ml) then dried under reduced pressure. The product was isolated as an air stable reddish brown powder in 0.064g (40% yield).

4.2.11. Synthesis of diacetyl-bis(2,6dimethylphenyl)imine palladium methylchloride [(D-MPI)PdMeCl]

A Schlenk tube equipped with a magnetic stirrer bar was charged with (COD)PdMeCl (0.080g, 0.308mmol)) in freshly distilled diethyl ether (20ml) and D-MPI(0.090g, 0.308mmol) in freshly distilled diethyl ether (10ml). The resulting brownish mixture was stirred for 18hours at room temperature under nitrogen atmosphere. The solvent was evaporated and the resulting brownish powder was washed with diethyl ether (1x10ml) then distilled hexane and then dried. The product was isolated as an air stable brownish powder in 0.109g (64% yield).

4.3 Polymerisation Reactions

4.3.1. Polymerisation of 1-hexene by (D-(iPr)PI)NiBr$_2$/MAO. [PH1]

An oven dried Schlenck tube equipped with a magnetic stirrer bar was charged with 1-hexene (10ml) in freshly distilled toluene (36ml) and

(D-(iPr)PI)$NiBr_2$ (10.0mg, $1.60x10^{-5}$mol) in toluene (10ml) was stirred at room temperature for 10 minutes before the addition of 10% MAO (100eq 1.6ml) in toluene. The resulting deep-green reaction mixture was stirred for 1hour at room temperature under nitrogen atmosphere. During the polymerisation reaction there was a rise in temperature to 40°C. The reaction was quenched with methanol(8ml) and the polymer was precipitated with acetone(1l) and then the precipitate was filtered off solution and dried under vacuum for 1day. The final polymer was isolated as a colorless plastic-like material in yield of 1.74g (26%).

4.3.2. Polymerisation of 1-hexene by (G-(iPr)PI)$NiBr_2$/MAO

An oven dried round bottom flask equipped with a stirrer bar was charged with 1-hexene (10ml) in freshly distilled toluene (35ml) and (G-(iPr)PI$NiBr_2$) (9.55mg, $1.60x10^{-5}$mol) in freshly distilled toluene (10ml) and stirred for 10 minutes at room temperature before the addition of 10% MAO (100eq, 1.6ml) in toluene. The resulting deep-purple solution was stirred for 1hour at room temperature under nitrogen atmosphere then quenched with methanol. The resulting polymer was precipitated in acetone(800)ml was filtered off, washed with acetone (3x10ml) then dried

under vacuum for 1day. The final polymer was isolated as a colorless amorphous material in yield of 3.70g (55%).

4.3.3. Polymerisation of 1-hexene by (G-(iPr)PI)PdMeCl/MAO

This polymerisation was conducted in the similar manner as 4.3.1 and 4.3.2 above under the same conditions. After mixing 1-hexene (10ml) in freshly distilled toluene (35ml) and (G-(iPr)PI)PdMeCl (8.53mg, $1.6x10^{-5}$mol) in freshly distilled toluene followed by addition of 10% MAO (100eq, 1.6ml) in toluene and stirred for 1hour at room temperature under nitrogen atmosphere The polymerisation was quenched by methanol and precipitated with acetone(1L). The precipitate was filtered off and washed with acetone (3x10m) and 10% HCl (100ml) then dried. The final polymer was obtained as a greyish powder in yield of 0.18g (2.8%).

4.3.4 Polymerisation of 1-hexene by (D-(iPr)PI)PdMeCl/MAO

This polymerisation was also conducted in the similar manner as above under the same conditions. After mixing 1-hexene (10ml) in freshly distilled toluene and (D-(iPr)PI)PdMeCl (8.98mg, $1.6x10^{-5}$mol) in freshly distilled toluene (10ml) followed by addition of 10% MAO (100eq, 1.6 ml) and stirred for 1hour at room temperature under a nitrogen atmosphere, the polymerisation was quenched by methanol and precipitated with acetone.

The precipitate was filtered off then and washed with acetone then 10% HCl (100ml). The final polymer was isolated as greyish powder in yield of 0.20g (3%).

4.3.5. Polymerisation of ethylene by (D-(iPr)PI)NiBr$_2$/MAO

An oven-dried three necked round bottom flask fitted with a septum (for monomer inlet), a glass tap (for monomer outlet), a glass stopper and equipped with a magnetic stirrer bar was charged with freshly distilled toluene (45ml) saturated with constant flow ethylene at 1atm pressure at room temperature. The toluene was stirred at constant purged with ethylene for 15 minutes before the addition of (D-(iPr)PI)NiBr$_2$ (10mg, 1.60x10^{-5}mol) and the resulting suspension was stirred for 10 minutes at constant flow of ethylene followed by addition of 10% MAO (100eq, 1.5ml) in toluene. The resulting deep-green polymerisation reaction mixture was allowed to stir for 40 minutes at room temperature under the constant flow of ethylene. During stirring there was a temperature increase from room temperature to 45°C, this was allowed to cooled down before the reaction was quenched with methanol. The polymer with precipitated from acetone and filtered-off then washed with 10% HCl (100ml) and dried under vacuum for 1day. The final

polymer was isolated as colourless amorphous polymer in 2.43g with activity of $13.7x10^3$g/h.mol/dm^3.

4.3.6.Polymerisation of ethylene by (G-(iPr)PI)NiBr$_2$/MAO

This polymerisation was conducted in the similar manner as 4.3.5. under the same conditions. After the addition of (G-(iPr)PI)$NiBr_2$ (9.53mg, $1.60x10^{-5}$mol) to the toluene saturated by a constant flow of ethylene the reaction was stirred for 15 minutes at room temperature under ethylene atmosphere followed by addition of 10% MAO (100eq, 1.5ml) in toluene. The resulting deep-purple mixture was stirred for 40 minutes at room temperature under a constant flow of ethylene. The polymerisation was quenched with methanol and the polymer was precipitated in acetone then filtered and washed with 10% HCl (100ml) and dried under vacuum for 1 day. The final polymer was isolated as white powder; yield 0.25g with activity of 1.41 $x10^3$g/h.mol/dm^3.

4.3.7. Polymerisation of ethylene by (G-MPI)NiBr$_2$/MAO

This polymerisation was carried on the same manner as 4.3.5 above. After addition of (G-MPI)$NiBr_2$ (7.73mg, $1.6x10^{-5}$mol) to the toluene saturated by

a constant flow of ethylene at 1atm pressure was stirred for 15 minutes before the addition of 10% MAO (100eq, 1.5ml) in toluene. The resulting deep-purple polymerisation mixture was stirred at room temperature for 40minutes under constant flow of ethylene. The reaction was quenched by addition of methanol and precipitated from ethanol then filtered-off and washed with 10% HCl (50ml) and dried under vacuum for 1 day. The final polymer was isolated as a hard milky solid polymer; yield 1.69g with activity of 9.51 $x10^3$g/h.mol/dm^3.

4.3.8. Polymerisation of ethylene by (D-MPI)$NiBr_2$/MAO

This polymerisation was also conducted in the same manner as 4.3.5. After addition of (D-MPI)$NiBr_2$/MAO (8.18mg, $1.60x10^{-5}$mol) to the toluene saturated by a constant flow of ethylene at 1atm the suspension was stirred for 10 minutes followed by addition of 10% MAO (100eq, 1.5ml) and stirred at room temperature for 40 minutes under a constant flow of ethylene. The resulting deep-green polymerisation mixture was quenched with methanol and the polymer was precipitated in ethanol then washed with 10% HCl (100ml) and dried under vacuum for 1day. The final product was isolated as amorphous colourless material; yield 2.01g with activity of 11.3 $x10^3$ g/h.mol/dm^3.

4.3.9. Polymerisation of ethylene by (G-(iPr)PI)PdMeCl/MAO

This polymerisation was also conducted in the same way as 4.3.5 above. After the addition of (G-(iPr)PI)PdMeCl (8.53mg, $1.60x10^{-5}$mol) to the toluene saturated with a constant flow of ethylene at 1 atm the resulting suspension was stirred at room temperature for 15 minutes before the addition of 10% MAO (100eq, 1.5ml) then stirred for another 40 minutes at room temperature. The resulting colourless homogeneous solution was quenched by methanol and the polymer was precipitated from acetone. The precipitate was filtered off then washed with 10% HCl (100ml) and dried under vacuum. The final polymer was isolated as a greyish powder; yield 0.19g with activity of 1.07 $x10^3$g/h.mol/dm^3.

4.3.10. Polymerisation of ethylene by (D-(iPr)PI)PdMeCl/MAO

This polymerisation was conducted in exactly the same way as the above reaction 4.3.5 and the observations were the same but no polymer was obtained in the first run, only black material was isolated. In the second run a sticky colourless material was isolated and in the third run greyish powder was isolated; yield 0.18g with activity of 1.01 $x10^3$g/h.mol/dm_3.

4.3.11. Polymerisation of ethylene by (G-MPI)PdMeCl/MAO

This polymerisation reaction was also conducted in the same way to 4.3.5. above. All other steps corresponded to those mentioned in 4.3.10. But when methanol was added to quench the reaction the solution turned black and after trying to precipitate this black product from acetone or ethanol and the mixture of two and also place the solution in the fridge no precipitate was obtained. So no polymer was obtained from this reaction.

4.3.12. Polymerisation of ethylene by (G-MPI)PdMeCl/MAO

This polymerisation reaction was conducted in the same way as 4.3.5 above. The polymerisation corresponded exactly to the reaction 4.3.9 above. The final polymer was isolated as a greyish powder; yield 0.15g with activity of 8.44 $x10^2$g/h.mol/dm^3

References

1. P.W. Atkins., D.F.Shriver., C.H. Langford., *Inorganic Chemistry,* 2nd ed, Oxford University press., Oxford, (1994), p715.

2. C. Masters., *Homogeneous Transition Metal Catalysis,* Chapman and Hall, London, (1981).

3. G. Odian., *Principles of Polymerisation,* 2nd ed, John Wiley& Sons, New York, 1981.

4. K. Ziegler., E. Holzlamp., H. Breil., H. Martin., *Angew Chem,* (1995), **67**, 541.

5. G. Natta., *J. Polym. Sc.* (1955), **16**, 143.

6. G. Natta., P. Pino., P. Corrandi., F. Danusso., E. Matinca., E. Mazzanti., G. Moraglio., *J. Am. Chem. Soc.,* (1965), **77**, 1708.

7. G. Fink., R. Mülhaupt., H.H. Brintzinger., *Ziegler Catalysts*, Springer-Verlag, Berlin and New York, 1995, p217.

8. J.C. Randall, *Macromolecules,* (1997), **30**, 803.

9. G. Natta, *J.Polym. Sci.,* (1959), **34**, 531.

10. B. Lotz., J.C. Wittman., A.L. Lovinger., *Polymer,* (1996), **37**, 4979.

11. H.H. Brintzinger., D.Fischer., B. Rieger., R.M. Waymouth., R. Mülhaupt ., *Angew. Chem. Int, Ed, Engl,* (1995), **34**, 1143.

12. P.C. Möhring., N.J. Coville., *J. Organomet. Chem,* (1994), **479**, 1.

13. W. Spaleck., F. Kube., A. Winter., J. Rohrmann., B. Bachmann., M.Antberg., V. Dolle, E.F.Paulus., *Organometallics,* (1994), **13**, 954.

14. D. Fischer., R. Mülhaupt., *J. Organomet. Chem,* (1991), **417**, C7.

15. V. Busico., R. Cipullo., *J. Am. Chem. Soc,* (1994), **116**, 9329.

16. R. Fierro., Z.Yu., M.D. Rausch., S. Dong., D. Alvareze., J.C.W. Chien., *J. Polym. Sci. Part A, Polym. Chem,* (1994), **32**, 661

17. X.Y.Chen., M.D.Rausch., *Macromolecules,* (1995), **28**, 5399.

18. X.Y.Chen., M.D. Rausch,. *J. Polym. Sci. PartA. Polym. Chem,* (1995), **35**, 2093.

19. J. Korvumaki., G.Fink., J.V.Seppala., *Macromolecules,* (1994), **27**, 6254.

20. C. Pellechia., D. Poppalardo., *Macromolecules,* (1996), **29**, 1158

21. U. Stehling., J. Diebold., R. Kirsten., W. Roll., H.H. Brintzinger., *Organometallic,* (1994), **13**, 964.

22. F.G. Sernetz., R. Mülhuapt., T. Amor., T. Eberle., J. Okuda., *J. Polym. Sci. Part A, Polym. Chem.,* (1997), **35**, 1571.

23 J. Suhm., M.J. Schneider., R. Mülhuapt., *J. Polym. Sci. Part A, Polym. Chem.,* (1997), **35**, 735.

24. G.H. Llinas., S.H. Dong., D.T. Mallia., D.M. Rausch., Y.G. Lin., H.H.Winter., J.C.W. Chien., *Macromolecules,* (1992), **25**, 1292.

25. G.W. Coates., R.M. Waymouth., *Science,* (1995), **267**, 217.

26. E. Hauptman., R.M. Waymouth., *J.Am. Chem. Soc,* (1995), **117**, 11586.

27. S. Suhm., J. Heinemann., Y. Thomann., R. Thomann., R.D. Maier., T. Schleis., J. Okuda., J. Kressto., R. Mülhaupt., *J.Mater. Chem,* (1998), **8,** 553.

28. H. Weiss., M. Ehrig., R. Ahlrichs., *J.Am.Chem. Soc*, (1994), **116**, 4919.

29. G.W. Parshall., S.D. Ittel., *Homogeneous Catalysis*, 2nd ed, Wiley, New York, 1992.

30. F.C. Rix., M. Brookhart., *J. Am. Chem. Soc.* (1995), **117**, 1137.

31. S. Mecking., L.K. Johnson., L. Wang., M. Brookhart., J. Am. Chem. Soc, (1998), **120**, 888.

32. L.K. Johnson., C.M. Killian., M. Brookhart., *J. Am. Chem. Soc,* **(1995), 117**, 6414.

33. G.J.P. Britovsek., V.C. Gibson., B.S. Kimberly., P.J. Maddox., S.J. Mctavish., G.A. Solan., A.J.P. White., D.J. Willams., *J. Chem. Soc. Chem. Comm,* (1998), 849.

34. M. Tanner., M. Brookhart., J.M. Desimone., *J. Am. Chem. Soc*, (1997), **119**, 7617.

35. L.K. Johnson., S. Mecking., M. Brookhart., *J. Am. Chem. Soc,* (1996), **118**, 267.

36. J.C.W. Chien., R. Sugimoto., *J. Polym. Sci. Part A, Polym. Chem,* (1991), **29**, 499.

37. C.M.Killian., D.J.Tempel., L.K. Johnson., M. Brookhart., *J. Am. Chem. Soc,* (1996), **118**, 11664.

38. L.B. Small., M.Brookhart., A.M.A.Bennett., *J. Am. Chem. Soc,* (1998), **120**, 4049.

39. C.M. Killian., L.K. Johnson., M. Brookhart., *J. Organomet. Chem,* (1997), **16**, 2005.

40. G. van Koten., K. Vrieze., *Adv. Organomet. Chem,* (1982), **21**, 151.

41. H. tom Dieck., K.D. Franz., W. Majunke., *Z. Naturforsch,* (1975), **30B**, 922.

42. J. Kliegman., R.K. Barnes., *Tetrahedron*, (1970), **26**, 2555.

43. H. Bock., H. tom Dieck., *Chem. Ber*, (1967), **100**, 228.

44. H. van der Poel., G. van Koten., K. Vrieze., *Inorg. Chem*, (1980), **19**, 1145.

45. G. van Koten., K. Vrieze., *Inorg. Chem.*, (1980), **19**, 181.

46. A.L. Balch., R.H. Holm., *J. Am. Chem.* Soc, (1966), **80**, 520.

47. H. Bock., H. tom Dieck., *Angew. Chem*, (1966), **18**, 159.

48. M. Svoboda., H. tom Dieck., C. Kruger., Y.H. Tsay., *Z. Naturforsch. B: Anorg. Chem. Org. Chem*, (1981), 36B, 814.

49. M. Svoboda., H. tom Dieck., T. Greiser., *Z. Naturforsch. B: Anorg. Chem. Org. Chem*, (1981), **36B**, 3823.

50. H. tom Dieck., M. Svoboda., J. Kopf., *Z. Naturforsch. B: Anorg. Chem. Org. Chem*, (1978), **33B**, 1381.

51. J. Chatt., L.M. Vallarino., L.M. Venanzi., *J. Chem. Soc*, (1957), Part IV, 344.

52. M. Rudler-Chauvin., H. Rudler., *J. Organomet. Chem*, (1977), **134**, 115.

53. G. Calvin., G.E. Coates., *J. Chem. Soc*. (1960), 2008.

54. R.E. Rulke, J.M. Ernsting., A.L. Spek., C. J. Elsevier., P.W.N.M. van Leeuen., K. Vrieze., *Inorg. Chem*, (1993), **32**, 5769.

55. E.A. Collins, J. Bares, F.W. Billmeyer., *Experiments in Polymer Science*., A Wiley-interscience Publication, London, 1974.

56. C.C. Price., E.J. Vandenberg., *Coordination polymerisation.*, Plenum Press, London and New York, 1983.

57. K.G. Virendra., S. Sheo., S.B. Ishwar., *J.M.S-Rev. Macromol. Chem. Phys*,(1994), **C34**, 439

58. Y. Sun, W.E. Piers., S.J. Rettig., *J. Chem. Soc. Chem. Comm*., (1998), 127.

59. *Reactivity, mechanisms and structure in Polymer chemistry*, eds. A.D. Jenkins, A Ledwith, A wiley Intersience Publication, London, 1974.

60. J. Boor Jr., *J. Polymer. Sci*, (1965), A, **3**, 995.

61. J. Boor Jr., *J. Polymer. Sci*, (1965), B, **3**, 7.

62. J. Boor Jr., *J. Polymer.Sci*, (1963), C, **1**, 257.

63. R.H. Grubbs., G.W. Coates., *Acc. Chem. Res*, (1996), **29**, 85.

64. K.J. Ivin, J.J. Rooney., C.D. Stewart., M.L.H. Green., R. Montab., *J. Chem. Comm.*, (1978), 604-606.

65. P. Cossee., *Tetrahedron Letters*, (1960), **17**, 12-16.

66. P. Cossee., *Tetrahedron Letters*, (1960), **17**, 16-21.

67. D.S. Breslow., N.R.J. Newburg., *J. Am. Chem. Soc*, (1959), **81**, 81

68. Z. Dawoodi., M.L.H. Green., V.S.B. Mtetwa., K. Prout *J. Chem. Soc. Chem. Comm.* (1982), 1410.

69. M.R. Kesti., R.M. Waymouth., *J. Am. Chem. Soc*. (1992), **114,** 3565.

70.W. Kaminsky., A. Ahlers., N. Moller-Lindenlof., *Angew. Chem. Int. ed.* (1989), **28**, 1216.

71. J.S. Eshius., Y. Tan., J. Teunben., J. Renkema., *J. Molecular Catalysis*, (1990), **62**, 277.

72. L. Resconi., G. Franciscono., L. Abis., F. Piemontesi., T. Fiorani, *J. Am. Chem. Soc*. (1992), **114**, 1025.

73. L. Resconi., S. Bossi., L. Abis., *Macromolecules*, (1990), **230**, 4489.

74. J.C.W. Chien., B.P. Wang., *J. Polymer. Sci.*, (1990), **28**, 15.

75. T. Tsutsui.,A. Mizumo., N. Kashiwa., *Polymer*, (1989), **30**, 428.

76. M. Bochman., *J. Chem. Soc. Dalton. Trans*, (1996), 255

77. K.G. Virendra., S. Sheo., S.B. Ishwar., *J.M.S-Rev. Macromol. Chem. Phys*,(1994), **C34**, 439.

78. S.S. Reddy., S. Sivoram., *Prog. Polymer. Sci.*, (1995), **20**, 309.

79. J.C.W. Chien., B.P. Wang., *J. Polymer. Sci, Polymer. Chem.*, (1988), **26**, 3089.

80. X. Yang., C.L. Stern., T.J. Marks., *J. Am. Chem. Soc*, (1994), **116**, 10015.

81. J. Chiu., *Polymer characterization by Thermal Methods of Analysis,*Marcel Dekker, Inc, New York, 1974.

82. E.C. Charsley., S.B. Warrington., *Thermal Analysis, Techniques and Application*, Royal Society of Chemistry, Cambridge, 1992.

83. B. Wunderlich., *Thermal Analysis*, eds. Academic Press Inc, San Diego, 1990.

84. W.W. Wendlandt., *Thermal Analysis.*, A wiley-interscience Publcation, New York, 1986.

85. A. Renfrew., P. Morgan., *Polyethene*, Interscience Publications Inc, New York, 1960.

86. M.L. Miller., *The Structure of Polymers*, Reinhold book corporation, New York, 1966.

87. P. Meares., *Polymer, Structure and Bulk properties*, eds. D. van Nostrand company, London, 1965.

88. R.A.V. Raff., K.W. Doak., *Crystalline Olefin Polymers*, Interscience Publications Inc, Part I., New York, 1965.

89. W.F. Msuya., C.Y. Yue., *J. Mater. Sci. Lett*, (1989), **8**, 1266.

90. B. Wunderlich., C.M. Comier., *J. Polymer. Sci.*, (1967), **A2**(5), 987

91. F.A. Quinn, Jr., L. Mandelkern., *J. Chem. Soc*, (1958), **80**, 3178.

92. D.D. Perrin., W.L.F. Armarego., *Purification of Laboratory Chemicals*. 3rd ed, Pergamon Press, New York, 1988.

93. B.S. Furniss., A.J. Hannsford., P.W.G. Smith., A.R. Tatchell., *Vogel's Textbook of Practical Organic Chemistry*. 5th ed, Longman Scientific & Technical, New York, 1989.

94. G.W.A. Fowles., D.A. Rice., R.A. Walton, *J. Inorg. Nucl. Chem*, (1989), **31**, 3119.

95. *Inorganic Synthesis*, 13, McGraw-Hill Book Cie, New York, 1972, p162.